uOttawa

L'Université canadienne
Canada's university

FACULTÉ DES ÉTUDES SUPÉRIEURES ET POSTOCTORALES

uOttawa

L'Université canadienne
Canada's university

FACULTY OF GRADUATE AND POSDOCTORAL STUDIES

Lin Zhang
AUTEUR DE LA THÈSE / AUTHOR OF THESIS

M.A.Sc. (Mechanical Engineering)
GRADE / DEGREE

Department of Epidemiology and Community Medicine
FACULTÉ, ÉCOLE, DÉPARTEMENT / FACULTY, SCHOOL, DEPARTMENT

Acoustics Signal Processing in Subject and Object in the Loop Configurations
TITRE DE LA THÈSE / TITLE OF THESIS

D. Necsulescu
DIRECTEUR (DIRECTRICE) DE LA THÈSE / THESIS SUPERVISOR

CO-DIRECTEUR (CO-DIRECTRICE) DE LA THÈSE / THESIS CO-SUPERVISOR

J.Z. Sasiadek

D. Dhillon

Gary W. Slater
Le Doyen de la Faculté des études supérieures et postdoctorales / Dean of the Faculty of Graduate and Postdoctoral Studies

# Acoustic Signal Processing in Subject and Object in the Loop Configurations

by

Lin Zhang

The thesis submitted to the

Faculty of Graduate and Postdoctoral Studies

In Partial Fulfillment of the Requirements

For the Degree of

Master of Applied Science in Mechanical Engineering

Department of Mechanical Engineering

University of Ottawa

*Your file Votre référence*
*ISBN:* 978-0-494-81335-5
*Our file Notre référence*
*ISBN:* 978-0-494-81335-5

## Abstract

Acoustic signal processing is a discipline dealing with the information extracted from sound signals with applications in industry, entertainment areas etc.

Two experimental configurations concerning real-time acoustic signal processing are developed for: voice manipulation and machine fault diagnosis, which share the same experimental equipment and signal processing software.

First experimental study is based on the voice manipulation technique in a subject-in-the-loop configuration. A human voice was altered and fed back to the human subject in a signal manipulation process. The experimental setup validity was verified and real-time applications were achieved.

Second experiment was conducted on a drive-motor-system to detect the fixture fault conditions due to loose bolts. An object-in-the-loop fault diagnosis system was developed using the acoustic signals acquired from loose/healthy conditions. The result presents that the loose versus healthy conditions can be identified in real-time. The numerical result illustrates the pattern of natural frequencies change under both conditions.

## Acknowledgments

I would like to express my gratitude to my supervisor Dr. Dan Necsulescu for the guidance, support, patience and generous help throughout my graduate study and more importantly, for the vision of finding such an interesting and rewarding thesis topic. Special thanks to my parents, my family, Charles and all my friends for being there for me and their continuous encouragement is the motivation for the accomplishment of the thesis.

## Table of Contents

## List of Figures

## List of Tables

## List of Terminology

| | |
|---|---|
| A/D | Analog-to-Digital |
| D/A | Digital-to Analog |
| DFT | Discrete Fourier Transformation |
| FFT | Fast Fourier Transformation |
| DSP | Digital Signal Processing |
| S/H | Sample-and-Hold |
| LTAS | Long-term-average-spectrum |
| MSSpectrum | Mean-square Spectrum |
| PSD | Power Spectral Density |
| GUI | Graphic User Interface |
| FIR | Finite Impulse Filter |
| DAQ | Data Acquisition |
| rpm | Revolutions per Minute |
| FEA | Finite Element Analysis |
| DOF | Degree of Freedom |
| NAF | None-altered Auditory Feedback |
| MAF | Masking Auditory Feedback |
| DAF | Delayed Auditory Feedback |
| FAF | Frequency-Altered Feedback |

# 1 Introduction

## 1.1 Introduction

Sound is omnipresent in this world: music from the radio, lectures given by the professor, vibration noise from the car, slight hum from our computer CPU fans, or even sound of air flowing through a vent etc. According to American Heritage Dictionary of the English Language, sound is defined as a travelling wave that is an oscillation of pressure passing through a solid, liquid or gas medium, which stays in the range of hearing frequency from 20Hz to 20,000Hz, or the sensation stimulated in organs of hearing by such vibration. [1]The oscillation of sound pressure comes from the change in an ambient pressure due to a sound wave. The scientific study of sound properties helps us to visualize this abstract entity in depth and more importantly, provides us with access to a large variety of applications.

In order to investigate sound, sensors such as a microphone are used to collect the acoustic signal we are interested. The function of microphone is to produce an analog voltage output dependent on a time-varying input of sound pressure. The analog voltage output, after analog-to-digital conversion, can be processed into a digital form by a computer.

The digital form of acoustic signal is represented either in time or in frequency domain, each one in a specific way convenient to have a general picture of the sound. A plot that uses sound pressure or sound power in a function of time is a time-domain representation, while when using a function of frequency as independent variables, is known as frequency-domain spectrum. A frequency domain representation is more intuitively interpretable for the applications in this thesis as the mechanism of mammalian auditory system, especially the cochlear, performs a type of spectrum analysis in converting vibrations of the eardrum into neutral impulses, and therefore our auditory perception is based on the frequency domain representation of sound. [2] A complete frequency domain representation is composed of a magnitude spectrum and a phase spectrum. Due to the fact that phase spectrum is less informative in our work, there is much less stress on it in this thesis.

The frequency domain representative of sound can be adopted for developing a broad range of scientific applications such as voice training for actors or actresses who are supposed to

achieve a voice output different from the natural one, accent training for foreigners, clinically diagnosis of laryngectomized patients or even pinpoint failures in machinery.

Two experimental configurations based on acoustic signal processing are introduced: Subject-in-the-loop system and Object-in-the-loop system. Both share the same equipment and sound signal processing software.

The subject-in-the-loop experimental setup contains a human subject in the loop, a microphone, a pair of earphones and a computer. The human voice signal is picked up by the microphone, digitized and transferred to the computer. MATLAB is used to achieve the acquisition of voice signal and manipulation in MATLAB / SIMULINK environment. Long-Term-Average-Spectrum (LTAS) is generated with customized codes for representing the information of frequency-amplitude response. At the same time, the output of the analog voice is fed back to human's hears through the earphones to achieve modified voice feedback and to test if we can obtain required new voice quality. The objective of this configuration is to illustrate how we can achieve voice manipulation in a controllable manner to enhance the voice mobility of human subjects. The experiment is conducted under two set of configurations: formant manipulation and real-time application.

A fault diagnosis scheme, called object-in-the-loop, is proposed in the thesis as well. The experimental configuration is composed of an object drive-motor-system, a DC power source, a microphone and a computer. This system provides a path to visualize the normal versus abnormal states of the rotating machine. Compared and analyzing the FFT spectrums generated, the damaged from the undamaged conditions of the device can be distinguished. The experimental results have been verified and improved by applying resonance tube measuring technique as a part of the experimental configuration to acquire more accurate and interpretable testing results. Therefore, the application of resonance tube measurement has helped to complete the entire object-in-the-loop fault diagnosis configuration in real-time. A simulation model of the drive-motor-system is also included in the thesis to illustrate the change of structural natural frequencies as a result of the alteration number of degrees of freedom (DOF).

## 1.2 Organization of the Thesis

In chapter 1, Introduction, organization and goal of the thesis are presented.

In chapter 2, literature review, focuses on acoustic signal processing and its related algorithms as well as on the background information regarding acoustic applications. A next section covers voice perception and acoustic faulty diagnosis issues used further in the thesis.

In chapter 3, experimental apparatus and experimental procedures for the subject-in-the-loop and object-in-the-loop are introduced.

In chapter 4, are presenting experimental results and discussion related to the experiments.

In chapter 5, Conclusions are presented.

References and Appendix are following after chapter 5.

## 1.3 Description of the Goal

Acoustic signal processing plays an important role in industrial applications, media and entertainment business. Two experimental configurations were developed for carrying out two important novel applications: voice training and acoustic failure detection in real-time.

According to previous studies, humans unconsciously compensate in changing their voice when hearing their altered auditory voice feedbacks. Based on the principle, the thesis introduces a voice feedback system accompanied by a formants manipulation method to take advantage of this feature and to realize the goal of modifying the voice as required. The voice feedback system is developed for people with professional training who can actually retrain their voice to obtain a different voice quality. Running the audio processing program in real-time is another challenge for the experimental setup development since most of real-life communications take place with little or no latency. Most published papers emphasize on the voice manipulation with professional software on dedicated analog or digital systems and little has been mentioned regarding the use of a readily available PC running MATLAB/SIUMLINK audio signal processing in real-time. This has been found to be an interesting and important topic to cover in this thesis.

The second experimental system refers to a condition monitoring system that is able to detect defects in a rotating system. The principle behind it is that any defects in a structure would lead to the changes in the natural frequencies of it and these frequencies can be captured by a microphone and processed to obtain a FFT spectrum. In this experiment, a drive motor system is operated under both healthy and defective conditions with same experimental setup. The objective is to differentiate the defective system from the healthy one based on the analysis of frequency changing patterns using FFT spectrums, besides to use the proposed resonance tube measurement to refine the existing experimental results.

# 2 Audio Signal Processing and Application

With the help of digital signal processing technique, signals can be acquired, processed, displayed, analyzed and manipulated as needed.

An analog input signal need to be converted into its digital form to be used in a computer. The function of an analog-to-digital converter is to convert a continuous signal into equally time-based discrete signals. Sometimes, if output of a signal is required, a digital-to-analog converter is a must for the process to be accomplished. [3]

Digital signals can be displayed in both time and frequency domain. Owing to the mechanism of our auditory system and signal properties contained in the frequency domain, the frequency representation is more useful. The transformation from time-domain to frequency-domain is conducted by Discrete Fourier Transformation (DFT). The efficient and fast algorithm of calculating DFT is Fast Fourier Transform (FFT), which only uses $N \log N$ steps to solve the problem while conventionally $N^2$ steps is required.

## 2.1 Digital Signal Processing

Digital Signal Processing (DSP) is a subfield of signal processing to modify signals in the digital domain to make them suitable for many purposes for real-world devices and applications such as mobile phone, digital camera, DVD player, audio processing and laser detection. Before a signal can be modulated, it has to go through a routine called digitalization, an essential procedure to convert an analog signal into its digital form.

The following section will introduce two important conversions in DSP: analog to digital conversion and time to frequency domain conversion.

### 2.1.1 Sampling

Most signals we confront are continuous, such as voice, microwave, laser beams etc. If these continuous signals are acquired for a signal processing purpose, they have to be converted into discrete digital forms to be processed by a computer or a digital device. An essential

procedure called digitalization is used to achieve this step. Digitalization of a signal is divided into two steps: Sample-and-hold (S/H) and the quantization.

S/H is a process to keep an analog signal constant for a short duration of time before it enters a subsequent system so that input value of the signal is stable enough to be accurately used for a conversion. The comparison between an original analog signal (shown in Figure 2.1) and the signal after S/H. (Figure 2.2)

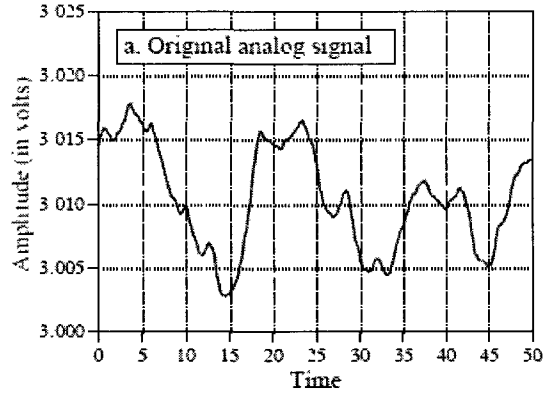


Figure 2.1 Original Input Signal [4]

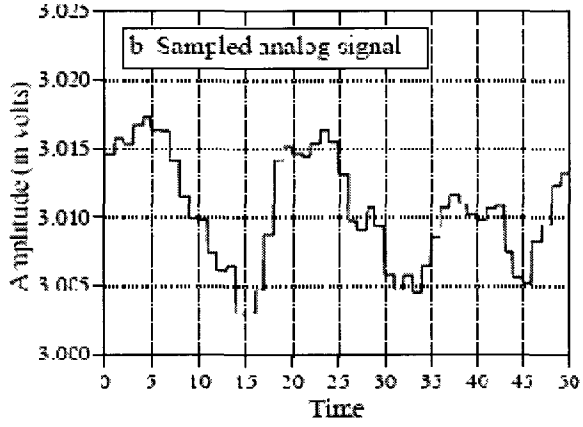


Figure 2.2 the Signal after S/H [4]

The following step is termed as quantization, which converts a sequence of continuous variables into digitized discrete signals as shown in Figure 2.3. A drawback of quantization is that it generates quantization errors or quantization noise, as shown in Figure 2.4. The errors are introduced due to the rounding errors between an input voltage value and an output digitized value. For example, input voltage values for 3.4500 volts and 3.4504 volts

will both be converted into digital number 3450. Quantization noise is uniformly distributed between $\pm \frac{1}{2} LSB$ (Least Significant Bit), with a mean of zero and a standard deviation of $\frac{1}{\sqrt{12}} LSB$ . [4]

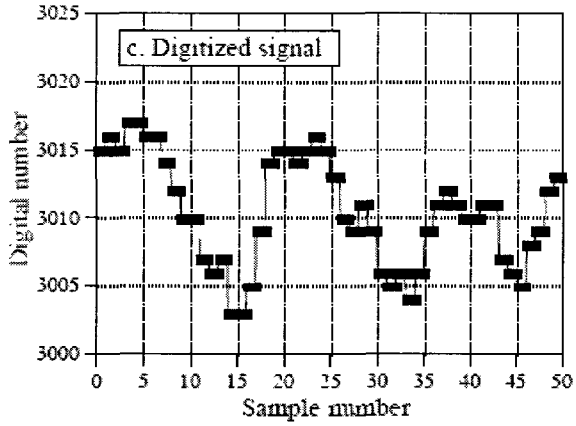


Figure 2.3 Digitized signal [4]

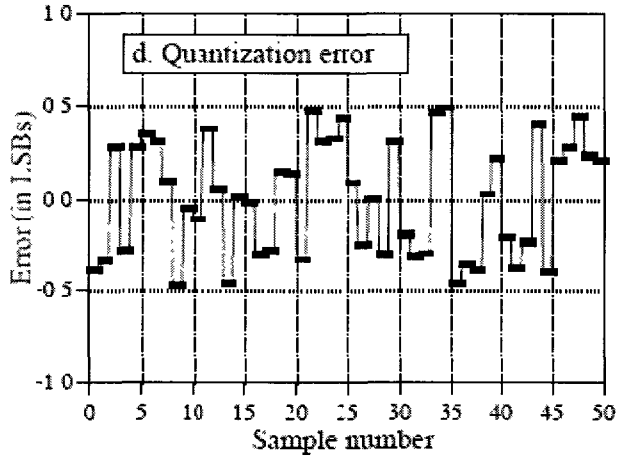


Figure 2.4 Quantization error [4]

## 2.2 Sampling Theorem

Sampling has a significant influence on signal content as it converts a continuous signal into a discrete signal which has a limited bandwidth. An appropriate sampling should contain the information that is able to reconstruct an original analog signal according to the chunk of data from a digitized signal. However, if the frequency in a sampled data is altered aliasing

will result in some part of the signal getting folded back or aliased. Two examples illustrate what is appropriate sampling. The continuous lines stand for the original analog inputs; the squared dots are the samples. In the Figure 2.5, although the sample data are sparsely distributed in the signal, the samples are still uniquely representing the original signal and the signal information is adequate for reconstructing the original analog input, which is defined as an appropriate sampling. However in the Figure 2.6, the sampled data totally lose the original frequency rate and could be mistakenly interpreted as a sine wave of 0.05 Hz frequency. Consequently, it is identified as an inappropriate sampling.

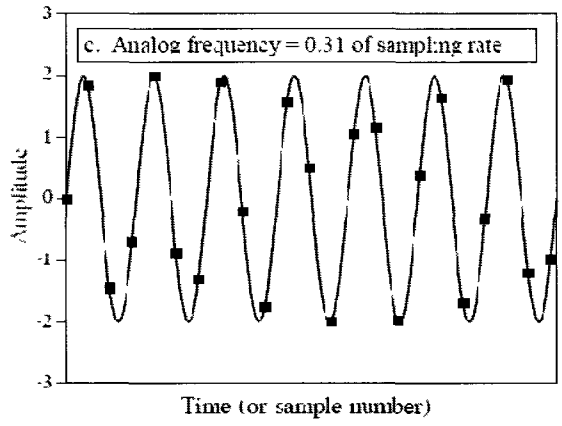


Figure 2.5 Appropriate sampling [4]

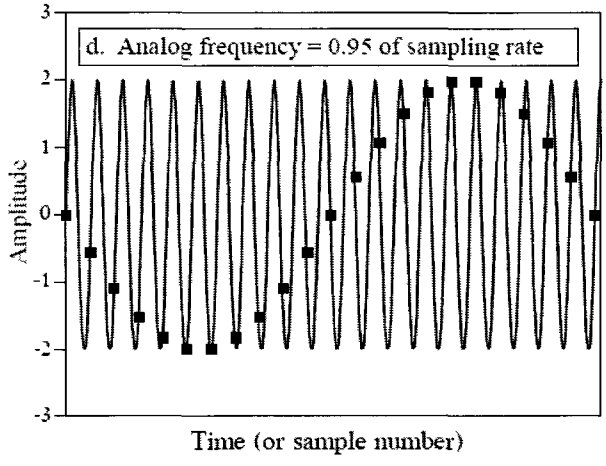


Figure 2.6 Inappropriate sampling [4]

To avoid having an aliased signal, led sampling theorem, or Nyquist sampling theorem require limit verification. The sample theorem points out that a continuous signal can be properly sampled only if the frequency is within one-half of the sampling rate. For instance, with a sample rate of 8000 samples/second, maximum frequency of the input signal should be below 4000 Hz. Any frequencies above 4000 Hz will be aliased within 4000 samples/second which could possibly lead to the lost or distorted important information of the input signal.

## 2.3 Discrete Fourier Transform (DFT)

Jean Baptiste Joseph Fourier, a French mathematician and physicist developed a mathematical technique based on an algorithm that decomposes input signals into sinusoids called Fourier analysis. [4] The reason of choosing decomposition of signals into sinusoids over other signals representations is because of its sinusoidal fidelity. That means when an input is formed of sinusoids, the output is guaranteed to be sinusoidal. Only the amplitude and phases change while frequency and wave shape stay the same. [4] This feature makes it simpler to interpret than the original analog signal.

Discrete Fourier Transform (DFT) is part of the Fourier analysis which deals with discrete and finite-in-length digitized signals. DFT also called decomposition analysis or the forward DFT is a procedure of calculating the frequency domain of a signal according to its counterpart in time domain. The input sample number is usually taken as a number which is positive and a power of 2, running from 32 to 406. It is owing to the binary form of the digital data storage in the computer and the algorithm calculation requirement for the Fast Fourier Transform (FFT).

DFT can be divided into real DFT and complex DFT. Real DFT deal with real numbers, while complex DFT deals with complex numbers or real numbers. Real DFT converts an input of N points signal into 2 output signals with N/2+1 sample points each, which are noted as real part ReX[] and Imagery part ImX[]. Complex DFT transforms two N points time domain signals into two N points frequency domain. Most of time, we only manage complex number in DSP, therefore only complex DFT is introduced. DFT is an operation to

convert a sequence of finite data $x_1, x_2 ... x_n$ in time-domain into its frequency-domain $X_1, X_2 ... X_n$.

The formula can be written as:

$$X(k) = \sum_{n=0}^{N-1} x(n) e^{-j2\pi nk/N}, k = 0,1,2...N-1 \quad (2.1)$$

x(n): An input signal at time sample n, n is an integral $n \geq 0$;

X(k): kth spectral sample;

N: Number of samples in the time-domain;

$j = \sqrt{-1}$: Basis for complex number;

$e = \lim_{n \to \infty} (1 + \frac{1}{n})^n = 2.718...$;

$e^{\frac{j2\pi}{N}}$: Primitive Nth root of unit;

Extensive use of Euler's identity can be seen in the equation 2.2 to express sinusoids.

$$e^{jx} = \cos(x) + j\sin(x) \quad (2.2)$$

Writing in Polar form, we have:

$$A_k = |X(k)| = \sqrt{\mathrm{Re}\, X(k)^2 + IMX(k)^2} \quad (2.3)$$

$$\varphi_k = \arctan \frac{IMX(k)}{\mathrm{Re}\, X(k)} \quad (2.4)$$

Formula of Inverse DFT can be expressed in 2.5, which can be used to reconstruct a frequency domain signal back into its time-domain.

$$x(n) = \frac{1}{N}\sum_{n=0}^{N-1} X(k)e^{j2\pi nk/N}, k = 0,1,2...N-1 \tag{2.5}$$

DFT has following important properties:

Completeness: N dimension of samples in DFT has N dimension of samples in IDFT:

$$Transform: c^n \rightarrow C^n$$

Periodicity: periodic sample with period N:

$$X_{k+N} = \sum_{n=0}^{N-1} x_n e^{-j\frac{2\pi}{N}(k+N)n} = \sum_{n=0}^{N-1} x_n e^{-j\frac{2\pi}{N}kn} = X_k \tag{2.6}$$

## 2.4 Fast Fourier Transform (FFT)

Fast Fourier Transform (FFT) is the fastest and most efficient algorithm to calculate DFT and is widely applied in the commercial spectrum analysis and computer-based applications such as signal process and analysis, device detection and adjustment, machine diagnosis and protection. [5]

Brief history background of FFT: J.W. Cooley and J.W. Tukey published the initial paper in the field "An algorithm for the machine calculation of complex Fourier Series". Although a century earlier, German mathematician Karl Friedrich Gauss had used the method; he did not put it into practical use because at that time, there was no digital computation system to solve this problem. [4]

In the next section we will talk about how FFT works and the mathematical algorithms behind it:

First of all, a N-sample-point-time-domain signal is broken into N time-domain signals each contain one sample point by using interlaced decomposition method. $Log_2 N$ steps are needed for the decomposition. FFT time-domain decomposition often needs to be treated by

bit-a-reversal sorting algorithm, which rearranges an order of N time-domain samples by counting in binary with the bits flipped left for right. [4]

Second step is to calculate the frequency spectrum corresponding to each time-domain point. All the frequency-domain spectrums are added up in a reverse order that the time domain decomposition had happened to form a complete frequency spectrum.

Mathematically FFT algorithm can be expressed as follows:

Given x[n] can be divided into even a[n] odd and b[n]:

$$a[n] = x[2n], n = 0,1...N/2-1 \tag{2.7}$$

$$b[n] = x[2n+1], n = 0,1...N/2-1 \tag{2.8}$$

We can compute N/2 points of a[n] and b[n] in equation 2.1, therefore:

$$A_k = \sum_{n=0}^{N/2-1} a[n]e^{-j2\pi nk/(N/2)}, k = 0,1...N/2-1 \tag{2.9}$$

$$B_k = \sum_{n=0}^{N/2-1} b[n]e^{-j2\pi nk/(N/2)}, k = 0,1...N/2-1 \tag{2.10}$$

And combine them into the equation, we can acquire $x(k)$:

$$x(k) = A_k + W_N^k B_k, k = 0,1...N/2-1 \tag{2.11}$$

$$x(k) = A_k - W_N^k B_k - N/2, k = N/2, N/2+1,...N-1 \tag{2.12}$$

Following procedure showing how can we obtain $x(k), k = 0,1,...N/2-1$

$$A_k + W_N^k B_k = \sum_{n=0}^{N/2-1} a[n]e^{-j2\pi nk/(N/2)} + W_N^k \sum_{n=0}^{N/2-1} b[n]e^{-j2\pi nk/(N/2)} \tag{2.13}$$

$$= \sum_{n=0}^{N/2-1} a[n] W_{N/2}^{nk} + \sum_{n=0}^{N/2-1} b[n] W_N^k W_{N/2}^{nk} \tag{2.14}$$

Because

$$W_{N/2}^{nk} = e^{-j2\pi nk/(N/2)} = e^{(-j2\pi/N)2nk} = W_N^{2nk} \tag{2.15}$$

Therefore, the equation becomes:

$$\sum_{n=0}^{N/2-1} a[n] W_N^{2nk} + \sum_{n=0}^{N/2-1} b[n] W_N^k W_N^{2nk} \tag{2.16}$$

$$= \sum_{n=0}^{N/2-1} a[n] W_N^{2nk} + \sum_{n=0}^{N/2-1} b[n] W_N^{(2n+1)k} \tag{2.17}$$

According to (2.7) and (2.8)

$$= \sum_{n=0}^{N/2-1} x[2n] W_N^{2nk} + \sum_{n=0}^{N/2-1} x[2n+1] W_N^{(2n+1)k} \tag{2.18}$$

The equation is combined of even points (first half) and odd points (second half). Comparing with the original equation (2.1) similarity can be found in the equation we have in half of the range.

Let us assume our total points is N/2-1, therefore, we can place $\sum_{n=0}^{N/2-1}$ by $\sum_{n=0}^{N-1}$ , while N=N/2,

And place 2n and 2n+1 by $n_{even}, n_{odd}$ , which is divided into odd and even points therefore, the original equation becomes:

$$\sum_{n=0}^{N-1} x[n_{even}] W_N^{nk} + \sum_{n=0}^{N-1} x[n_{odd}] W_N^{nk} \tag{2.19}$$

$$= \sum_{n=0}^{N-1} x[n] W_N^{nk}$$

$$= \sum_{n=0}^{N-1} x[n] \; e^{-j\frac{2\pi}{N}kn}$$

$$= X(k)$$

## 2.5 Windows

Audio signal is quasi-stationary that may vary within milliseconds or stay constant for a few milliseconds. Therefore, a window function is needed to choose a period of time to keep it constant for analysis. Nevertheless, window function is a compromise between spectral and temporal resolution. A long window provides high spectral resolution but lowers temporal resolution. [6]

Leakage (smearing) is the problem we have to face in the process of FFT calculation. It leads to the signal energy dispersing out of a narrow band frequency range, which blurs the amplitude, frequency and overall shape of a signal. The reason why Leakage happens is due to the edge effects from FFT calculation: FFT only picks finite samples of data out of a continuous input signal and assumes they are periodic and endpoints are connected. This gives rise to the problem when dealing with finite samples of data because it results in a truncated waveform which is disconnected at certain endpoints, see Figure 2.7. In order to eliminate disconnections, window functions are introduced to solve this problem. See Figure 2.8.

Figure 2.7 Disconnected at the Endpoints [4]

Figure 2.8 Continuous Waveform after applying Window [4]

Window builds an input time signal into a bell shaped curve on the time-domain spectrum, which start and end at zero, big arc in the middle. Different windows have different width for the curve in the time domain. See Figure 2.9. When the window function is applied in the frequency domain, it consists of a major peak and different small peaks called side lobs. See Figure 2.10.

An ideal window function is the one with low side lobs that can be effective in reducing leakage and narrow major peak that can catch spectral details. However, practically there is always a compromise between both. A disadvantage of window function is that it attenuates beginning and ending of a signal curve so that averages out the whole spectrum. In order to receive a more statistical accurate spectrum, increasing of sampling time is needed. [7]

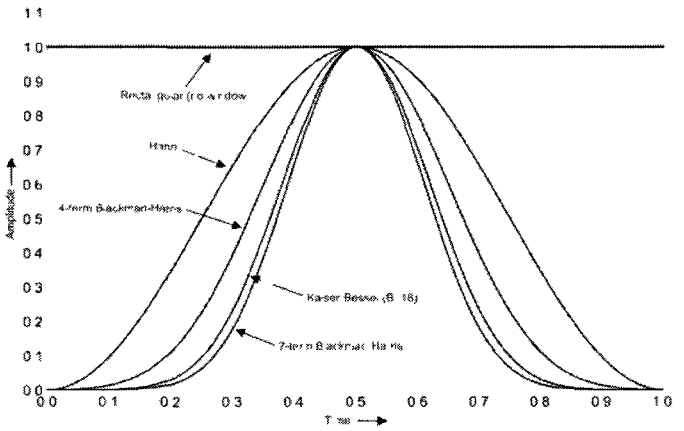


Figure 2.9 Windows in time domain [8]

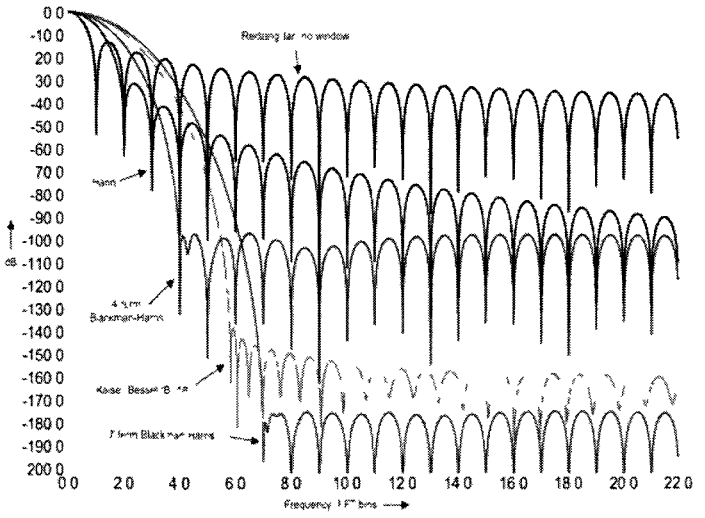


Figure 2.10 Windows in frequency domain [8]

It is difficult to conclude which window is better than another because different purposes are served in different applications. Most common windows used these days are Hanning, Hamming, Blackman, Flattop and etc. The following

Table 2.1 shows how to choose windows for different applications

According to previous study, Hamming window is the most popular one for voice analysis. Mathematical function of Hamming window is:

$$\omega(n) = 0.54 - 0.46\cos(2n\frac{\pi}{N-1}) \tag{2.20}$$

And Hanning window is good at discerning signals near in frequencies and noise measurement because it has better frequency resolution and moderate side lobes which will not place problems in the accuracy of a spectrum. [8][9]

Algorithm of Hanning window is expressed as:

$$\omega(n) = 0.5[1 - \cos(2\pi\frac{n}{N})], 0 \le n \le N \tag{2.21}$$

| Type of Signal | Window |
|---|---|
| Transients whose duration is shorter than the length of the window | Rectangular |
| Transients whose duration is longer than the length of the window | Exponential, Hanning |
| General-purpose applications | Hanning |
| Spectral analysis (frequency-response measurements) | Rectangular (for pseudorandom excitation) Hanning ( for random excitation) |
| Separation of two tones with frequencies very close to each other but with widely differing amplitudes | Kaiser-Bessel |
| Separation of two tones with frequencies very close to each other but with almost equal amplitudes | Rectangular |
| Accurate single-tone amplitude measurements | Flat top |
| Sine wave or combination of sine waves | Hanning |
| Sine wave and amplitude accuracy is important | Flat top |
| Narrowband random signal (vibration data) | Hanning |
| Broadband random (white noise) | Uniform |
| Closely spaced sine waves | Uniform, Hamming |
| Excitation signals (hammer blow) | Force |
| Response signals | Exponential |
| Unknown content | Hanning |

Table 2.1 Window Selection [8]

## 2.6 Voice Perception and Manipulation

### 2.6.1 Human Auditory and Voice Production System

Human ear is one of the most important and sensitive organ of entire body which has a wide range of hearing response from 12 Hz to 20000 Hz. In order to have a better understanding of how auditory system affects voice perception, we need to acquire some basic information about how they work.

The following including a brief description of the structure of our auditory system and how we are able to capture sound. The structure of a human ear is shown below, see Figure 2.11

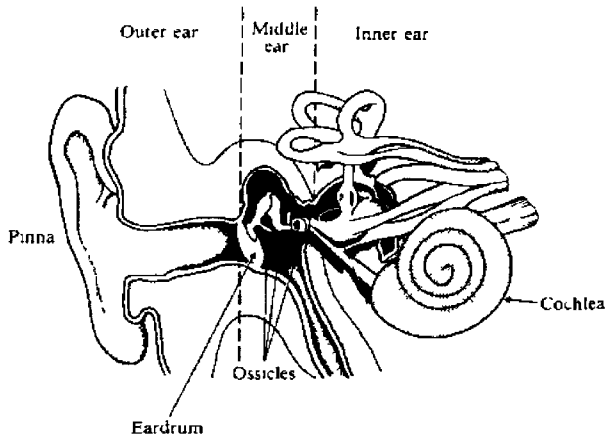


Figure 2.11 Human Ear [10]

Our ear is composed of 3 parts: outer ear, middle ear and inner ear. The outer ear contains Pinna and ear canal which is a tube of 0.5 mm in diameter and 3 cm in length. At the end of inner side of ear channel is eardrum or tympanic membrane, the function of which is that it vibrates when there is sound coming in. Middle ear consists of small bones called Ossicles which begin where ear drum is and ends at oval window to transfer vibration. Opening into the middle ear is the Inner ear, also called Cochlea. It is a liquid-filled tube; starts from the oval window and coverts vibrations into neural impulse. About 1200 sensory cells on the basilar membrane contained in the cochlea form cochlea nerve. When exposed to high frequency, nerve cells are stimulated where the basilar membrane is more stiff which is the part close to the oval windows. Vice-versa when it happens to the low frequency. This feature makes the fibers in the cochlear nerve response to specific frequencies, which lead to the perception of sound. [11] Next part let us have a look at how voice is produced, see Figure 2.12.

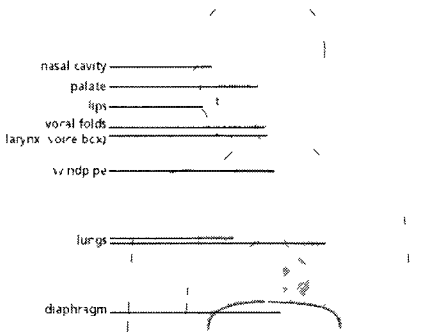


Figure 2.12 Voice Production Mechanism

Air pressure from the lungs, the diaphragm forms a steady air flow to the Larynx, windpipe and back of the throat. Vocal folds in the Larynx vibrate the air generating sound waves. Corresponding to the different conditions of the tongue, jaw, lips and speech organs, resonances in the vocal tracts change the sound waves to form different formants of frequency that is how different sound is made. Finally, voiced comes out from our mouth and/or nose.

### 2.6.2 Long-Term-Average Spectrum (LTAS)

In order to adjust their voice as desired singers, actors, public speakers need auditory feedbacks technology to help them to train their voice. In the past decades, an audio analysis method, called long-term-average spectrum (LTAS), has played an important role in the auditory feedback area and provides us with access to visualize and manipulate our own voice. A number of previous research publications have employed LTAS to analysis normal and impaired voice features. [12][13][14][15][16]

LTAS reveals the audio source and resonance characteristics of a signal, which help us to see the average frequency distribution of sound energy in a continuous voice sample. [17] The spectrum excludes pauses and voiceless segments before analyzing and averaging the remaining discrete spectra by leveling out the short-term variations. The advantage of LTAS is that it has direct physical interrelation about the location of the vocal tract resonances therefore, is a complementary to audio analysis. [15] Averaging a long-duration signal can be more accurate to allocate the right power to the frequencies. Additionally, noise-induced

fluctuations can be reduced to a lower level. With the application of window functions, LTAS becomes more accurate and favorable.

The algorithm of LTAS in MATLAB environment is established based on the Mean-Square Spectrum (MSSpectrum) that gives intuitive voice information about a signal's power distribution in respect to frequency. Unlike Power Spectral Density (PSD) that peak stands for the power in a frequency band in a spectrum, the peak in the MSSpectrum represents the power at a given frequency. [18] Two estimation methods are employed to calculate MSSpectrum: Periodogram and Welch, a modified Periodogram method.

Periodogram method computes an entire input signal at once, while Welch method breaks an input signal into segments, computing a periodogram of each segment and then averages them out to form a power spectrum. Periodogram estimation method is going to be applied in the first experiment and therefore the algorithm will be stressed next.

The formula for the periodogram method can be written as:

$$Periodogram = \frac{|abs(X(k))|^2}{F_s L} \tag{2.22}$$

X(k): DFT of the signal

$F_s$: Signal sampling frequency

L: Length of the signal

In most cases, FFT is applied in the operation and usually the result is one-sided, that means the negative side of frequencies are omitted. The calculation can be improved by applying window function [19] and Hamming window is most popular for the speech or singing signal. One-sided Periodogram function with a Hamming window can be written as:

$$Periodogram = \frac{|X(k)|^2}{2F_s L \frac{1}{m}\sum_{n=0}^{N-1}\left|0.54-0.46\cos(2\pi\frac{n}{N})\right|}, 0<n<N \tag{2.23}$$

m: length of the hamming window, m=N+1

### 2.6.3 Auditory Feedback Manipulation

Auditory feedback is a term that describes a cortical processing mechanism for voice productions that occurs when a produced message is compared and verified with the intended message while a speaker's auditory system perceives their voice outputs. Auditory feedback manipulation involves with altered auditory feedback which referring to the alternations to recurrent auditory information. [20] Auditory feedback manipulation has been of great importance in all sorts of applications from clinical to the laboratory-induced function; from voice training for singer/ actors to the treatment of disorder of shuttering. [21] Due to the adaptability of our human motor mechanism response to variance from internal and external conditions, any changes in the auditory feedback can affect our voice production system. [22] [23]

Typically, in an auditory feedback voice manipulation system input of a human voice that is routed into a computer or a signal processor will be routed back to the human subject with altered/non-altered auditory feedbacks (NAF) as the output. The relationship between input and output of an acoustic signal is called transfer function. Auditory feedback is a function of magnitude and phase of the signal; however, only frequencies that are reinforced as they traverse the loop will be adopted as feedback. [24] Masking auditory feedback (MAF), delayed auditory feedback (DAF) and frequency-altered feedback (FAF) are 3 common forms of auditory feedback alternations. [25]

When an auditory feedback is altered, a human subject changes his voice to compensate for the changes in the voice. The compensation is only related to the perturbation magnitude; therefore, it is a part of a control system that we can use to manipulate people's voice. Biologically, auditory feedback stimulates our neural mechanics, which has impact on our sensory feedback. [26] The feedback offers a means to alter source characteristics, pitch and the vocal tract transfer function, formant frequencies. [27]

In order to facilitate the voice training for singers, actors or public speakers, studies have been conducted based on the manipulation of formant frequencies, called formant manipulation, to enhance the mobility of voice formants. As an alternative to the traditional voice training method, a human based closed-loop control system used for voice

manipulation technique has been generated. In this case, the human subject is an audio signal generator, whose voice is picked up by a microphone that is connected to a computer that processes acoustic signals. The output of filtered signals from the computer is fed back to the subject through a loudspeaker or earphone. The audio manipulation system assists us also in determining if filtered auditory feedback is helpful to facilitate the subject who has no voice training background to produce different voice qualities. The configuration of the audio manipulation mechanism is shown in the Figure 2.13. An analog voice signal is going through different frequency manipulations, filters are applied to the voice signal to adjust to the voice signal as desired.

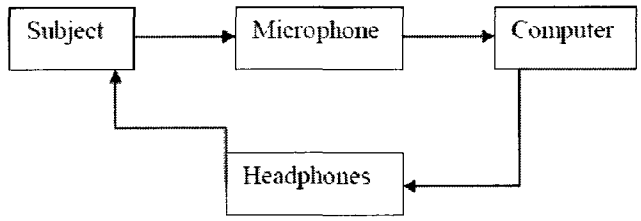


Figure 2.13 Audio Manipulation Mechanism Diagram

## 2.7 Acoustic Analysis for Fault Diagnosis of Vibro-acoustic System

The same equipment shown in the Figure 2.13 and the same signal processing program can be used for the case when the subject is replaced by an object that generates vibro-acoustic signals. In the service life of rotating machinery like automotive, rolling mills, aeronautical, inevitably occurs the deterioration from loose mechanical fixtures, cracks in structure, environment erosion, long running hours due to the heavy production requirements etc. Failures of machinery could cause dramatic loss for the economy or catastrophic effects on human life and. Therefore, great consideration has been given to prevent and detect failures in structures and in moving mechanical parts. [28] Several non-destructive test methods have been proposed based on acoustic signals, vibrations signals, ultrasonic, thermal field

etc. The justification is that local damage changes the acoustic characteristic of a system and, by examining the processed data, we will be able to identify to the faulty parts. [29]

### 2.7.1 Vibration

Vibration is one of the most common oscillatory movements in high-speed running cars, manufacturing machine-tools, industrial motors etc. Vibration can be classified as free vibration and forced vibration. Free vibrations are defined as the vibrations coming from the system itself with no external and a free vibration system has its own natural frequencies. Forced vibrations are driven by external forces. When the excitation is oscillator the affected system is forced to vibrate at the same frequency as the excitation. When the frequency coincides with one of the system's natural frequencies, large oscillations occur, i.e. resonance. Resonance can be stimulated by harmonic excitations from unbalance in a rotating device, force produced by a reciprocating machine, or the motion of a machine itself. [30] Resonance can be catastrophic to the structure, and sometimes can destroy the whole structure causing tremendous economic catastrophe as recalling of the collapse of Tacoma narrow bridge (1940).

Resonance can be reduced by adding damping system to lessen the vibration level. We can, however, take advantage of the resonance to use in machinery fault diagnosis technology. Given the natural frequencies of a system, we can manually add excitation frequency as equal or close to one of the natural frequency to create resonance. By using proper measuring equipments, a small defect can be detected in a more efficient manner owing to the amplified changes in amplitude and the shift of natural frequencies locations due to the defects. [30] The function of creating resonance in a system works the same way as a zoom function in a camera or a microscope that helps us to "see" better the situation. For example, a drive motor can be used an excitation drive; the vibration of the system can be transmitted through its structure and the structure itself has numerous natural/resonance frequencies. If motor's frequency matches one of the structural resonant frequencies, a stronger vibration occurs. Any defects under this situation will also be magnified and therefore easier to be perceived. [31]

### 2.7.2 Fault Diagnosis Technology

Fault diagnosis technique has been significantly progressed with the advancement of signal processing technique and algorithm in the last two decades, most popular signal processing methods are FEA and FFT, more advanced technique are Pattern Recognition, neutral/fuzzy system, wavelet transform etc. [32]

The fundamental basis for using fault diagnosis lies in that any defects in a structure lead to the changes in the modal parameters. Changes in the modal parameters vary from point to point, as well as to the differences of the locations and severity of the damage. Modal parameters can be determined by using transducers, such as a microphone or an accelerometer in a dynamic test. During the test signals are sent to a computer or signal analyzer to obtain a spectrum for analysis. According to some published research, damages or deterioration in a structure can be detected when there are at least 5% of changes in the frequency domain. [33]

Vibration analysis and acoustic analysis are two important fault detection methods, closely related to each other. Vibration is macroscopic oscillation of a structure while sound is microscopic oscillation of a substance. For example, vibration analysis results as a direct study of a force applied on a body, while sound analysis results from its impact.

Acoustic signals contain significant information that can help to characterize the dynamic behavior of a machine and it is closely associated with obtaining a sound spectrum from a microphone or microphone arrays. Acquired sound spectrums permit to detect defects in their early stage, which could save a company the cost of downtime of machinery. Previous research indicates that frequency domain spectrum is better for defects detection than its time-domain representation. The reasons are: 1. it is easy to recognize sound radiation in the frequency domain as major peaks are frequently associated with the structure resonant/natural frequencies or rotation speed etc. 2. Frequency analysis of machine condition can give an earlier warning of the defects than in the time domain as faults usually result in the change of vibration level in the frequency domain. While in the time domain, the variation of the vibration level occurs only when the faults are so maturely developed that they are destructive enough to affect the overall vibration level. [34]

The acoustic analysis methodology is carried on by applying baseline sound spectrums that are taken under well-defined operating system when a machine is running in healthy condition. Using this spectrum sets as references to compare with other spectrums which are running under similar operating system but in unhealthy conditions. The comparison is completed on a logarithmic scale of the amplitude. The changes between 6-8dB are considered as significant, while changes above 20 dB are considered as corresponding to a seriously defective system. [35]

Two approaches have been used to introduce defects to a vibro-acoustic system to employ the condition monitoring for fault diagnosis. First one is to run a system until failure occurs and then monitor the changes. Second one is to manually introduce defects to the system and measure the vibration response and to compare with the undamaged ones. First approach is time-consuming and unrealistic for the practice use. The second one is relatively flexible and controllable for the simulated defects we use in this thesis. [36]

### 2.7.3 Acoustic Signal Testing

A new non-destructive technology, called acoustic resonance testing, has proved to be an effective and cost-friendly defect diagnosis method for quality assurance in the industrial field. The test is based on the theory that a defective component changes the characteristic of vibration patterns while acoustic signals are the precursors of the vibration. Through the "communication" with the machinery, we will be able to differentiate the defective and healthy condition by measuring the frequency response from the excited work-piece with some appropriate sensors and devices.

Microphone is suitable for the measuring task in the environment without much background noise and dusty [37] and is usually placed at the near-field of a target. The location of a microphone has an important effect on the accuracy of data. Field points we choose for the acoustic measurements should be both unique and complete. Uniqueness means that each measurement point should contain the information that can be only obtained at this point and it is different from other points. Problematic situation occurs when more than one point contains the same information. This issue arises when we set points too close to each other under similar conditions. Completeness means the captured information should be enough to

represent the state of the object. This issue occurs when we separate points too far away from each other, which leaves out important information which we need.[38]

In order to accurately differentiate different structural conditions such as healthy versus unhealthy, we should let the object run in a reliable and consistent environment. Numerical descriptions of the changes in the amplitude and frequency can be used as important criteria to separate the healthy and unhealthy conditions. Amplitude can help us visualize the severity of the vibration and frequency can help us decide the oscillation rate. Changes in the following patterns can also be used to recognize defects: If the amplitude of curves has increased or decreased; If the locations of frequencies have been shifted; If the distance between resonances has changed; if there's any splits in the resonance frequency. [37]

In order to obtain detailed and accurate diagnosis data, some other factors should be considered as well. Diagnostic techniques using acoustic signals are efficient when the sound pressure caused by the defect area is high. When the degree of the defects is light, the changes in the frequencies cannot be detected by the microphone. As a result, purchasing some high-resolution, high sensitivity microphone and reducing sound reflection and perturbation form nearby surfaces should greatly improve the accuracy and success of test results. Due to the fact that acoustic signals are picked up by a microphone, the background noise could impact the sound generated from the device, therefore some effective filters should be applied to decrease the effects from the noise. [39][40]

# 3 Subject-in-the-loop Auditory Feedback Voice Manipulation Experiment

Auditory feedback plays an important role in voice training for singers and public speakers etc. Computer-based voice training technology can assist them to learn to take control of their voice by using the knowledge of voice perception and manipulation in an adequate setting.

In this section, an experimental setup for such voice training methodology called subject-in-the-loop auditory feedback control system (Figure 3.1) will be demonstrated. Previous studies show that speakers presented with auditory feedbacks containing a persistent shift of the formant frequencies of their own voices adapting to the alternation by changing the formants of their voices in the opposite direction of the shifts because of the mismatch between the auditory expectation and auditory signal fed back to the subject. [41] By using this knowledge, we should be able to increase our ability in the control of our own voice through the auditory feedback manipulation. LTAS is an effective acoustic measurement providing speech/singing voice spectra over time; by studying LTAS we can not only recognize our own voice formant but manipulate it as desired.

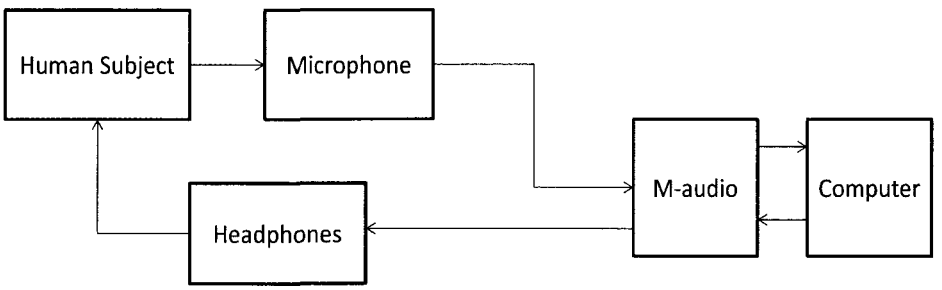


Figure 3.1 Subject-in-the-loop auditory feedback control system

The following experiment is based on the setup for voice training methodology in conjunction with the applications of filters to achieve formant-frequency manipulation. The experiment is divided into 2 steps, formant manipulation and real-time audio processing.

## 3.1 Experiment Procedure for Formant Manipulation

The experiment takes place in the Dynamics and Control Laboratory in the University of Ottawa. The voice signals are generated by a student with normal hearing condition. The microphone is connected to a M-audio soundcard input jack. A pair of earphones is connected to the output jack in the device. The M-audio is connected at the USB port on the computer. The Latest M-audio soundcard driver is installed to guarantee the proper function of M-audio. MATLAB from MATHWORK is installed on a desktop computer and Signal Processing Blockset from the SIMULINK platform is used. The important Parameters of M-audio and Microphone can be seen in the Appendix A. A customized Graphic User Interface (GUI) is designed for the experiment (Figure 3.2), see Appendix B for the M code.

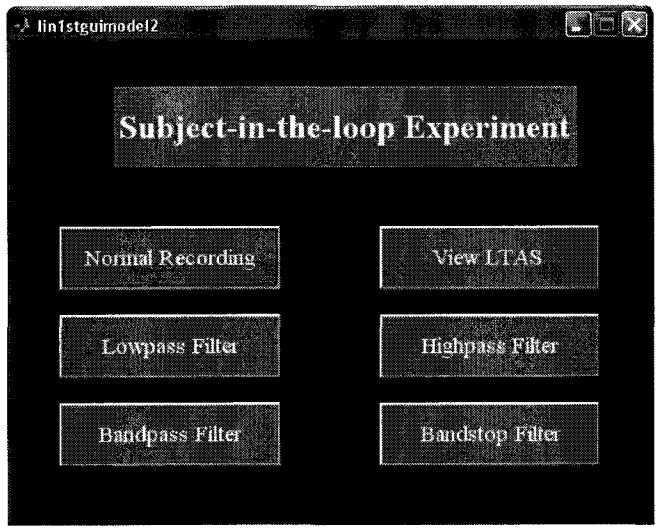


Figure 3.2 GUI for the Subject-in-the-loop experiment

Prior to any alternation of auditory feedback, a normal recording procedure is conducted with a sample time of 30 seconds to determine the formants we need to manipulate in the successive experiments by analyzing the LTAS of which. 3 blocks from the Signal Processing blocksets are used: From Audio Device, To Audio Device, To Wave File. The blocks are linked by the arrow-end line (Figure 3.3). 30 seconds of singing of an English song is recorded and played back at the same time.

The voice file in the format of .wmv is saved under C:\Documents and Settings\Grad Student\My Documents\MATLAB. The Long-term-average-spectrum (LTAS) using Periodogram estimation algorithm is applied to obtain the spectrum of the recording voice by clicking View LTAS in the GUI panel.

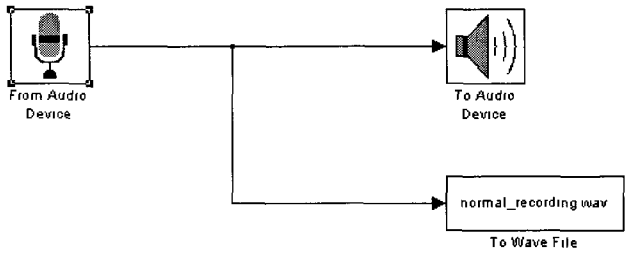


Figure 3.3 Blocks for normal recording

From the acquired LTAS, formant frequencies of interest can be determined to apply formant frequency manipulation in conjunction of different filters to achieve the goal of attaining desired voice characters. The Frequency-altered feedback (FAF) is simultaneously fed back to the human object to validate the managed voice. At the same time, voice manipulation purpose is achieved owing to the human object responses to the altered auditory feedback by producing different voices as reflections.

Four types of response applied in the experiment with the realization of Equiripple Finite Impulse Filter (FIR) are: low-pass, high-pass, band-pass and band-stop. The blocks (Figure 3.4) illustrate the voice manipulate scheme utilizing a low-pass High-Pass, band-pass and band-stop voice manipulation schemes share the similar blocks as the low-pass except substituting with its corresponding digital filter.

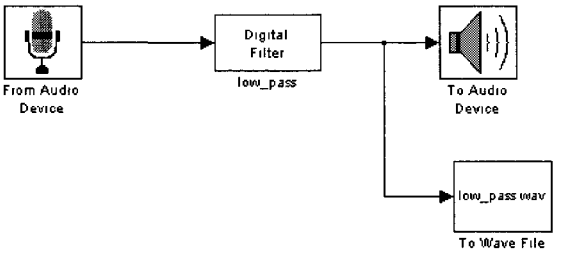


Figure 3.4 Formant Manipulation scheme with low-pass response auditory feedback

A low-pass filter designed with equiripple FIR method is designed to pass all the frequencies below a designated level while blocking all the frequencies above. Magnitude response of the Low Pass filter can be seen in the Figure 3.5. High-pass response has the opposite effect on the signal that is, blocking frequencies below the passing band.

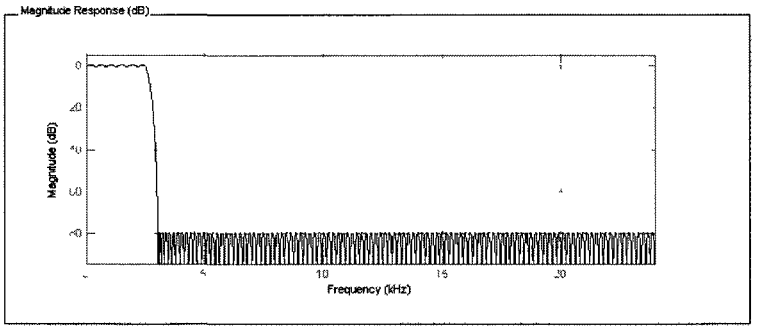


Figure 3.5 Low-Pass filter magnitude response

Equiripple FIR band-pass filter allows all the frequencies in between two frequencies, that is, passing band and stop band, to pass, while banning the other frequencies. Magnitude Response is shown in Figure 3.6.

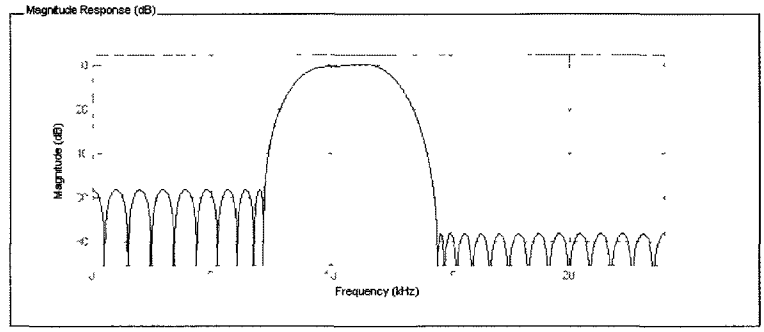


Figure 3.6 Band-Pass filter magnitude response

## 3.2 Experiment Procedure for Real-time Audio Processing in MATLAB

### 3.2.1 Real-time technology

xPC Target is one of the MATLAB platforms that allow us to run SIMULINK blocks in real time. The technology is based on the communication between a host computer and a target computer. Host computer, the "commander", can be a desktop computer or a laptop that has MATLAB software installed and with an Ethernet card supported by MATLAB. [42]Target computer, the "executor", can be any computer or device that has an Ethernet card recognized by MATLAB. The Host-Target communication can be either by Network communication or Serial communication. Considered data transferring speed, network communication either by connection with a cross-over cable or fast LAN is more efficient and favorable. The generated code of designed SIMULINK blocks by using Visual Basic as a compiler in the Real-Time Workshop environment is transferred to a target computer through a cross-over cable to be operated in real-time. [43]

Latency is one of the critical factors to evaluate voice training software's practicality as most of the voice analysis software we use today is in real time. However, how to accomplish this in interactive software like MATLAB is not an easy task. The problem has been investigated by several audio processing researchers who want to use MATLAB as the interface. The main reason is as opening the MATLAB, all the functions related to the start-up commands are called up, besides other Windows operating programs also running in the

background, which significantly slows down the MATLAB running speed. What xPC Target does is to separate SIMULINK from the MATLAB and the operating system to avoid competing for the operation time in the Host computer.

This part of the experiment contributes to the real-time audio processing in MATLAB, of interest in particular for those who work in audio DSP, as resulting from several papers concerning this application in MATLAB.

### 3.2.2 Experiment procedure

Real-time audio processing procedure in MATLAB is similar to the previous stated. Instead of using M-Audio as the voice input/output interface, PCI-6024e DAQ from National instrument is used. The participant's voice is transferred into electrical signals by the Microphone we used for the last experiment. The input signals are digitized with 12-bits precision using NI PCI-6024e DAQ. Real-time analysis and filtering of the voice are accomplished in the xPC Target interface of MATLAB. NAF and FAF are routed back to the human object from the output of the DAQ; see Figure 3.7 for the control system of real-time Object-in-the-loop experiment.

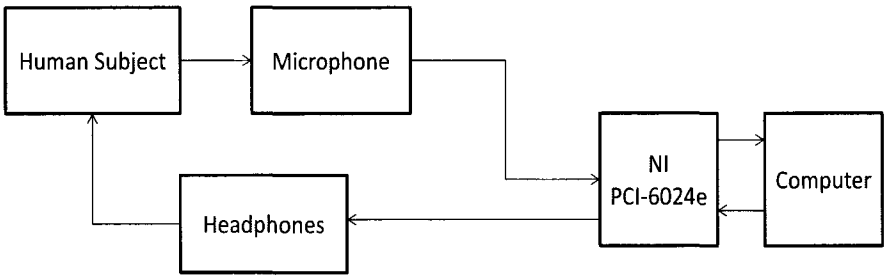


Figure 3.7 Real-time object-in-the-loop feedback control system

MATLAB offers us three options to achieve real-time applications with xPC Target, real-time workshop and real-time workshop embedded code. The real-time object-in-the-loop experiment is conducted under xPC Target module in the Dynamics and Control Lab at University of Ottawa, with a Host laptop, a Target desktop, PCI-6024e DAQ from National Instruments, a microphone and connecting cables. No detectable background noise is noticed during the experiments. The experimental procedure and setup of xPC Target are shown as follows:

Step 1, connecting the host computer and the target computer. The host computer is a HP laptop with Ethernet card Realtek RT 8101E Family PCI-E Fast Ethernet NIC and has MATLAB installed. The Target computer is a Dell desktop with Ethernet card Inter(R) Pro/100M Desktop Adapter with NI PCI-6024e DAQ installed. Two computers are connected by a Crossover cable CAT-6.

Step 2, assigning TCP/IP protocols to both computers. The host computer's TCP/IP: 192.168.1.120 with subnet 255.255.255.0. The target computer's TCP/IP: 192.168.1.119 with subnet: 255.255.255.0.

Step 3, starting MATLAB. In the command line typing in xpcexplr, a xPC Target Explorer window should appear. Selecting a correct path for the compiler, see Figure 3.8

In the communication protocol under Target PC1, filling in the following the data, see Figure 3.9.

Choosing Network Boot; Creating Boot image and rebooting the target computer, see Figure 3.10

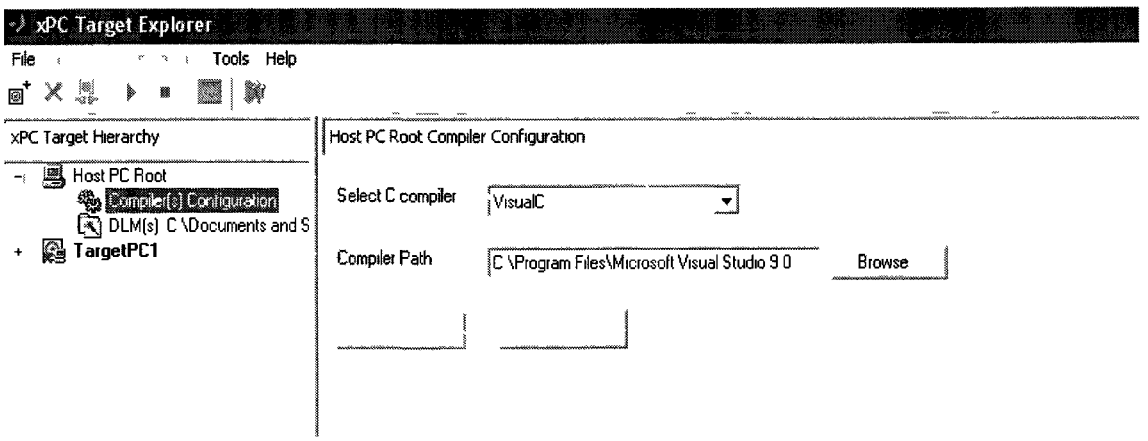


Figure 3.8 Selecting a C compiler for the xPC Target

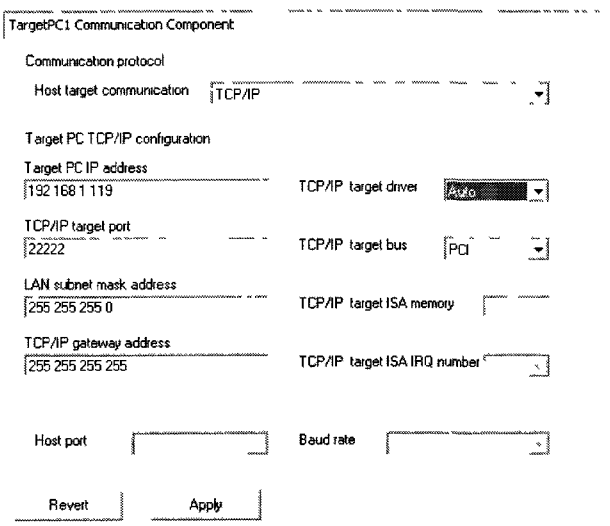


Figure 3.9 Target PC communication window

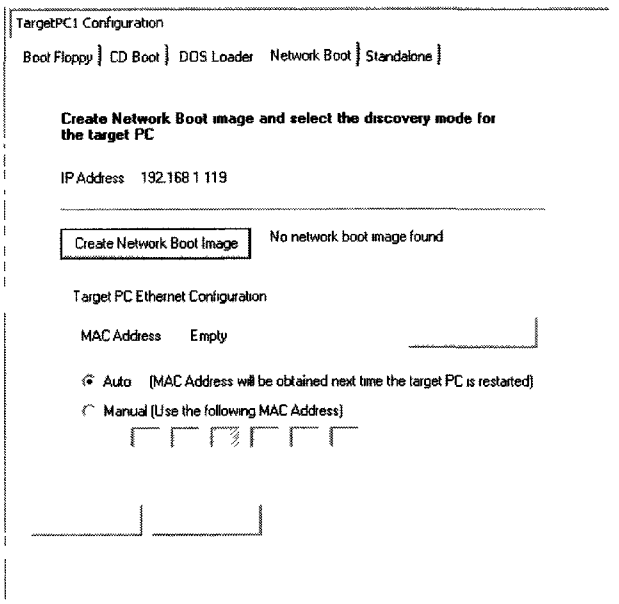


Figure 3.10 Creating network boot image

Step 4, the target computer looking for the right MAC address of the host computer that contains boot image which should bring the target computer into the DOS interface with xPC Target command, as shown in Figure 3.11. This means the Target boot is successfully booted with the boot image.

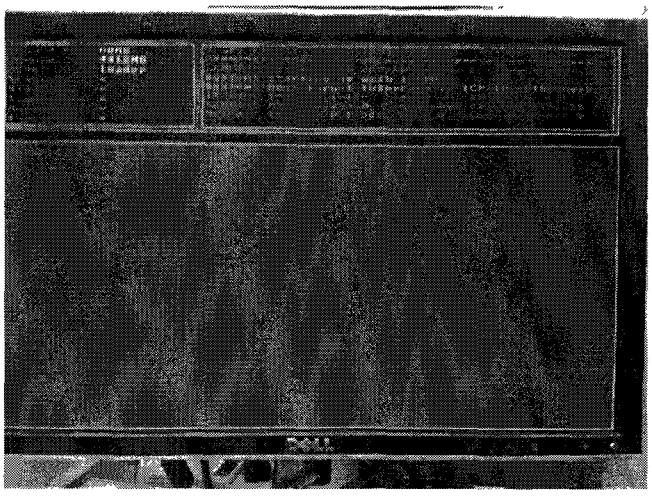

Figure 3.11 Target computer successfully boot with boot Image

A follow-up check of the configuration is required to examine the communication between the Target computer and Host computer by typing xpctest in the commend line. MATLAB starts to check the connection in 8 steps. If the communication is set correctly, it displays Test Suite successfully finished in the commend line, see Figure 3.12.

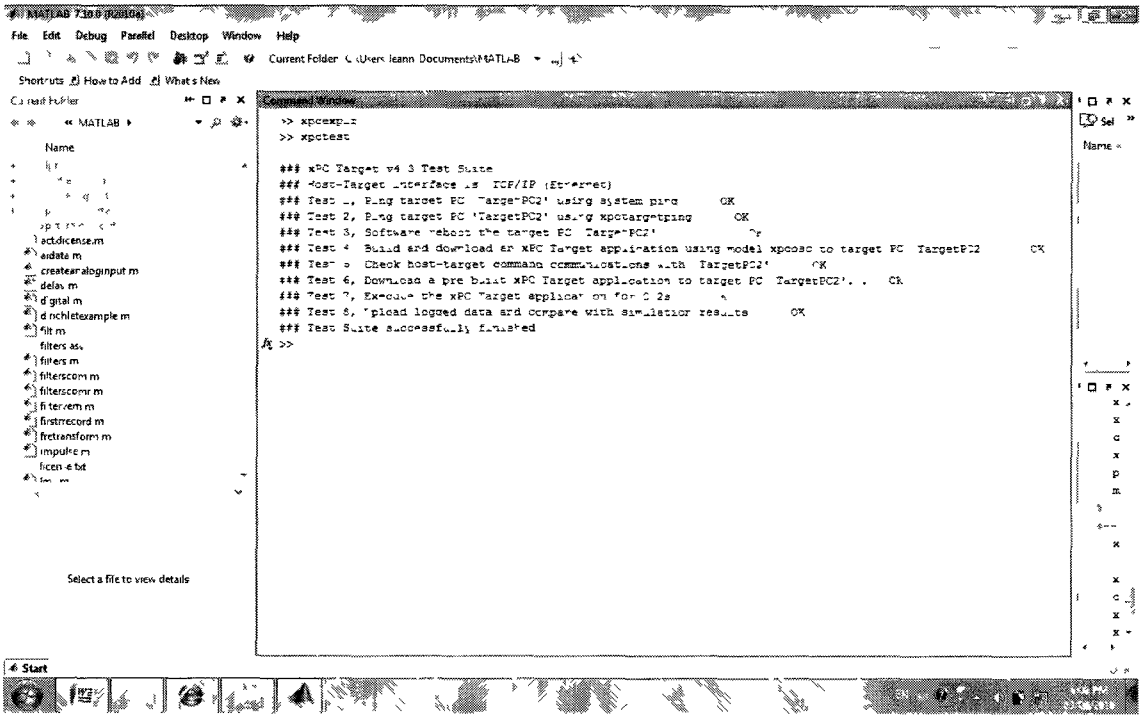


Figure 3.12 Communication test

Step 5, connecting input to the analog input of the DAQ at Channel 7 and earphone sets to the analog output at Channel 1, see Figure 3.13. The cable is connected to the microphone via single-ended connection, as shown in Figure 3.14.

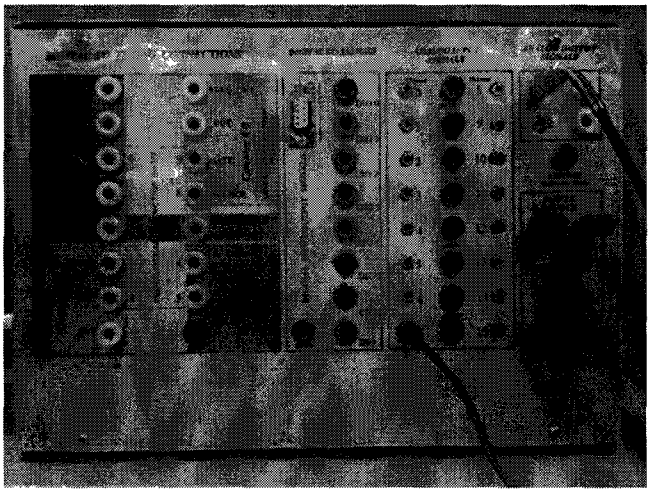

Figure 3.13 NI PCI-6024e DAQ I/O channel connection

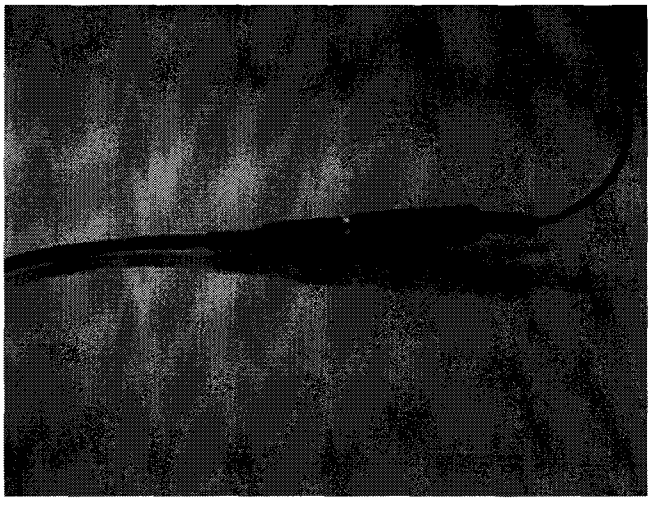

Figure 3.14 Cable connection with the microphone

Step 6, building blocks in SIMULINK for real-time test. GAIN block needs to be added to the blocks because the input voltage was below 0.005 volts so that it could not be captured by as the analog output in the DAQ. The SIMULINK blocks are shown in Figure 3.15

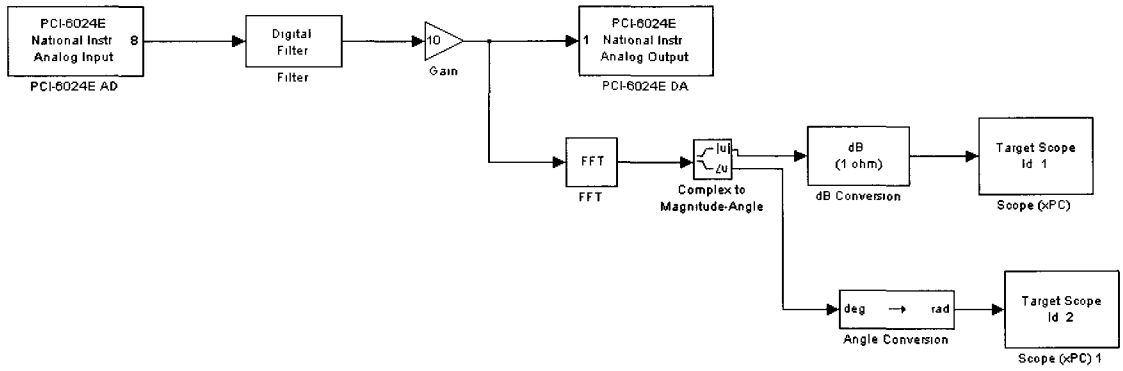


Figure 3.15 Real-time audio processing blocks

Step 7, running the model, target file should be chosen as xpctarget.tlc; execution time as real-time. Building the model and choosing external as simulation method in the simulation menu; connecting the host computer to the target and running the model.

# 4 Object-in-the-loop Real-time Fault Diagnosis Experiment

In order to validate the correctness of the proposed method, a drive-motor-system running under healthy and unhealthy conditions is analyzed in this experiment. FFT spectrums of the acoustic signals are investigated to perform fault diagnosis. Post-diagnostic resonance tube measurement method is applied to validate and improve the prior experimental result, and therefore to complete the object-in-the-loop configuration.

The Acoustic signals are picked up by a microphone at 6 different spots close to the motor case. The motor is operated at 10 different speeds. Acoustic signals are transferred to a computer for the acoustic signal processing. Analysis is conducted on the acoustic signatures output on the FFT spectrums. Sound pressure in magnitude and frequency are the resulting values of the signals in the FFT spectrums. The difference shown in the baseline spectrums and spectrums from the defective situations can be taken for the comparison purpose for the detection of faults.

The Object-in-the-loop experiment requires 3 main steps: Data Acquisition, Feature Extraction and Condition Identification. [44] In this experiment, data acquisition process employed a unidirectional dynamic microphone to collect at different places the acoustic signals radiated from the drive motor system. Feature extraction is achieved by utilizing Fast Fourier Transform to obtain its signal patterns. Condition identification is carried out based on the FFT spectrums to recognize the defective states.

A simple simulated model of the drive-motor-system is also presented for modal analysis in ANSYS to illustrate the changes in the natural frequencies of the structure before and after the structure contains defects.

## 4.1 Introduce of Experiment Apparatus

The experiment is implemented to demonstrate the practicality of utilizing a proposed fault diagnosis system in real life. The completed experimental arrangement includes a microphone, M-audio (as sound card), a high-end computer and an object drive-motor-

system to generate acoustic signals. The object-in-the-loop control system is shown in Figure 4.1

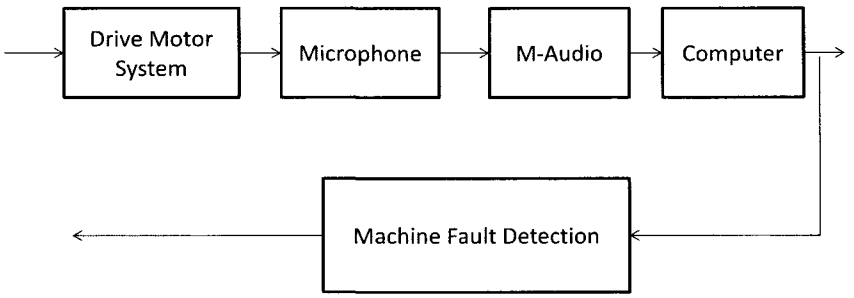


Figure 4.1 Real-time object-in-the-loop configuration

The object drive-Motor-system is shown in Figure 4.2. The motor has a voltage supply from 0 to 12 volts, gear ratio of 75 to 1 and a variable speed from 0 to 3600 revolutions per minute (rpm). The shaft connects with the wheel by a coupling to reduce transmission of vibration from motor and misalignment. A hole with diameter 1 centimeter is introduced to amplify the imbalance of the system. In order to let the structure realize free vibration, two metal plates are extra added to support the structure.

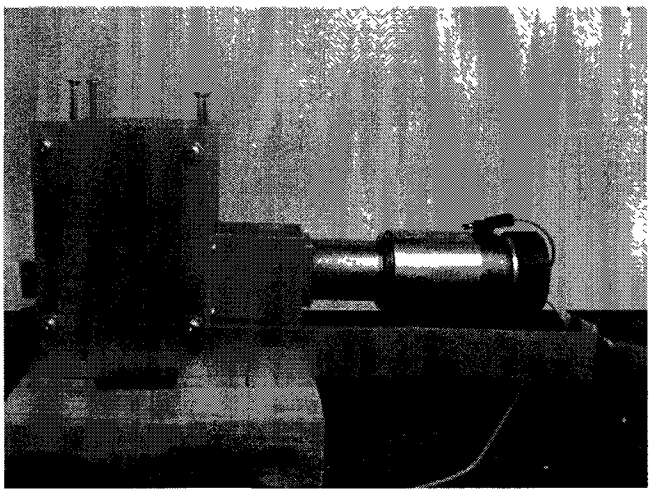

Figure 4.2 Drive motor object

The DC power supply has a range of 0 to 25 volts and a level knob is used to adjust to the required voltage for the experiment. Positive and negative voltages from the power supply are transmitted to the motor through two wires, see Figure 4.3.

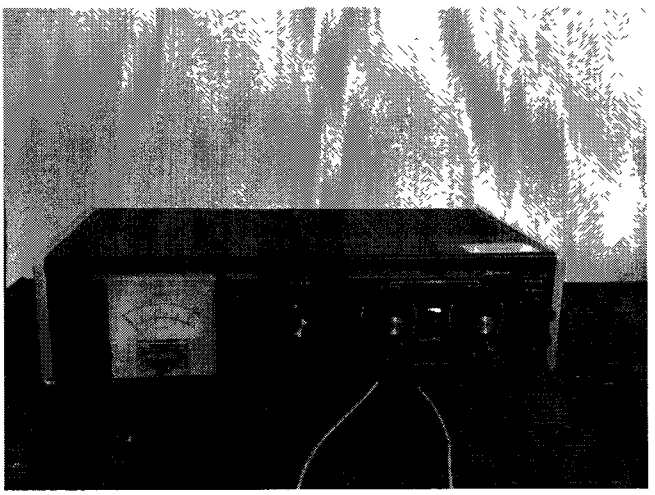

Figure 4.3 DC power supply

A dynamic unidirectional microphone was used to convert sound energy into electrical output. In order to reduce the near-field noise disturbance and improve its unidirectional ability, it was wrapped around with a thick layer of foam, which is a sound absorbing material, and is taped to reinforce it, as shown in Figure 4.4.

Figure 4.4 Microphone with the sound absorbing material

In order to reduce the surrounding noise, reflections and stray radiations from other subjects in the lab, the drive-motor-system is placed in a cardboard box (as seen in Figure 4.5) to increase the determination of defects. [36][45] Sufficient space is left in the chamber for the system to operate freely.

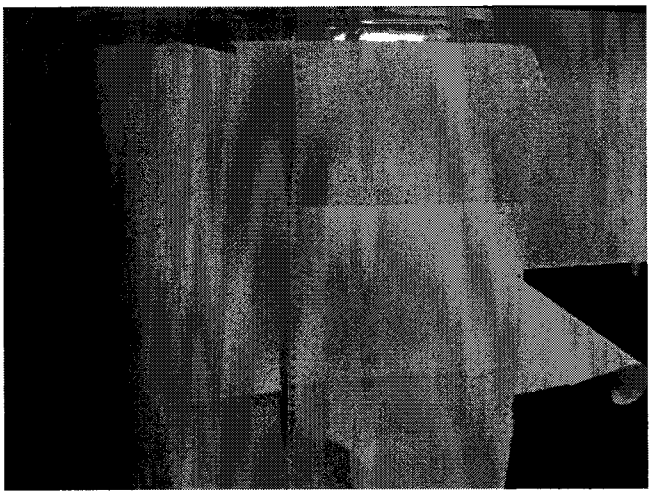

Figure 4.5 Sound-proof chamber

Resonance tube is used to validate the correctness of the prior test results and improve the experimental scheme. The tube we use for the experiment is made of Aluminum 24.6cm long and has a diameter of 3.2cm. One end of the tube is attached to the microphone (bonded by the thick tape) and another end is placed at where the measurement points are, therefore it is a half-open-half-close tube, see Figure 4.6.

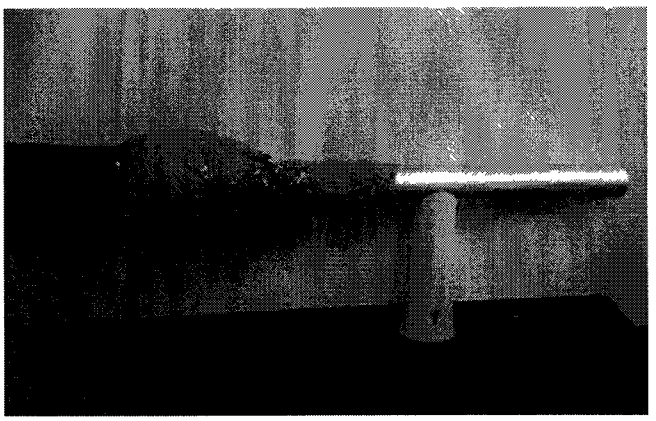

Figure 4.6 Resonance Tube

The resonance of the tube is calculated by: [46]

$$f = \frac{v_{air}}{4 \cdot (L + 0.4D)} \tag{4.1}$$

$$v_{air} = 331.13 \cdot \sqrt{(1 + \left(\frac{T}{273.15}\right)}$$

L: Length of the resonance tube. L=24.6 cm

D: Diameter of the resonance tube. D=3.2 cm

T: Temperature of the experiment environment. T=18 Celsius degree

## 4.2 Procedure of the Object-in-the-loop Experiment

Health condition of the system is defined by the tightness of the bolts on the front panel. Defects are manually introduced by setting the bolts loose on the front panel. The structure is fixed to a heavy table. There is no audible noise detected during the experiment.

The test is initially operated under a healthy condition that is, setting all the bolts tight, Figure 4.7. The starting speed is set at 600 rpm. In order to obtain accurate acoustic results and to see how speed is going to affect them, the test uses speeds of 600 rpm to 3300 rpm, which correspond to the increase of voltage by 1 volt steps up to 11 volts.

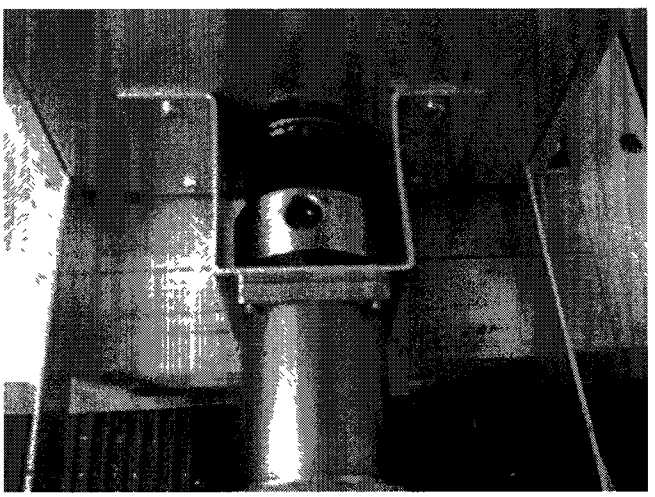

Figure 4.7 Tight bolts on the front panel

Six acoustic signals are sampled separately as seen in the Figure 4.8, using a microphone 0.5 cm away from the structure. At the beginning of each set of the experiments, the motor is settled by running for 5 minutes waiting to reach its stable condition.

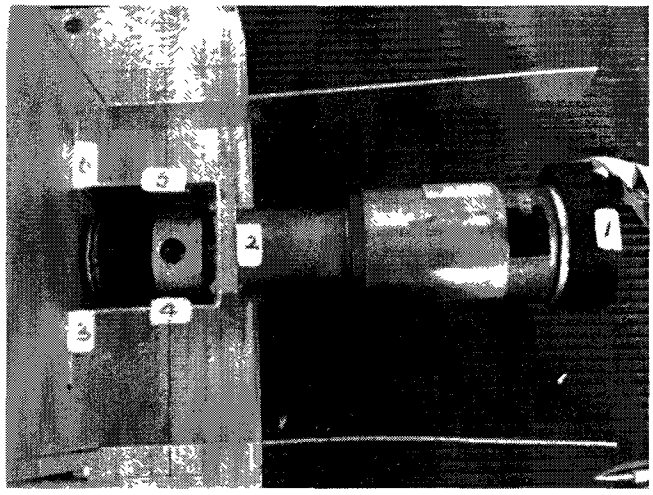


Figure 4.8 Sampling locations

Motor's speed in revolutions per minute (rpm) is calculated according to its driven shaft speed. Measured driven shaft speed and its corresponding motor speed are shown in the

Table 4.1.

| Measured DATA | | |
|---|---|---|
| Voltage (volts) | Shaft Rotating Speed (rpm) | Corresponding Motor Rotating Speed (rpm)/(Hz) |
| 2 | 8 | 600/10 |
| 3 | 10 | 750/12.5 |
| 4 | 14 | 1050/17.5 |
| 5 | 18 | 1350/22.5 |
| 6 | 24 | 1800/30 |
| 7 | 28 | 2100/35 |
| 8 | 32 | 2400/40 |
| 9 | 36 | 2700/45 |
| 10 | 40 | 3000/50 |
| 11 | 44 | 3300/55 |

Table 4.1 Measured Shaft Speed and its corresponding Motor Speed

Previous study on rotating machinery indicates that for proper measuring results, a minimum of 6 to 10 revolutions of the shaft under observation are needed for the accuracy of the test results. [47]

The sample time is given by

$$Sampletime T(\text{sec}onds) = \frac{60 \cdot n(neededrevolutionsofshaft)}{rpmofthemotor} \tag{4.1}$$

According to this equation, 5 seconds is chosen for the measurement time of the experiment.

The measured acoustic signals are transmitted to the computer. Fast Fourier Transform (FFT) is performed on every single input signal. Hanning window is applied to shape up the spectrum to reduce the effect of smear before the signals are processed by FFT. Generated FFT spectrums from the healthy condition are then used as baseline spectrums to be compared with the ones collected from the defective systems. The FFT plots are accomplished by use MATLAB code given in the Appendix C.

Defects are manually introduced to the structure by loosing up the bolts on the front panel as seen in the Figure 4.9 where four bolts are set loose to initiate a defective structure. Data acquisition procedure is as the previous one.

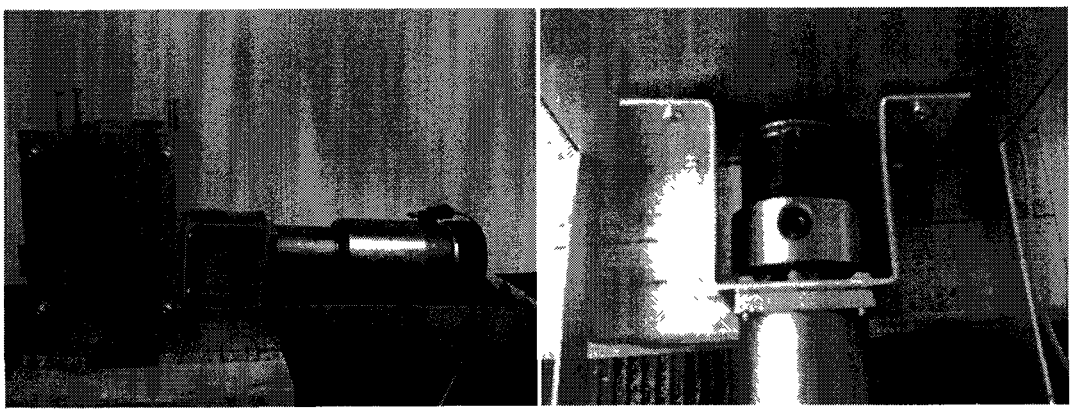

Figure 4.9 Loose bolts on the front panel

In order to examine if the degree of failures could also be detected from the acoustic analysis, looser bolts are considered for the completion of the experimental scheme as seen in Figure 4.10.

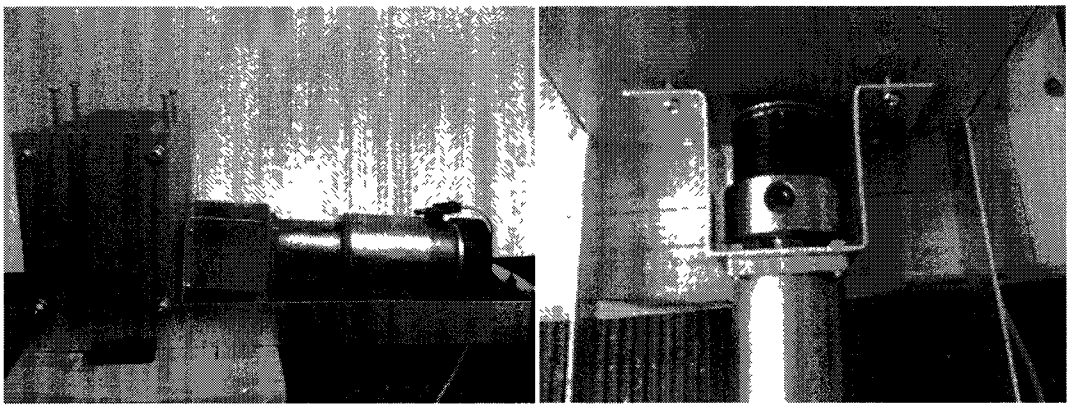

Figure 4.10 Looser bolts on the front panel

Test results are generated and collected in the MATLAB with different health conditions of the system running at the same speed on the same plot. The FFT spectrums are used for the fault identification and for the following resonant tube measurement.

Only the resonant frequencies are at or close to the resonance tube's frequency can be qualified for the resonance tube testing. According to the dimensions of the tube, the resonance frequency can be calculated and then comparing with the resonance frequencies from the obtained FFT spectrums to determine which set(s) of speed of the motor structure is/are eligible for the test. The procedure for the resonance tube measurement shares the same as the prior testing.

## 4.3 FEA Simulation Method

A simulated model of the drive motor system is considered here as shown in Figure 4.11. The purpose is to illustrate how Finite Element Analysis (FEA) method can be used to determine the natural frequencies of a given structure and if the constraints corresponding to the defective components in the motor system could affect the structure's natural frequencies.

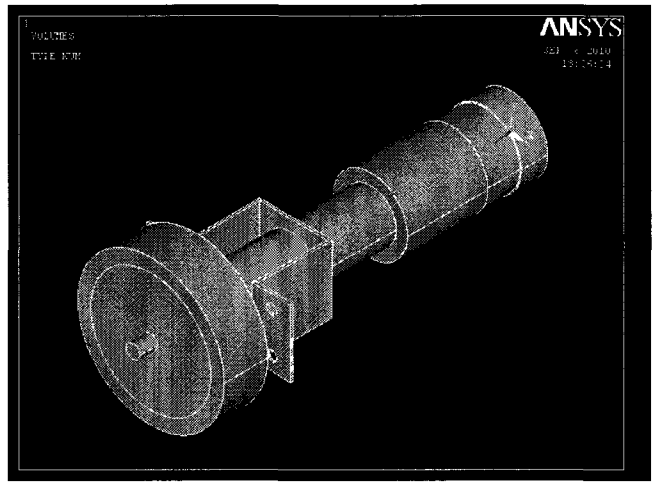


Figure 4.11 Modeling of the drive motor system

Four element types are used: Solid 45, Shell 63, Shell 43 and Shell 181, chosen for the model. The material models are set according to the material Poisson Rate, density and volume. In a healthy condition analysis, the connection areas have full degree of freedom (DOF), as seen in Figure 4.12

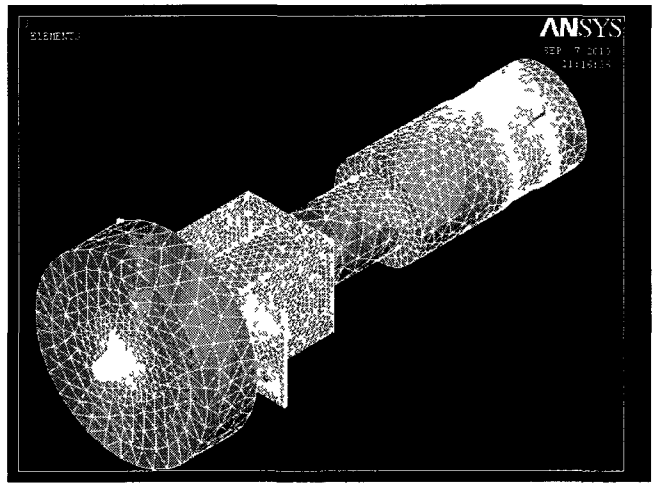


Figure 4.12 Bolts area applying with full DOF after mesh

Defective condition of the drive motor system is reflected on the FEA model by setting z direction free in the displacement and rotation. Modal Analysis is adopted for the structural analysis method. 10 modes are chosen to be extracted for the analysis using Black Lancozs methods.

# 5 Results and Discussion

## 5.1 Results and Discussion for the Subject-in-the-loop Experiment

The configuration of subject-in-the-loop experiment is designed for the voice training purpose. Previous studies show that humans subconsciously change their voice according to the auditory feedbacks. The configuration is based on the principle in conjunction with filters to achieve the goal of voice manipulation. NAF and FAF are under analysis in the form of LTAS, a popular speech/singing signal representative used in the acoustic researches.

30 seconds of normal recording voice in LTAS can be seen in the Figure 5.1 obvious formants are noticed from the spectrum, first formant ( $F_0$ ) happens at 89 Hz, $F_1$ at 354 Hz, $F_2$ at 697 Hz, $F_3$ at 1057 Hz. Each formants stand for the pitches in the voice.

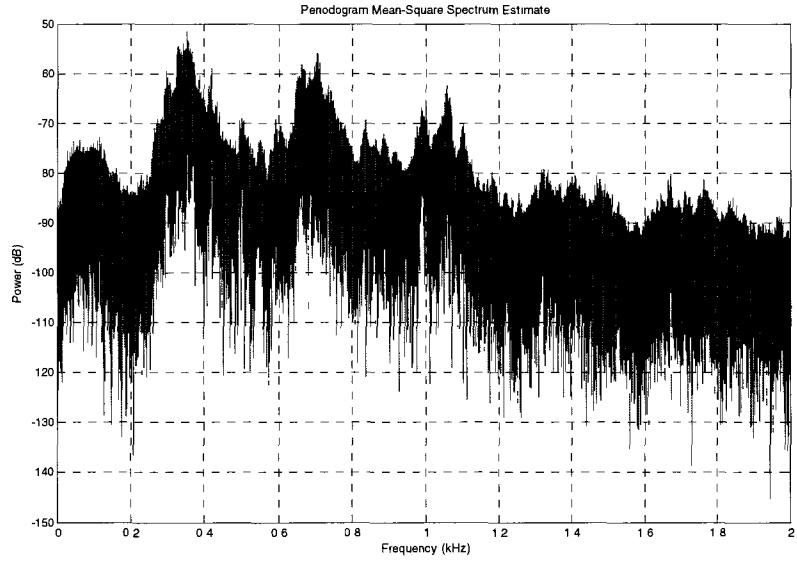


Figure 5.1 LTAS from normal recording

Formant at 697 Hz with a bandwidth of 115 Hz (from 646 Hz to 761 Hz) were selected for the target frequencies because it's dominant role in the LTAS up to 2000 Hz

The experimental result applied with the low-pass filter can be seen in the Figure 5.2. Stop frequency was chosen at 761 Hz, which blocked all the frequencies above 761 Hz. The voice was guttural and aphonic and content of the voice cannot be heard clearly.

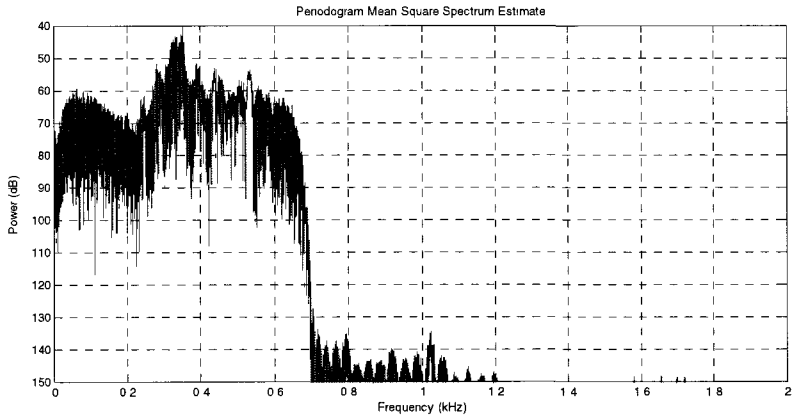


Figure 5.2 LTAS of low-pass response auditory feedback

In the High-pass response auditory feedback experiment, pass frequency was set at 761Hz. See Figure 5.3. Voice is high-pitched in this case. The content of the recorded voice can be perceived clearly but not pleasant because the voice sounds squeaky and twangy.

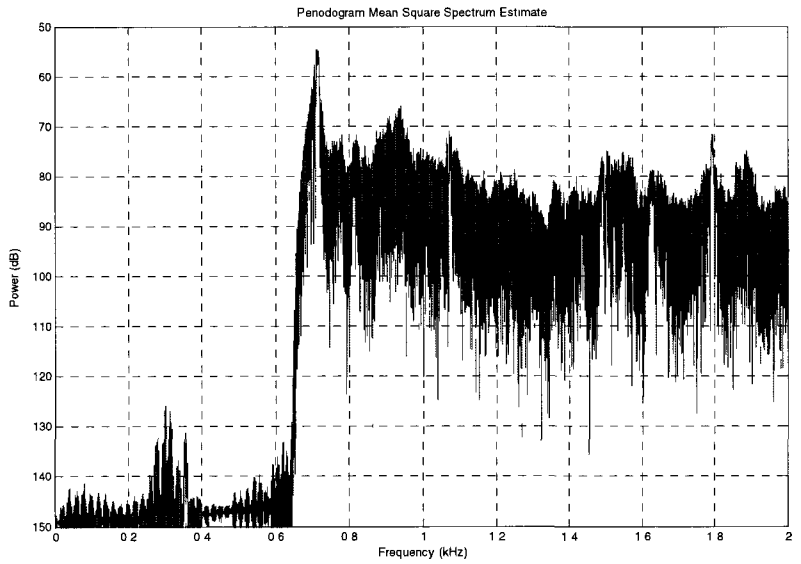


Figure 5.3 LTAS of high-pass response auditory feedback

In the band-pass response auditory feedback experiment, only frequencies range from 646Hz to 761Hz were allowed to pass, see Figure 5.4The voice is barely recognizable from the recorded file, which is very hollow and resonant.

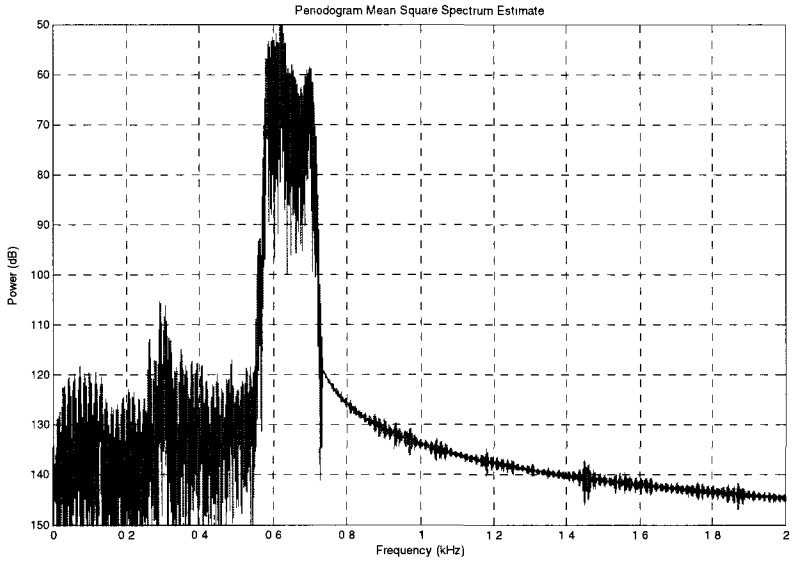


Figure 5.4 LTAS of band-pass response auditory feedback

In the band-stop response auditory feedback experiment, frequencies from 464 Hz to 761 Hz were filtered out. See Figure 5.5. The voice is most similar to the original voice, clear and pleasant.

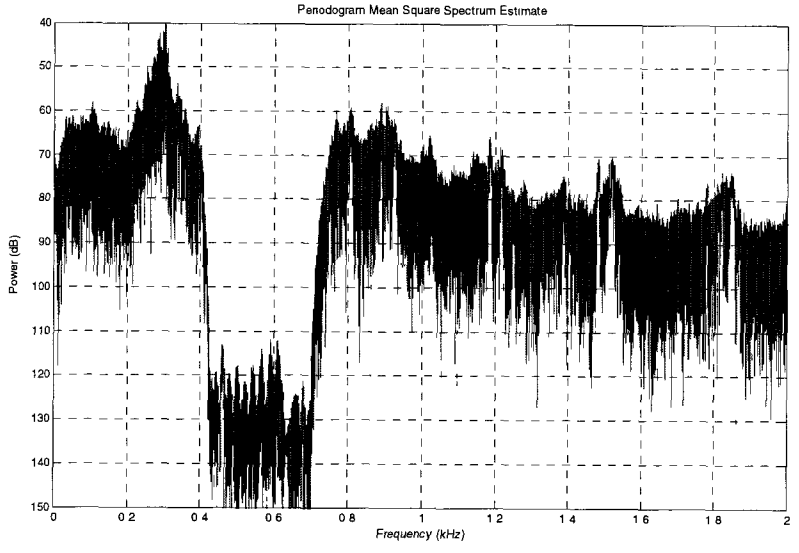


Figure 5.5 LTAS of band-stop response auditory feedback

With the help of the xPC Target, we were able to achieve the goal of real-time audio processing in this experiment. There was no latency in the audio input and output process. The FFT spectrums in the magnitude and angle are shown as Figure 5.6. Formant manipulations with filters were running in real time during the entire process. However the voice quality was not as satisfactory as what we had obtained in the previous experiment.

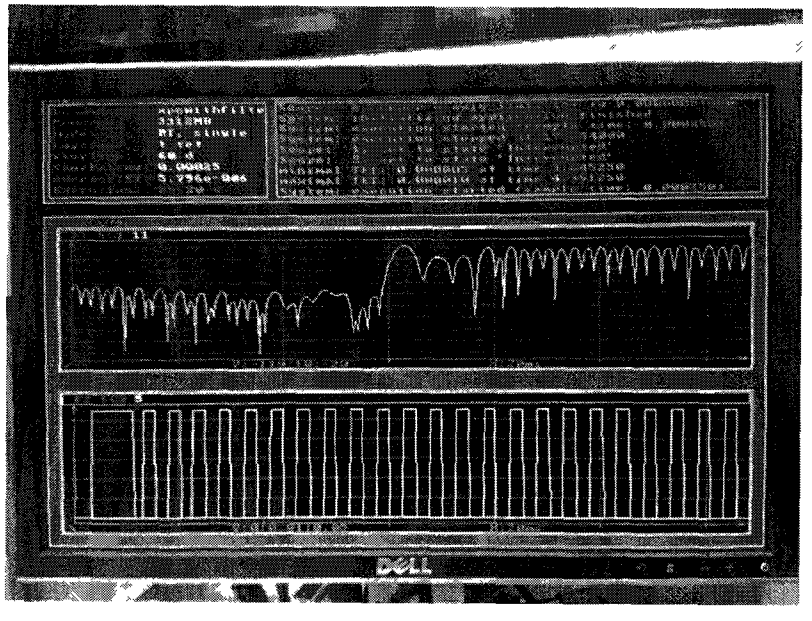

Figure 5.6 FFT in magnitude and angle

The Figure 5.7 illustrates the latency improvement concerning the audio record/playback processing in the xPC Target environment and SIMULINK environment. From the Figure.13, under xPC Target environment, the audio processing was 22338 samples ahead of that under SIMULINK environment, which is 456 mseconds faster compared to the SIMULINK's. As a result, xPC Target greatly improve the audio processing speed.

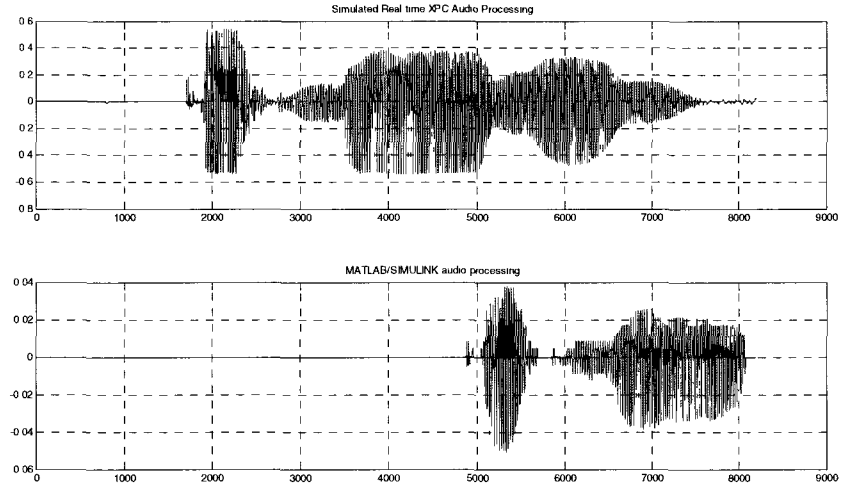


Figure 5.7 Delay improvement comparison: xPC Target Vs SIMULINK

The subject-in-the-loop experiment configurations are designed for the voice training purpose based on the human's auditory reflections to the voice feedback. The designed scheme for voice manipulation is for the goal of achieving activity control our voice in a controlled manner based on the auditory feedback knowledge we mentioned early. Such voice manipulation method can be used for voice training of acting, singing, public addressing etc. 4 kinds of filters were implemented in the experiment to illustrate the functionality of the scheme in creating desired voice characters. In addition, the configuration can be used for the speech analysis, synthesis and recognition purpose as well as for the voice formant studies, moreover, in the prediction of the speaker's emotional and psychological state. However, a noticeable delay was detected throughout the entire experiment process, which greatly affected the auditory feedback speed and quality. Numerous methods in accelerating SIMULINK operating speed have been tried, such as resetting SIMULINK configuration, refiguring computer's operating environment, adding a RT block to the designed blocks, applying Data Acquisition blockset of MATLAB etc.

nevertheless, none of them could really achieve real-time application. Obvious latency existed more or less.

xPC Target / MATLAB is a milestone technique for the accomplishment of running SIMULINK in real-time. Nevertheless, the same blocks used for voice manipulation cannot be operated under xPC Target due to the incompatibility of the audio library in MATLAB. As the solution, Data Acquisition Board (DAQ) NI PCI-6024e was applied. Compared with NI PCI-6024e, M-audio, used for the voice manipulation experiment, has 24bits of precision and 44100 maximum of sample rate which is an excellent choice for the audio processing. However, due to the limitation of the MATLAB functionality, M-audio could not be recognized as a DAQ, instead a low-cost NI PCI-6024e with self limits of 12 bits of analog input and out precision was chosen to achieve real-time operation at the cost of losing satisfactory sound quality. Additionally, owing the connection between microphone and analog input jack, system noise was noticed, yet which was greatly reduced by applying a low-pass filter.

A real-life voice training technology requires high quality of voice and low latency in audio processing, which can be achieved by either developing our own program or if, it is a requirement for using MATLAB, a high-end DAQ board or installing WaveWarp from the MATLAB company is essential for achieving such goal. As for the practicability of the voice perception configuration which will be long-term goal to test, therefore we are not able to show the final result in this paper.

## 5.2 Result and Discussion for the Objective-in-the-loop Experiment

The purpose of the object-in-the-loop experimental setup is to achieve condition monitoring and fault diagnosis in real-time for the drive-motor-system by examining the FFT spectrums. Initial experiment was conducted under undamaged condition and the FFT spectrums were saved as the baselines to compare with the acoustic signatures from the other two defective conditions. Resonance tube measurement method was applied to improve the accuracy of the measured results, consequently to bring to the completion of the experimental scheme.

Defects were intentionally introduced to the system by setting loose the bolts to study how impaired structure would affect the spectrums for these conditions. The experiments were carried out for 10 different speeds, from 600rpm up to 3300rpm. The acoustic samples were collected at 6 different spots on the motor case, shown on the Figure 4.8, for the sound sources near the structure linking the motor to a base.

### 5.2.1 Pre-experiment Hypothesis

Pre-experiment hypothesis for the drive-motor system was that at the free end of the motor, point 1, shown on Figure 4.8, would occur the largest vibration. We assumed that the motor was a practically rigid body so that the vibration distributed on the motor was proportional at the linear distance. Therefore, compared to point 1, at point 2, a lower overall vibration amplitude would result. Point 3 and point 6 were firm bolted to the structure; therefore, not much vibration should be seen. However due to the special location of which, some defective acoustic signatures could appear. Point 4 and 5 were at symmetric sides, one relative to the other, and the test result should be similar. The connectivity of the bolts to the frame was very significant and no obvious vibration changes were discerned in the experiment.

### 5.2.2 Experimental Result and Discussion

A drive-motor system has been chosen to demonstrate the diagnosis of faults. The experiment reveals the acoustic variations in the frequency spectrums as a function of the different structure conditions. Amplitude shift and resonance frequency shift are among the most distinctive features that enable faulty diagnosis. Detailed experimental results are given in the Appendix D.

Each set FFT spectrum contains 3 different conditions of the structure, healthy conditions (green lines), loose-bolts conditions (blue lines) and looser-bolt conditions (red lines) running at the same speed. Owing to the diagnostic ability of the proposed acoustic signal measurement method, the frequency range of the figures was set up to 3000Hz to achieve the best diagnostic result.

Acoustic samples taken at point 1 (see Figure 4.8) show apparent overall amplitudes changes due to the vibration changes under different conditions, as seen in the Figure 5.8, for the motor's running speed of 1350rpm. Due to the defective structure, the acoustic signal amplitude varies, compared to the acoustic result at point 2 at the same speed, from Figure 5.9The overall amplitude of the defective case results decreased, however, at the peaks, we can still notice the amplitude variation and frequency locations shifts.

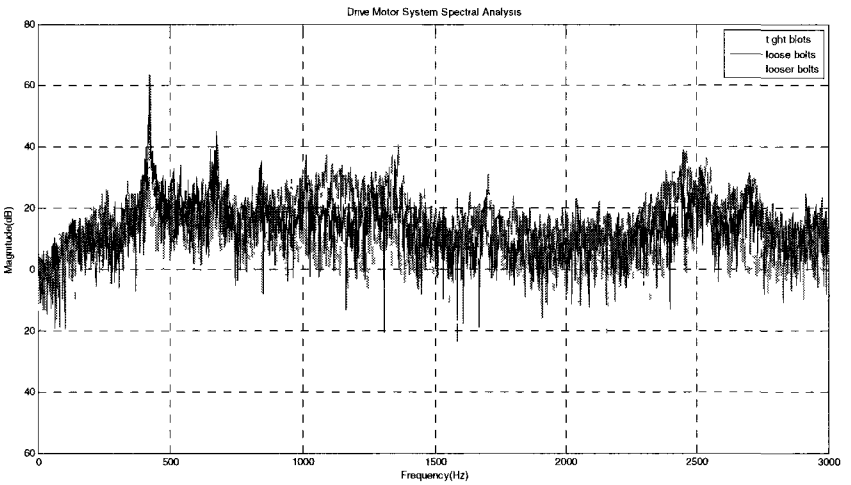


Figure 5.8 2700 rpm at point 1

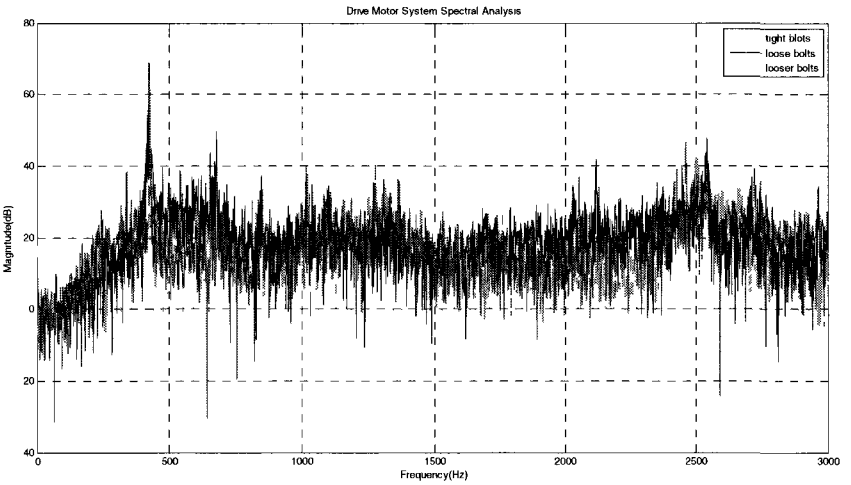


Figure 5.9 2700 rpm at point 2

At point 3 and point 6, near which the bolts were tight, we cannot notice large amplitude change. At the around 2500 Hz, however, an interesting phenomenon occurs, due to the

looseness of the bolts and this can be discerned at point 6 in some of the spectrums, for ex. Figure 5.10 and Figure 5.11. Due to the vibration excitation frequency, spectrum at motor running speed of 1050rpm show much higher amplitude shifts. This special phenomenon can be only seen at point 6, and therefore we conclude that the occurrence of the peak spikes is due to the changes in conditions. Frequency shift is another feature that is noticeable at points 3 and 6.

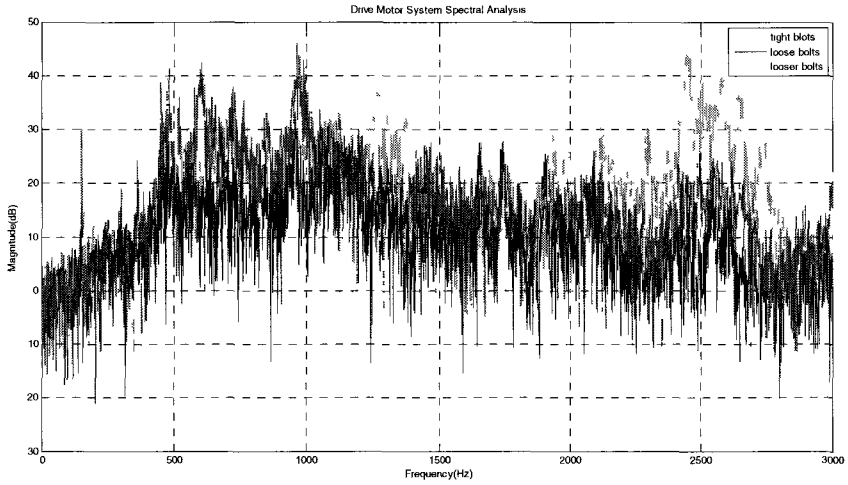


Figure 5.10 1050 rpm at point 6

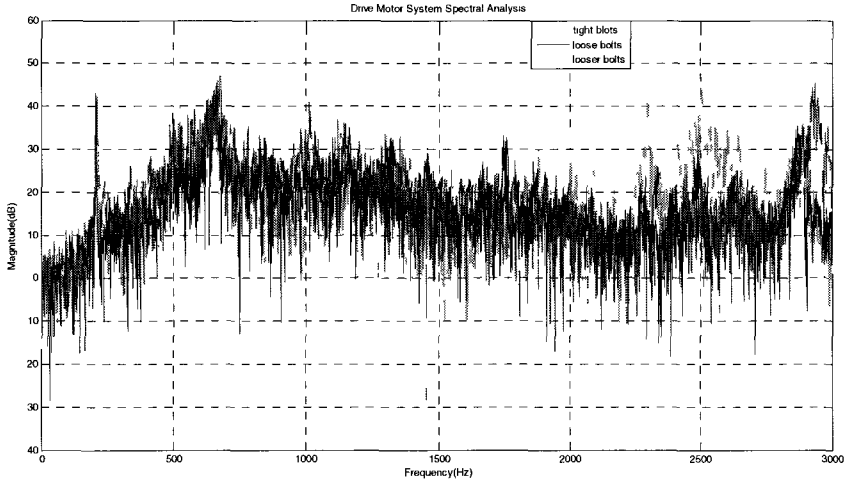


Figure 5.11 1350 rpm at point 6

At point 4 and 5, the results are close to the prediction that more significant amplitudes shifts are present those points than at point 3 and 6.

In addition to the comparison with the prediction, more phenomena due to the defective conditions are visible in the FFT spectrums.

Frequency location shifts due to the change of the conditions can be discerned when the motor was running at low speed, for example at 600 rpm. From the spectrum, we can notice that the peak frequencies under healthy conditions have shifts to the right of about 100 Hz. According to the references, frequency shift can be taken as the evidence for the fault diagnosis, while the speed at 600 rpm illustrate the most clear picture of such pattern.

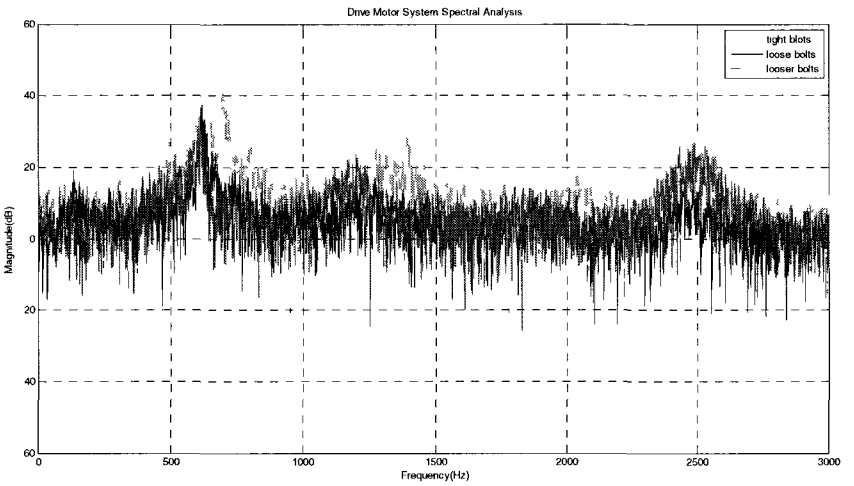


Figure 5.12 600 rpm at point 1

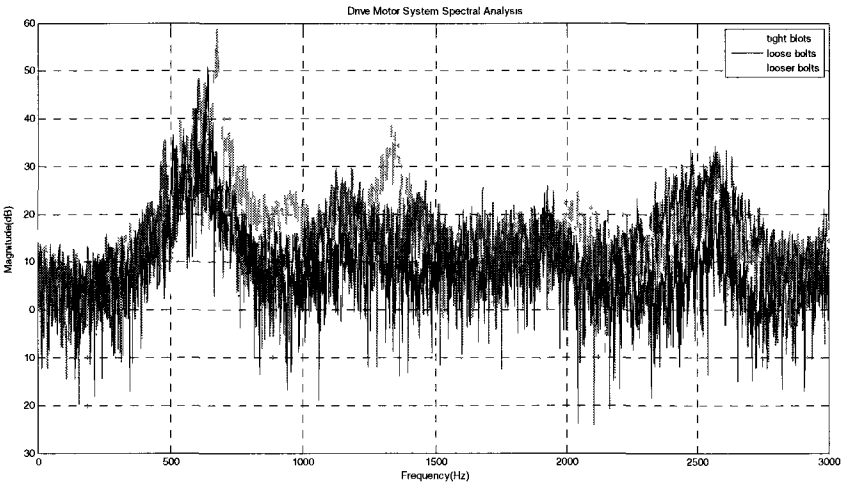


Figure 5.13 600 rpm at point 4

At speeds from 1050 to 3000 rpm, there are less significant changes when compared to spectrums for 600 to 750 rpm, for example, (compare Figure 5.8 and Figure 5.12). Obvious frequency shifts cannot be discerned as easily as those from lower speeds of motor. Amplitude change is the main sign that indicates the defective condition of the structure. However, at the speed of 3300 rpm, frequency shift can be discerned again where peaks are obvious in the spectrums, besides the big amplitude shift due to the defective conditions. In Figure 5.14, we can easily see the changes in the vibration level due to the changes of conditions. Figure 5.15 was taken at point 2, while Figure 5.13 is for point 1, and we can see that the vibrations decrease as assumed in the prediction. At point 3, although there is no obvious amplitude change, the frequency shift can be noticed, and this corresponds to the prediction as well.

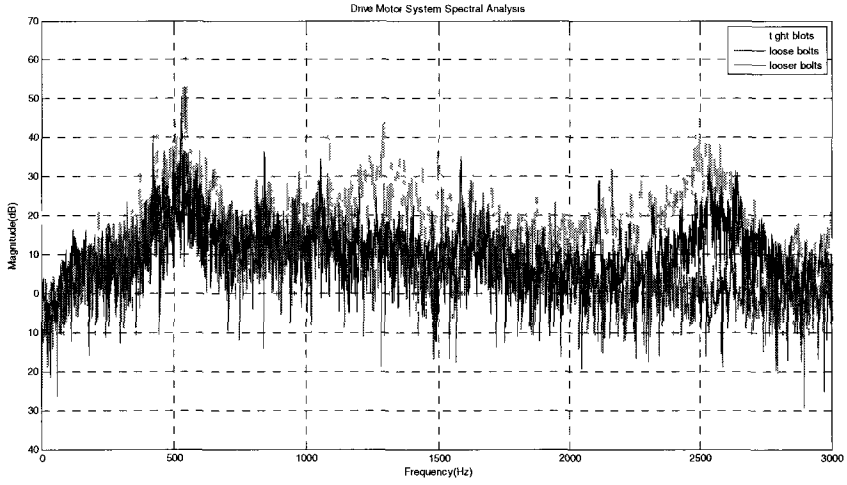


Figure 5.14 3300 rpm at point 1

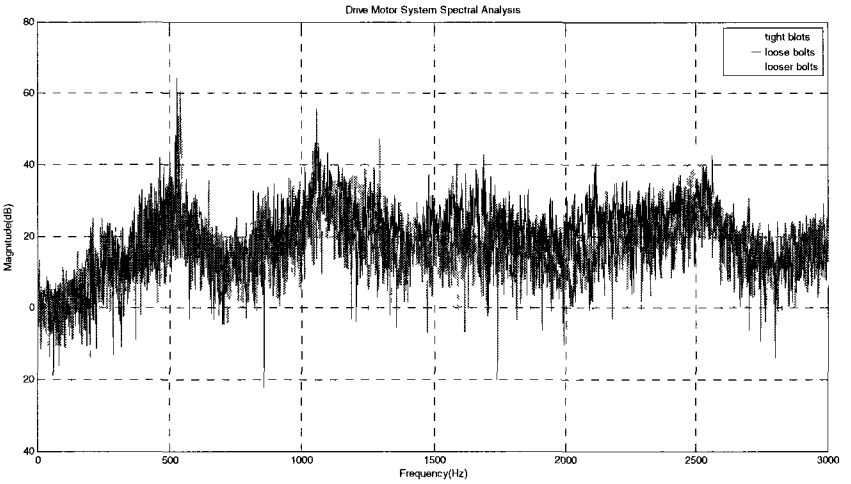


Figure 5.15 3300 rpm at point 2

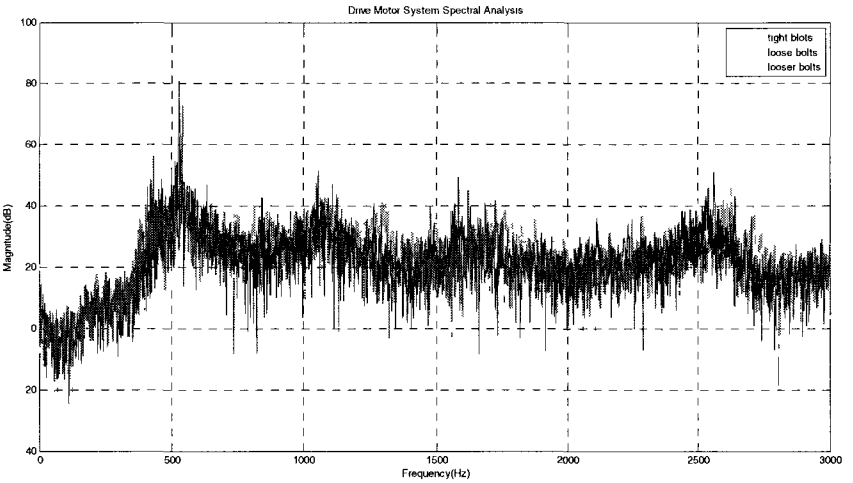


Figure 5.16 3300 rpm at point 3

Another feature that helps us to discern the defective conditions from the healthy ones, besides the amplitude and the frequency location shift, is the wave shape. From the spectrums, we can notice that defective conditions, somewhat loose and significantly loose bolts, share a similar pattern of spectrum, regardless the amplitudes, while for healthy conditions the results are different.

It is easier for us to discern healthy conditions from the defectives ones; however, it is more difficult to differentiate the somewhat loose conditions from more significantly loose conditions from the acoustic signal due to the way bolts are connected to the structure and

due to the measurement equipment accuracy. Looking at the amplitude changes, such as Figure 5.7, we can see that looser bolts have higher amplitude than the loose ones, which fits the assumption because looser conditions are expected to show more significant vibrations. However, such conditions are not visible on all the spectrums.

The motor speed has a significant influence on the accuracy of the results due to the fact that when the excitation frequencies are close or at the structural modal frequencies, structural resonance occurs and this can help to discern the changes resulting from defects. For results at speed values of 600 rpm, 750 rpm, 1050 rpm, 1350 rpm, 3300 rpm more diagnostic indications are visible than from other speeds. In addition, due to the frequency response of the microphone which starts at 80 Hz, all the important frequency response less than 80 Hz is omitted from the spectrums, including the structural resonance frequencies. After analysis the FFT spectrums, we can notice that the first resonant frequency due to the speed of the motor occurs only on speeds higher than 750 rpm, as seen from the first peak in the figures, and this frequency increases proportional to the speed of the motor.

The resonance tube experiment was taken place in the room temperature of around 18 Celsius degree The calculated resonance of the tube according to the stated equation is 330.24 Hz while the measured resonance is around 318 Hz, (refer to Figure 5.17), the first small peak is related to the resonance tube. The difference could be caused by the measurement errors or microphone sensitivity.

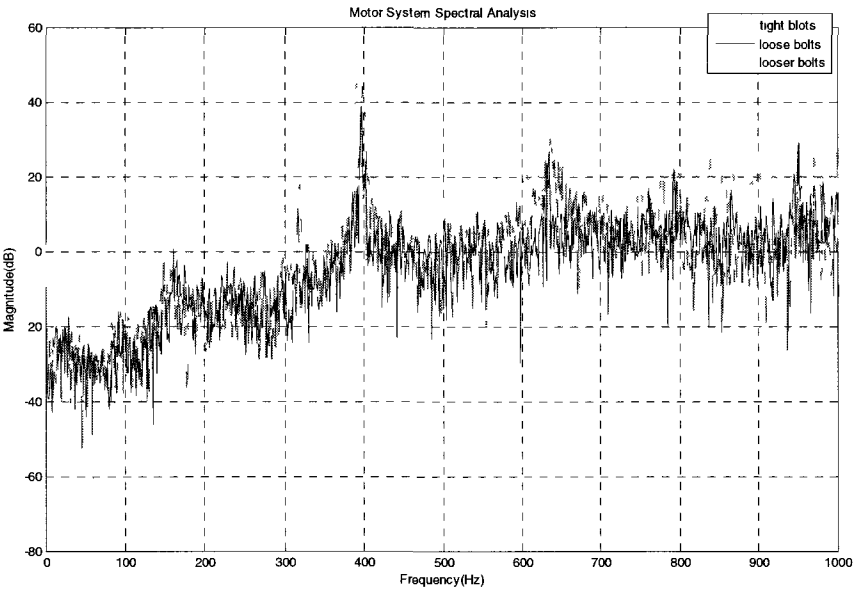


Figure 5.17 2400 rpm at point 2

The list of first resonant frequency set measured from the FFT spectrums from the prior experiment is shown in the

Table 5.1.

| Detected First Resonant Frequency | |
|---|---|
| Motor speed (rpm) | Frequency (Hz) |
| 600 | 600 |
| 750 | 629 |
| 1050 | 152 |
| 1350 | 205 |
| 1800 | 261 |
| 2100 | 315 |
| 2400 | 365 |
| 2700 | 425 |
| 3000 | 476 |
| 3300 | 543 |

Table 5.1 First Resonant Frequency on different Speed

Drive-motor-system with running speed of 2100 rpm and 2400 rpm were chosen for the resonance tube experiment for the reason that their resonance frequencies are closer to the resonant tube than the rest of the frequencies. And for the test of effects in choose a resonance tube at and about the structural resonance frequencies on the experimental results. As attested by the previous studies, the closer the structural frequency to that of the resonance tube, more accurate the measuring results will be.

6 sample locations were chose to collect the acoustic signals on the motor case, which share the same signal processing software and experiment procedure. The experimental results are presented in the Appendix E.

The results measured with the resonance tube contain a clearer picture of defective versus healthy condition. Instead of extending the frequency rang to 3000 Hz, we can recognize the defective situation even within the frequency range up to 1000 Hz. Resonance frequency shift can be detected from most of the spectrums regardless the amplitude shifts due to the defective situation. The experimental results illustrate a more recognizable defects-induced condition compare to the prior experiment, for example, see Figure 5.18, measured at 2100 rpm at point 2. Clearly we can see the resonance frequency shifts due to the loose blots conditions. Compared with the prior experiment result in the frequency rang 0 to 1000 Hz measured at 2100 rpm at point 2 (Figure 5.19  2100 rpm at point 2), frequency shift is not invisible, refer to Appendix F for the previous experiment results at 2100 rpm when ranged limited to 1000 Hz. The resonance tube measurement results illustrate refined diagnostic indications by showing both frequency shifts and amplitude shifts due to the defects.

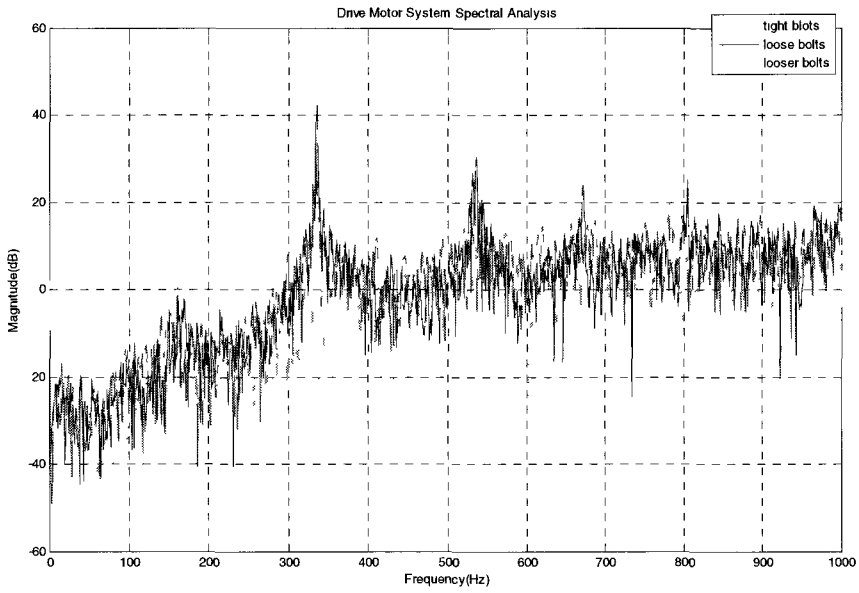


Figure 5.18 2100 rpm at point 2

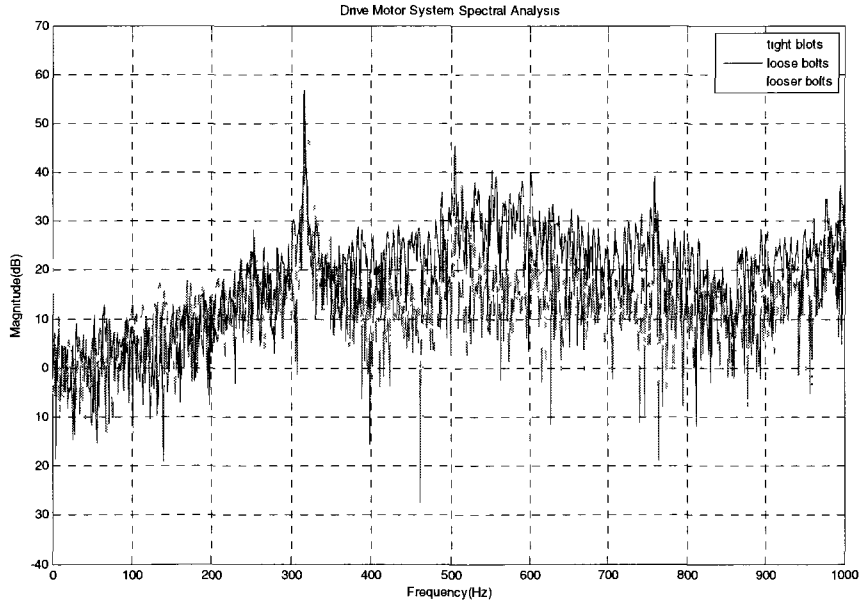


Figure 5.19 2100 rpm at point 2

From the resonance tube measurement results we can also verify the importance of choosing a resonance tube that is close to the structural resonance frequencies. The method improves the prior measuring result by displaying the frequency shift more visible and clarified the defective signature versus the healthy one. By selecting a resonance tube that is close to one

of the structural resonance frequencies can yield a better measurement results. Speed at 2100 rpm has a resonance frequency at 317 Hz and speed at 2400 rpm has it at 365 Hz, while the tube has it at 330 Hz. From the test results we can see more frequency shift due to the defects occur in the 2100 rpm set of experiment than the 2400 rpm's, for example see the comparison of Figure 5.20 and Figure 5.21. More visible frequency shift can be discerned from the spectrum that has the resonance frequency closer to the tube's resonance frequency. From the spectrum measured at 2400 rpm (Figure 5.21) different conditions of figures masking each other and there exists the frequency shift if you look closely but not as obvious as the one at 2100 rpm. Same situation also can be noticed on the rest of the points measured.

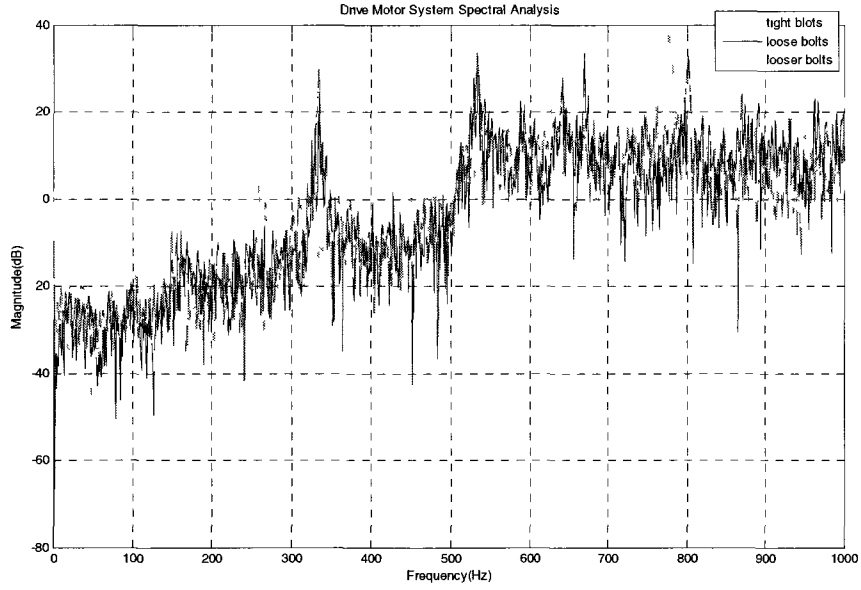


Figure 5.20 2100 rpm at point 3

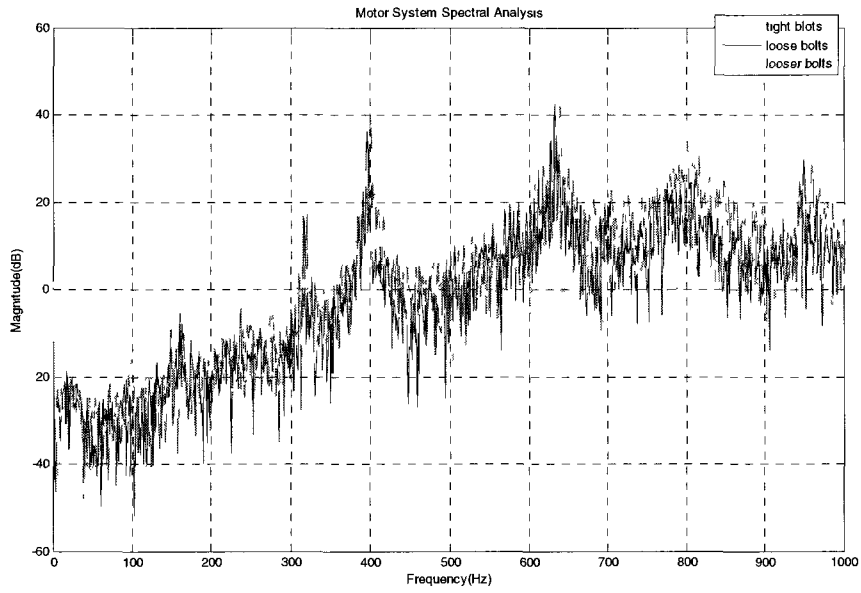


Figure 5.21 2400 rpm at point 3

First acoustic measurement method has illustrated its ability to detect fault condition of the structure and identification of defective versus healthy condition of the structure. With the assistance of resonance tube measurement, we were able to acquire more accurate and refined FFT spectrums as the diagnostic cues to apply condition monitor and fault diagnosis, therefore the employment of the resonance tube completed the entire object-in-the-loop fault diagnosis configuration. The experiments result also reveals the importance of choosing a close-by resonance frequency for the experiment. Nevertheless, we were not able to run the resonance tube test on all the speeds set we obtained from the prior experiment due to the lack of measurement equipment. As a result only limited test results are presented. Additionally, it is still difficult to localize location of the defect simply by observing the spectrums. More prior information about the structure is needed to perform a detailed analysis. We cannot simply diagnose the defects just from one plot and all the measured point related should be taken into consideration for the diagnosis of the fault situation.

The advantage of using acoustic measurement method is that there is no need to mount the microphone on the device for measurement owing to the possibility of remote measurement of acoustic signals. Compared with vibration measurement, this reduces the chances of misalignment of the sensors and the measurement of vibrations due to extraneous sources,

transmitted by the housing structure. [48] However, the sensitivity of the microphone plays an important role in the accuracy of the results because sometimes, small defects of certain component cannot be easily captured. Low-pass filter needs to be employed if the measurement environment involves significant background noise. The points for collecting acoustic data are another important aspect affecting the accuracy. It is advisable to have a prior analysis of the structure and more than one filed points for the measurement to achieve a higher accuracy for the results.

The real-time object-in-the-loop condition monitor and fault diagnosis configuration demonstrates the generic nature of the acoustic measurement method using sensor data. The purpose of the experiment is to identify the faulty conditions in the system and use a conventional fault diagnosis method based on FFT spectrum. FFT is adequate for the case of stationary signals. However, it is not appropriate to apply this algorithm for non-stationary signals as it averages out the frequencies. In that case, a better option, according to the previous studies, would be wavelet transformation. [38] In addition, Acoustic Emission technology proved to be efficient in detecting early stage of defects within materials and in machinery with rotating speed less than 600rpm. [49]

### 5.2.3 ANSYS Simulation Results

In order to understand better experimental results, ANSYS simulations were carried out.

The simulation results from ANSYS are shown in Table 5.2. The changes of the natural frequencies of the structure were evaluated for the structure before and after the defects in the components occurred.

ANSYS was used for modal analysis of the structures that have same shape, mass and material. The results cannot be used to calculate the actual values for the drive motor system the motor system because the model was a rigid body due the lack of the information about the 17-year-old motor used in experiments. The study shows, however, that without constrains in the z direction, natural frequencies from the structural change significantly. This illustrates the natural frequency changes due to the loss of constraint in z direction and confirms qualitatively the results obtained experimentally.

| Results from ANSYS | | |
|---|---|---|
| Frequency Order | Natural Frequency of Healthy Condition (Hz) | Natural Frequency of Unhealthy Condition (Hz) |
| 1 | 104.83 | 0 |
| 2 | 121.55 | 20.2 |
| 3 | 174.3 | 56.65 |
| 4 | 209.18 | 120.39 |
| 5 | 252.23 | 206.73 |
| 6 | 420.07 | 244.8 |
| 7 | 503.37 | 411.93 |
| 8 | 640.66 | 499.33 |
| 9 | 780.72 | 726.24 |
| 10 | 875.43 | 864.09 |

Table 5.2 Comparison of Natural Frequencies under Healthy and Unhealthy Conditions

# 6 Conclusions

Two user-friendly computer-based experimental configurations, subject-in-the-loop and object-in-the-loop, presented in this thesis, serve the purpose acoustic signal processing for voice manipulation and fault diagnosis using the same experimental setup components, the same signal processing procedures and software. The experiments illustrated the possibility of using a personal computer to conduct complex signal processing in a laboratory-induced environment. No professional signal processing equipments is necessary for this study. The experiments are based on the signal processing module available in MATLAB.

## 6.1 Conclusion for the Subject-in-the-loop Experiment

Past research shows that it is possible to compensate the response in voice production when modified signal feedback is applied. The subject-in-the-loop auditory feedback voice manipulation scheme is designed based on the knowledge that natural voice can be modified with the assistance of a voice training system. The same configuration can also be applied to voice analysis, synthesis and recognition and additional contributions to the study of voice formants and in the prediction of the speaker's emotional and psychological state. Formant manipulation was conducted in the first part of the experiment to illustrate the manipulation function in association to frequency based on the voice training principle that formant production is sensitive to auditory feedback. The validity of the manipulation configuration was verified. The second part of real-time audio processing was achieved under MATLAB interface, which confirm the possibility of carrying on an audio processing project without the need of professional acoustic equipment. Moreover, the real-time application compensates the lack of documentations regarding the real-time audio processing serviceability in the MATLAB. It has been long recognized that altered audio feedback has great impact on voice production, as a basis for voice training and language training in foreign languages. How to draw a direct line between this voice perception and production mechanism and how to apply the theoretical knowledge in practice individually still are, however, two unsolved problems. In addition, long term and strictly controlled studies are further needed to investigate the effectiveness of using the proposed configuration for voice training.

## 6.2 Conclusion for the Object-in-the-loop Experiment

The experiment focuses on the interrogation of acoustic signals, acquired from a drive-motor-system, to detect the loss of mechanical integrity, in the investigated case loose bolts. Acoustic measurement is the basis of the diagnosis system for the structure with the assistance of FFT. Post-diagnostic configuration using resonance tube measurement method has refined prior acoustic measurement by showing more accurate and noticeable frequency-shift test results. The application has completed and improved the accuracy of the object-in-the-loop experimental configuration. The experimental characteristics of the natural frequencies related to the structure were confirmed by numerical simulation result using ANSYS. Experimental results demonstrate that loose-bolts conditions can be identified by the changes in the amplitudes and shifts of frequencies and illustrate that acoustic analysis of a simple rotating machine is convenient and reliable for the fault diagnosis and condition monitoring. The proposed object-in-the-loop acoustic measurement configuration is able to detect early development of the damage and configuration has significant potential to be applied in industrial applications to improve manufacturing productivity and reduce the machine downtime and maintenance cost. However, the configuration still lacks the capability to preciously localize defective components and which would be possibly solved by using more accurate measuring device such as infrastructure equipment.

## References

[1]http://education.yahoo.com/reference/dictionary/entry/sound (definition for sound).

[2] http://www.batecho.eu/letters/SpectrumAnalysis.pdf (*A Biologist's introduction to Spectrum Analysis, Raven 1.2 User's Manua*l).

[3] Jerry Whitaker, Blair Benson, *Standard handbook of audio and radio engineering, 2nd ed,* McGraw-Hill, 2004.

[4] Smith, Steven W, *The Scientist and Engineer's Guide to Digital Signal Processing,* California Technical Pub, 1997.

[5] Yukun Liu, Liwei Guo, Qixiang Wang, Guoqing An, Ming Guo, Hao Lian, "Application to induction motor faults diagnosis of the amplitude recovery method combined with FFT", *Mechanical System and Signal Processing,* Vol 24, pp. 2961-2971, 2010.

[6] Anderson, T., "Applications of Speech Based Control." Paper presented at the RTO Lecture Series on Alternative Control Technologies: Human Factor Issues. Ohio, USA, 1998.

[7] http://microblog.routed.net/wp-content/.../an014-understanding-fft-windows.pdf (fft windows)

[8] http://zone.ni.com/devzone/cda//tut/p/id4844 (windows: optimizing FFTs using window Functions)

[9] http://www.irdbalancing.com/downloads/SIGCOND2_2.pdf (*Signal procesing for effctive vibration analysis*).

[10] http://personal.cityu.edu.hk/~bsapplec/thehuman.htm (the human ear).

[11] http://en.wikipedia.org/wiki/Voice_organ (voice organ).

[12] Maria Nordenberg, Johan Sundberg, "Effect on LTAS of vocal loudness Variation" ,

*Logoped Phoniatr Vocol,* Vol. 29, pp.182-191, 2004.

[13] Zangger Borch, D. and Sundberg,J, "Spectral distribution of solo voice and accompaniment in pop music" , *Logoped Phoniatr Vocol,* Vol. 27, pp.37-41, 2002.

[14] Kristine Tanner, Nelson Roy, Andrea Ash, Eugene H.BudeR, "Spectral Moments of the Long-term-average Spectrum: Sensitive indices of Voice Change after Therapy?", *The Voice Foundation,* Vol. 19, pp.211-222, June 2005.

[15] Tomi Kinnunen, Ville Hautamaki, Pasi Franti, "On the use of Long-term Average Spectrum in Automatic speaker Recognition", presented in Singapore at International Symposium on Chinese Spoken Language Processing, 2006, pp. 559-567.

[16] Manwa L.Ng, Hanjun Liu, Qin Zhao, Paul K.Y.Lam, "Long-term average spectral characteristics of Cantonese alaryngeal speech", *Auris Nasus Larynx,* Vol. 36, pp.571-577, October 2009.

[17] Leino, Timo, "Long-term Average Spectrum in Screening of Voice Quality in Speech: Untrained Male University Students", *The Voice Foundation,* Vol. 23, pp.671-676, November 2009.

[18] http://www.mathworks.com/help/toolbox/signal/spectrum.html (spectrum estimation).

[19] http://www.wavemetrics.com/products/igorpro/dataanalysis/signalprocessing/powerspectra.htm. (powerspectra).

[20] Elena A. Antipova, Suzanne C. Purdy, Marjorie Blakeley, Shelley Williams, "Effects of altered audiotry feedback (AAF) on stuttering frequency during monologue speech production", *Journal of Fluency Disorders,* Vol. 33 , pp.274-290, 2008.

[21] Joy Armson, Sheila Foote and Colleen Witt,Joseph Kalinowski and Andrew Stuart, "Effect of frequency altered feedback and audience size on stuttering: *European Journal of Disorder of Communication,* Vol. 32 , pp.359-366, 1997.

[22] http://www.research.kevinghanrahan.com (*Kevin Hanrahan's Research Papers*).

[23] David W., Purcell, Kevin G. Munhall, "Compensation following real-time manipulation of Formants in isolated vowels", *Acoustical Society of America*, Vol. 119, pp.2288-2297, April 2006.

[24] http://www.rane.com/note158.html (*Understanding Acoustic feedbacks and suppresors).*

[25] Michelle Lincoln, Ann Packman, Mark Onslow, "Altered auditory feedback and the treatment of stuttering: A review", *Journal of Fluency Disorders,* Vol. 31, pp.71-89, 2006.

[26] Theresa A. Burnett, Jill E. Senner, Charles R. Larson, "Voice responses to Pitch-shifted auditory feedback: a Preliminary Study", *Journal of Voice,* Vol. 11, pp.202-211, June 1997.

[27] Ewen N. MacDonald, Robyn Goldberg, Kevin G. Munhall, "Compensations in response to real-time formant perturbations of different magnitudes", *Acoustical Society of America*, Vol. 127, pp.1059-1068, Feburary, 2010.

[28] Yong xia, Hong Hao, "Statistical damage identification of structures with frequency changes", *Journal of sound and vibration,* Vol. 263, pp.853-870,12 June 2003.

[29] Ali Md. Younus, Achmad Widodo and Bo-suk Yang, "Evaluation of thermograph image data for machine fault diagnosis", *Nondestructive Testing and Evaluation,* Vol. 25, pp. 231-247,.02 June, 2010

[30] Thomson, Willam T, *Theory of Vibration with Applications,*$4^{th}$ ed, Prince Hall, 1993.

[31] Hong Joo Lee, Shi Uk Chung ,Sang Moon Hwang, "Noise source identification of a BLDC motor", *Journal of Mechanical Science and Technology,* Vol. 22, pp.708-713, 2008.

[32] Yukun Liu, Liwei Guo, Qixiang Wang, Guoqing An, Ming Guo, Hao Lian, "Application to induction motor faults diagnosis of the amplitude recovery method combined with FFT" *Mechanical System and Signal Processing,* Vol. 24, pp.2961-2971,

November 2010.

[33] O.S.Salawu, "Detection of structural damage through changes in frequency: a review", *Engineering Structures,* Vol. 19, pp.718-723, September 1997,

[34] Juan Dai, L.L. Philip Chen, Xiao-Yan Xu, Ying Huang, Peng Hu, Chi-Ping Hu, and Tao Wu, "Machinery Vibration Signals Analysis and Monitoring for Fault Diagnosis and Process Control", *Advanced Intelligent Computing Theories and Applications. With Aspects of Theoretical and Methodological Issues",* Vol. 5226, 2008.

[35] http://adt.lib.swin.edu.au/uploads/approved/adtVSWT20050715.092623/public/05chapter4.pdf *(review of vibration analysis techniques).*

[36] N.Tandon, A. Choudhury, "A review of vibration and acoustic measurement method for the detection of defects in rolling element bearings", *Tribology International,* Vol 32, pp. 469-480, 1999.

[37] Ignolf Hertlin, Detleve Schultze, Acoustic Resonance Testing: the upcoming volume oriented DNT method, prestend at Pan-American Conference for nondestructive testing, Rio de Janeiro, June 2-6, 2003.

[38] F. Martinus, D.W. Herrin, and A.F. Seybert, "Practical Consideration in reconstructing the surface vibration using inverse numerical Acoustics", *Society of Automotive Engineers.* Vol. 112, pp.1633-1640, 2003.

[39] Jian-Da Wu, Chao-Qin Chuang, "Fault idiagnosis of internal combustion engines using visual dot patterns of acoustic and vibration signals", *NDT & E International,* Vol. 38, pp.605-614 , December,2005.

[40] Katsuhiko Shibata, Atsushi Takahashi And Takuya Shirai, "Fault Diagnosis of Rotating Machinery through Visualization of Sound Signals", *Mechanical system and Signal Processing.* Vol. 14, pp.229-241, March 2000.

[41] Jason A. Tiurville, Kevin J. Reilly, and Frank H. Guenther, "Neural Mechanisms underlying auditory feedback control of speech", *NeuroImage,* Vol. 39, pp.1429-1443, 1 February 2008.

[42] http://www.mathworks.com/products/xpctarget/xPC_Target_Supported_Ethernet_Chipsets.pdf.( xPC target supported ethernet card).

[43] *Xpc Target, User's Guide Version 3*,The MATHWORKS Inc, 1999-2003.

[44] JD, Halderman, *Diagnosis and troubleshooting of automotive electrical, electronics, and computer system,5th ed,* Prentice Hall, 1997.

[45] Sujata S. Agashe, Sagar D. Birkar, Priti P. Rege,"Acoustic signal analysis for fault identification of a control valve", *ICGST-ACSE Journal,* Vol. 8, pp.29-36, January 2009.

[46] http://en.wikipedia.org/wiki/Acoustic_resonance (acoustic resonance).

[47] http://www.unitechinc.com/pdf/IntroductiontoTimeWaveformAnalysis.pdf (wave analysis)

[48] S.Devi, Dr. L. Siva Kumar, N.R. Shanker and K. Prabakaran, "A comparative Study between Vibration and Acoustic Signals in HTC cooling pump and chilling pump", *IACSIT international Journal of Engineering and Technology,* Vol. 2, pp.273-2,77, June 2010.

[49] D.Mba, "Applicability of acoustic emission to monitoring the mechanical integrity of bolted structures in low speed rotating machinery: case study", *NDT&E International,* Vol. 35, pp.293-300, 2002.

# Appendix A: Important Specifications for the Experimental Apparatus

Microphone:

Type: Dynamic; Directivity: Unidirectional; Sensitivity: -74 dB+/-3 dB; Frequency Response: 80~14,000 Hz

Frequency Response Curve

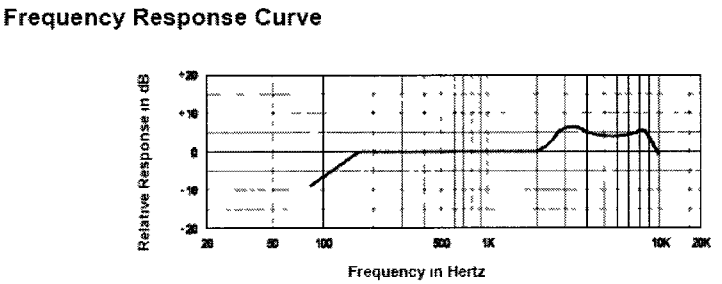


M-Audio

Name: M-audio Fast track Pro; Maximum Sample Rate: 48 KHz; Sample depth: 24 bits

Latency: 80 samples to 2048 samples

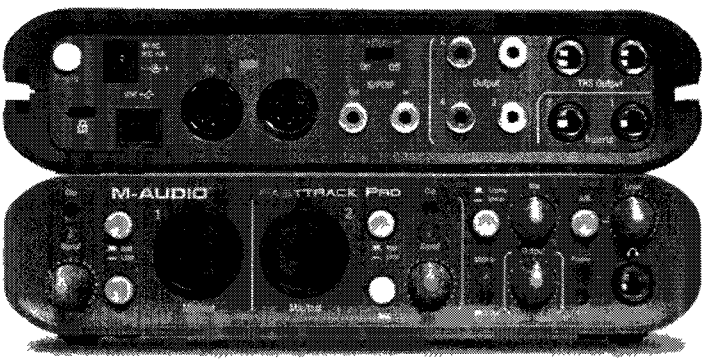

## Appendix B: MATLAB Code for the Subject-in-the-loop Experiment

```
% The following codes are designed for the subject-in-the-loop voice manipulation GUI. %
The codes start with "%" sign are the explanations

function varargout = lin1stguimodel2(varargin)

%LIN1STGUIMODEL2 M-file for lin1stguimodel2.fig

%      LIN1STGUIMODEL2, by itself, creates a new LIN1STGUIMODEL2 or raises the
existing

%      singleton*.

%      H = LIN1STGUIMODEL2 returns the handle to a new LIN1STGUIMODEL2 or the
handle to

%      the existing singleton*.

%      LIN1STGUIMODEL2('Property','Value',...) creates a new LIN1STGUIMODEL2
using the given property value pairs. Unrecognized properties are passed via

%      varargin to lin1stguimodel2_OpeningFcn.  This calling syntax produces a

%      warning when there is an existing singleton*.

%      LIN1STGUIMODEL2('CALLBACK')    and
LIN1STGUIMODEL2('CALLBACK',hObject,...) call the

%      local function named CALLBACK in LIN1STGUIMODEL2.M with the given input

%      arguments.

%      *See GUI Options on GUIDE's Tools menu.  Choose "GUI allows only one

%      instance to run (singleton)".

% See also: GUIDE, GUIDATA, GUIHANDLES
```

```
% Edit the above text to modify the response to help lin1stguimodel2

% Last Modified by GUIDE v2.5 12-Aug-2010 14:50:59

% Begin initialization code - DO NOT EDIT

gui_Singleton = 1;

gui_State = struct('gui_Name',       mfilename, ...

                   'gui_Singleton',  gui_Singleton, ...

                   'gui_OpeningFcn', @lin1stguimodel2_OpeningFcn, ...

                   'gui_OutputFcn',  @lin1stguimodel2_OutputFcn, ...

                   'gui_LayoutFcn',  [], ...

                   'gui_Callback',   []);

if nargin && ischar(varargin{1})

  gui_State.gui_Callback = str2func(varargin{1});

end

if nargout

   [varargout{1:nargout}] = gui_mainfcn(gui_State, varargin{:});

else

   gui_mainfcn(gui_State, varargin{:});

end

% End initialization code - DO NOT EDIT
```

```
% --- Executes just before lin1stguimodel2 is made visible.
function lin1stguimodel2_OpeningFcn(hObject, eventdata, handles, varargin)
% This function has no output args, see OutputFcn.
% hObject    handle to figure
% eventdata  reserved - to be defined in a future version of MATLAB
% handles    structure with handles and user data (see GUIDATA)
% varargin   unrecognized PropertyName/PropertyValue pairs from the
%   command line (see VARARGIN)
% Choose default command line output for lin1stguimodel2
handles.output = hObject;
% Update handles structure
guidata(hObject, handles);
% UIWAIT makes lin1stguimodel2 wait for user response (see UIRESUME)
% uiwait(handles.figure1);
% --- Outputs from this function are returned to the command line.
function varargout = lin1stguimodel2_OutputFcn(hObject, eventdata, handles)
% varargout  cell array for returning output args (see VARARGOUT);
% hObject    handle to figure
% eventdata  reserved - to be defined in a future version of MATLAB
% handles    structure with handles and user data (see GUIDATA)
```

```
% Get default command line output from handles structure
varargout{1} = handles.output;
% --- Executes on button press in pushbutton1.
function pushbutton1_Callback(hObject, eventdata, handles)
% hObject    handle to pushbutton1 (see GCBO)
% eventdata  reserved - to be defined in a future version of MATLAB
% handles    structure with handles and user data (see GUIDATA)
open('recordwithRTblock.mdl')
% --- Executes on button press in pushbutton2.
function pushbutton2_Callback(hObject, eventdata, handles)
% hObject    handle to pushbutton2 (see GCBO)
% eventdata  reserved - to be defined in a future version of MATLAB
% handles    structure with handles and user data (see GUIDATA)
open('low_pass.mdl')
% --- Executes on button press in pushbutton3.
function pushbutton3_Callback(hObject, eventdata, handles)
% hObject    handle to pushbutton3 (see GCBO)
% eventdata  reserved - to be defined in a future version of MATLAB
% handles    structure with handles and user data (see GUIDATA)
open('high_pass.mdl')
```

```
% --- Executes on button press in pushbutton4.
function pushbutton4_Callback(hObject, eventdata, handles)
% hObject    handle to pushbutton4 (see GCBO)
% eventdata  reserved - to be defined in a future version of MATLAB
% handles    structure with handles and user data (see GUIDATA)
open('band_pass.mdl')
% --- Executes on button press in pushbutton5.
function pushbutton5_Callback(hObject, eventdata, handles)
% hObject    handle to pushbutton5 (see GCBO)
% eventdata  reserved - to be defined in a future version of MATLAB
% handles    structure with handles and user data (see GUIDATA)
open('band_stop.mdl')
% --- Executes on button press in pushbutton6.
function pushbutton6_Callback(hObject, eventdata, handles)
% hObject    handle to pushbutton6 (see GCBO)
% eventdata  reserved - to be defined in a future version of MATLAB
% handles    structure with handles and user data (see GUIDATA)
% Generation of the LTAS spectrum using periodogram method with Hamming window
[filename,path]=uigetfile('*.wav','Desktop')
file=fullfile(path,filename);
figure;
```

```
[y,Fs,nbits]=wavread(file);
h2 = spectrum.periodogram('hamming');
hopts = psdopts(h2,y);  % Default options based on the signal x
set(hopts,'Fs',Fs,'SpectrumType','onesided','CenterDC',false);
plot (msspectrum(h2,y,hopts))
xlim([0 2]);
ylim([-150 -50]);
% --- Executes on button press in pushbutton8.
function pushbutton8_Callback(hObject, eventdata, handles)
% hObject    handle to pushbutton8 (see GCBO)
% eventdata  reserved - to be defined in a future version of MATLAB
% handles    structure with handles and user data (see GUIDATA)
% --- Executes during object creation, after setting all properties.
function pushbutton8_CreateFcn(hObject, eventdata, handles)
% hObject    handle to pushbutton8 (see GCBO)
% eventdata  reserved - to be defined in a future version of MATLAB
% handles    empty - handles not created until after all CreateFcns called
open('P1000669.JPG')
% --- Executes on mouse press over figure background, over a disabled or
% --- inactive control, or over an axes background.
function figure1_WindowButtonDownFcn(hObject, eventdata, handles)
```

```
% hObject    handle to figure1 (see GCBO)
% eventdata  reserved - to be defined in a future version of MATLAB
% handles    structure with handles and user data (see GUIDATA)
function edit2_Callback(hObject, eventdata, handles)
% hObject    handle to edit2 (see GCBO)
% eventdata  reserved - to be defined in a future version of MATLAB
% handles    structure with handles and user data (see GUIDATA)
% Hints: get(hObject,'String') returns contents of edit2 as text
%        str2double(get(hObject,'String')) returns contents of edit2 as a double
% --- Executes during object creation, after setting all properties.
function edit2_CreateFcn(hObject, eventdata, handles)
% hObject    handle to edit2 (see GCBO)
% eventdata  reserved - to be defined in a future version of MATLAB
% handles    empty - handles not created until after all CreateFcns called
% Hint: edit controls usually have a white background on Windows.
%       See ISPC and COMPUTER.
if ispc && isequal(get(hObject,'BackgroundColor'),
get(0,'defaultUicontrolBackgroundColor'))
   set(hObject,'BackgroundColor','white');
end
```

## Appendix C: MATLAB Code for the Object-in-the-loop Experiment

### a. Signal collecting

```
% the program is use for measuring the frequency response of the motor

% system. The recording part is lasted for 5 seconds. Afterwards, the audio

% data information is sent to collect magnitude and frequency information to

% form the frequency-magnitude plot. The program can also check the

% fundamental frequency of the system.

clear all;

close all;

clc;

ai=analoginput('winsound');  %create the analog input

chans=addchannel(ai,1);  %add 2 channels

daqmem(ai);  %use daqmem to check the system

duration=5;  %the recording is set to be 5 seconds

set(ai,'SampleRate',44100);  %set sampl erate at 441000

actualrate=get(ai,'SampleRate');  %actual rate equals to sample rate;sample rate is the number of samples acquire per second

set(ai,'SamplesPerTrigger',duration*actualrate)  %Samplepertrigger is the number of samples to acquire to each analog input channel to each trigger

set(ai,'TriggerType','manual') % TriggerType is set to Manual

blocksize=get(ai,'SamplesPerTrigger');

Fs=actualrate  %set the sample rate equals to the actual rate we get from the matlab
```

```
start(ai)    %Date Acquisition will be running as soon as the start commend is issued

trigger(ai)

wait(ai,duration+1)    %Wait till data acquisition completes or time-out elapses. If time-elapse occurs, an error comes out, Adding 1 second to the duration allow some margin for the time out

data=getdata(ai);

N=length(data);

win=hanning(N);

data1 = win.*data;

[f,mag]=daqdocfft(data1,Fs,blocksize);    %daqdocfft outputs the data in frequency-magnitude plot

xfft=abs(fft(data1));

index=find(xfft==0);   %avoid taking log of 0

xfft(index)=1e-17;

mag=20*log10(xfft);

mag=mag(1:floor(blocksize/2));

f=(0:length(mag)-1*Fs/blocksize);

f=f(:);

plot(f,mag,'red')

axis([0,1000,-60,60])

xlabel('Frequency(Hz)')   %set x axis to be shown as frequency

ylabel('Magnitude(dB)')   %set y axis to be shown as magnitude
```

```
title('Motor System Spectral Analysis')

[ymax,maxindex]=max(mag);   %find out actual fundamental frequency

grid;

maxfre=f(maxindex)

delete(ai)
```

## b. Data post-processing

```
% The following codes explains how to merge 3 different figures containing with different conditions into one figure.

get(gca,'Children'); % collecting figure data

fig=get(get(gca,'Children'));

x1=fig.XData; % x and y coordinates data

y1=fig.YData;

get(gca,'Children');

fig=get(get(gca,'Children'));

x2=fig.XData;

y2=fig.YData;

get(gca,'Children');

fig=get(get(gca,'Children'));

x3=fig.XData;

y3=fig.YData;
```

```
plot(x,y,'green',x1,y1,'blue',x2,y2,'red')

xlabel('Frequency(Hz)')   %set x axis to be shown as frequency

ylabel('Magnitude(dB)')   %set y axis to be shown as magnitude

title('Motor System Spectral Analysis')

grid on

legend('healthy','unhealthy-loose-bolts','unhealthy-looser-blots')
```

# Appendix D: Results for the Object-in-the-loop Experiment

1) 6-point acoustic measurement experiment results from 600 rpm :

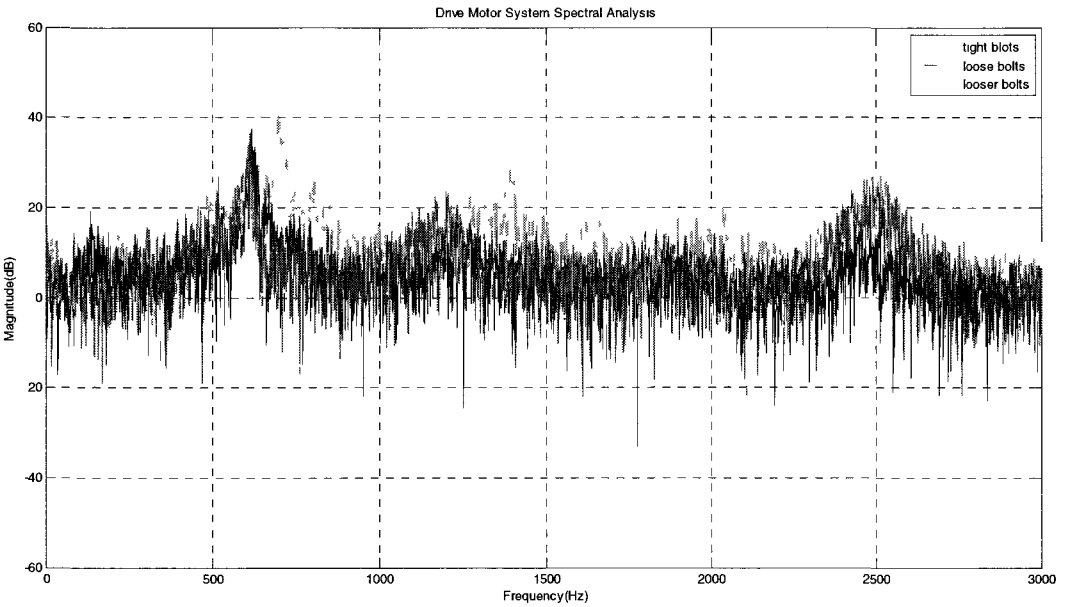


Fig. 1 600 rpm at point1

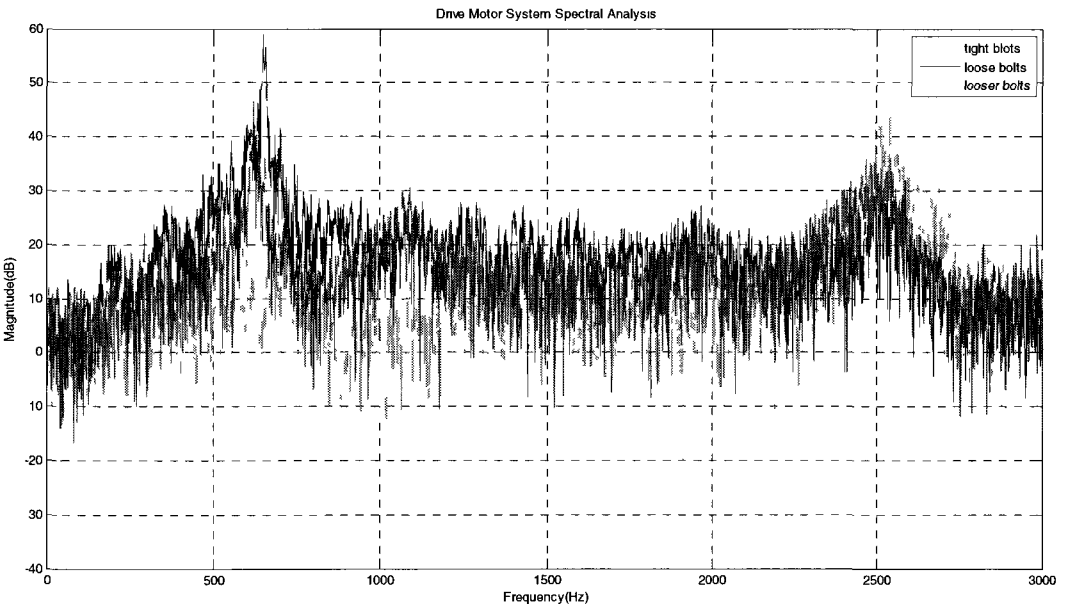


Fig. 2 600 rpm at point 2

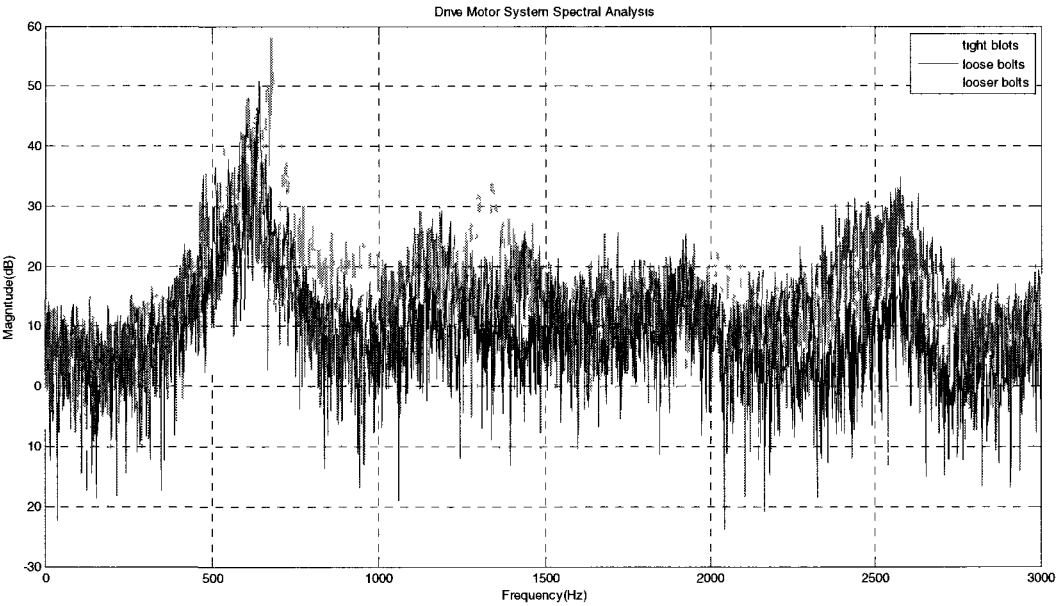


Fig.3 600 rpm at point 3

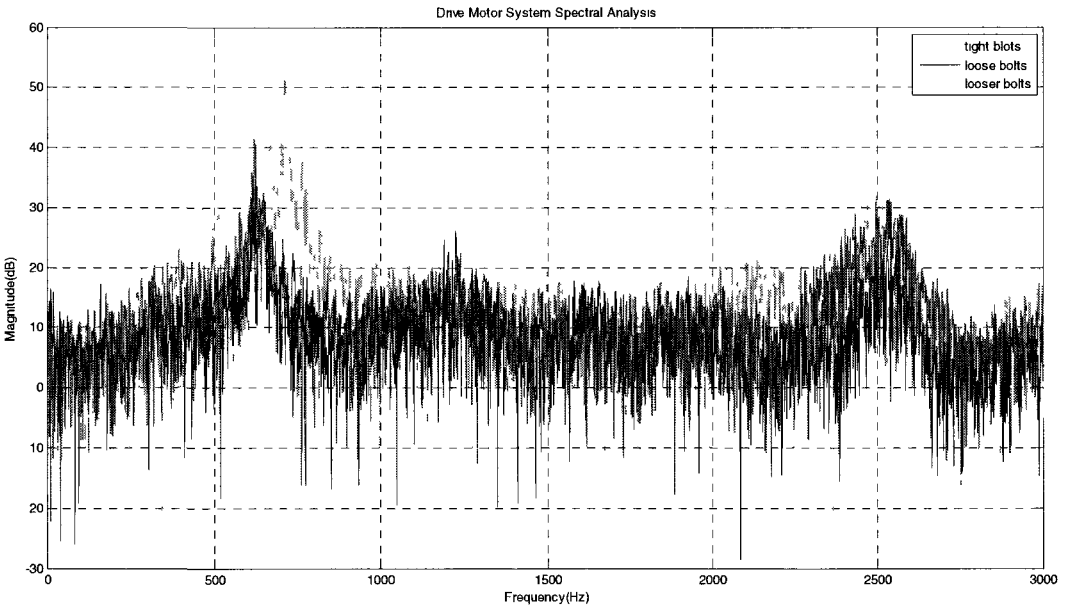


Fig. 4 600 rpm at point 4

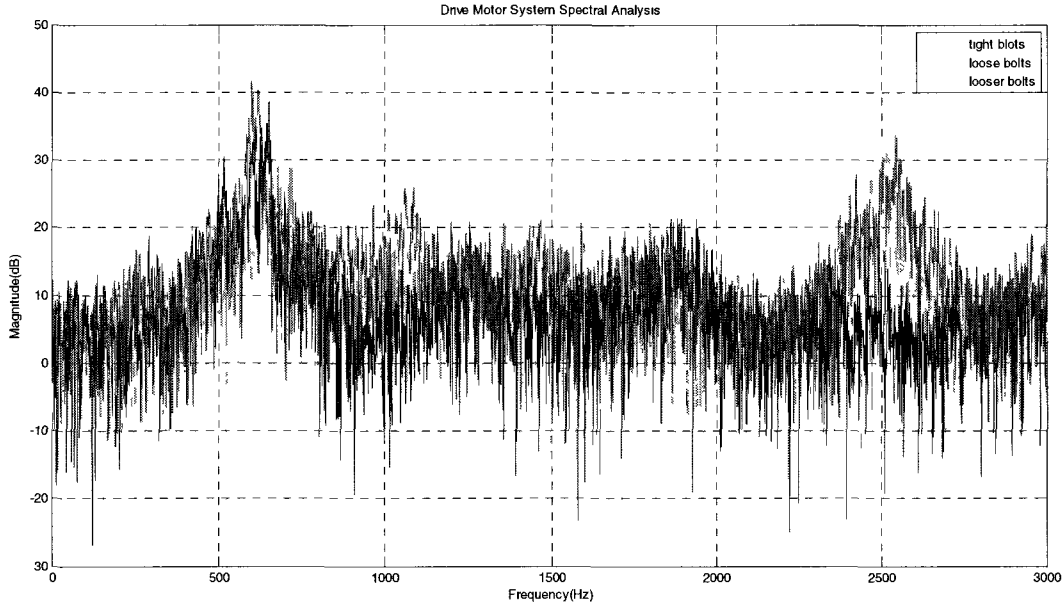


Fig. 5 600 rpm at point 5

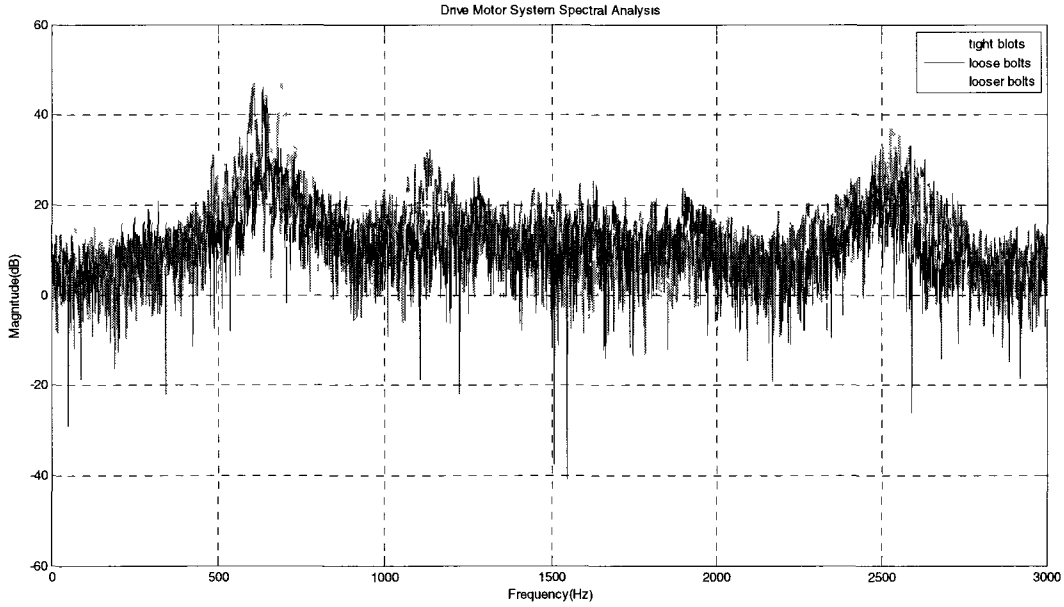


Fig. 6 600 rpm at point 6

2) 6-point acoustic measurement experiment results from 750 rpm :

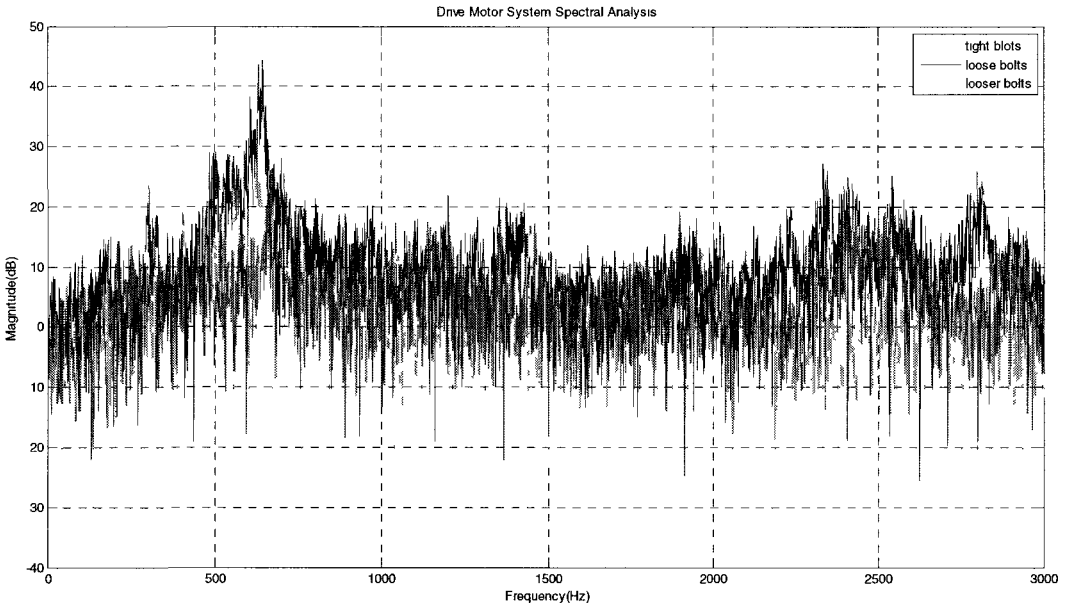


Fig. 5.7 750 rpm at point1

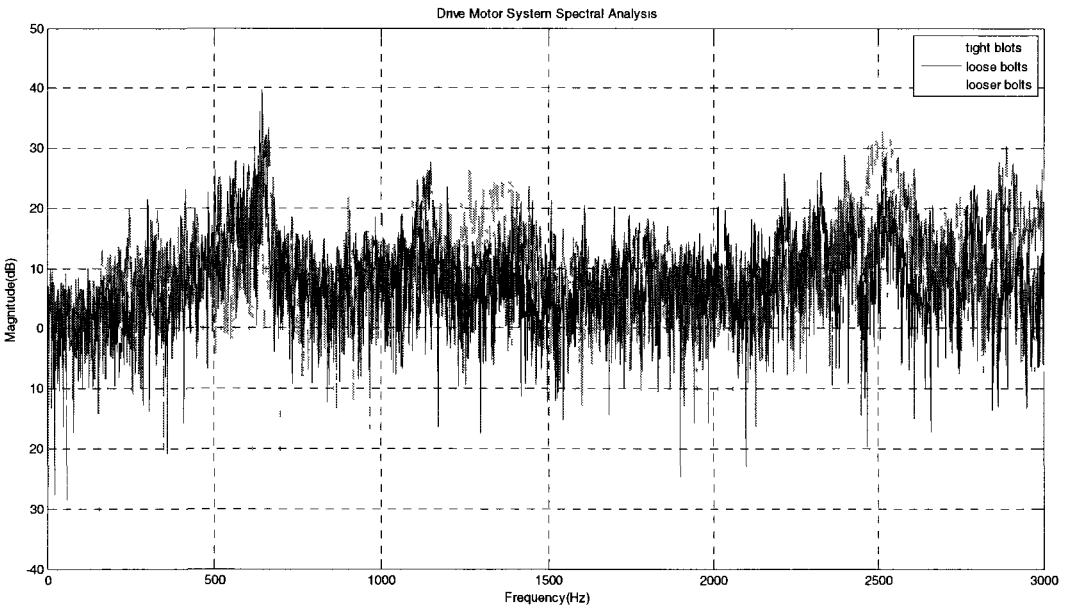


Fig. 8 750 rpm at point 2

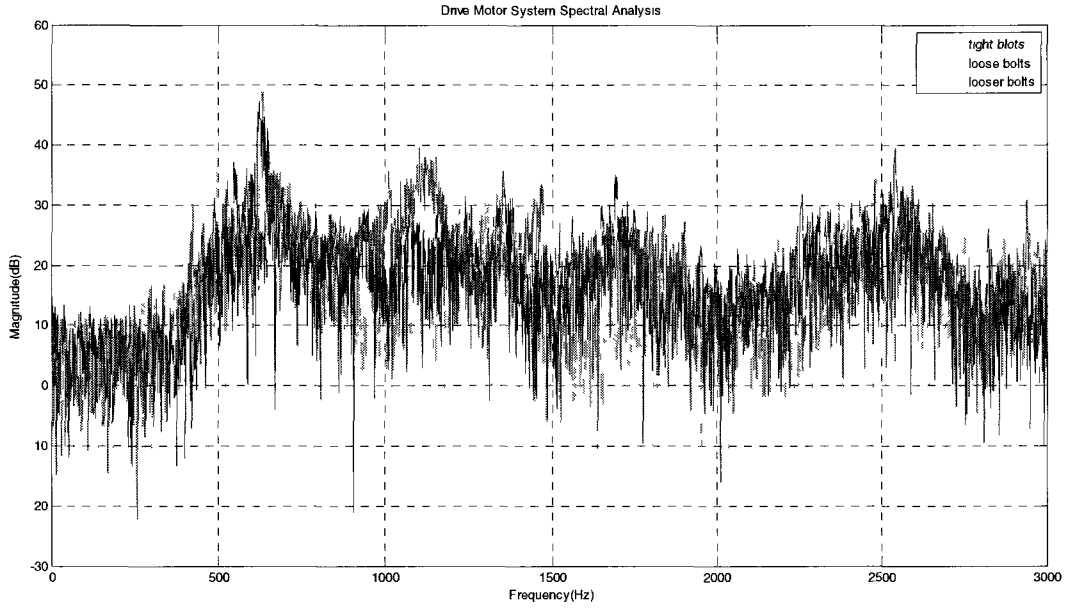


Fig. 9 750 rpm at point 3

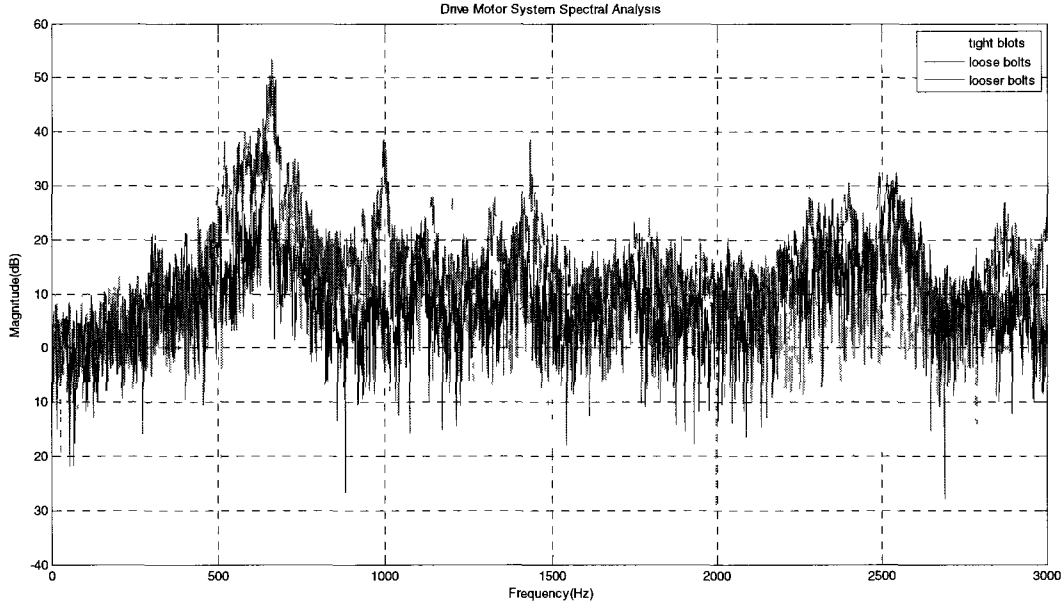


Fig. 10 750 rpm at point 4

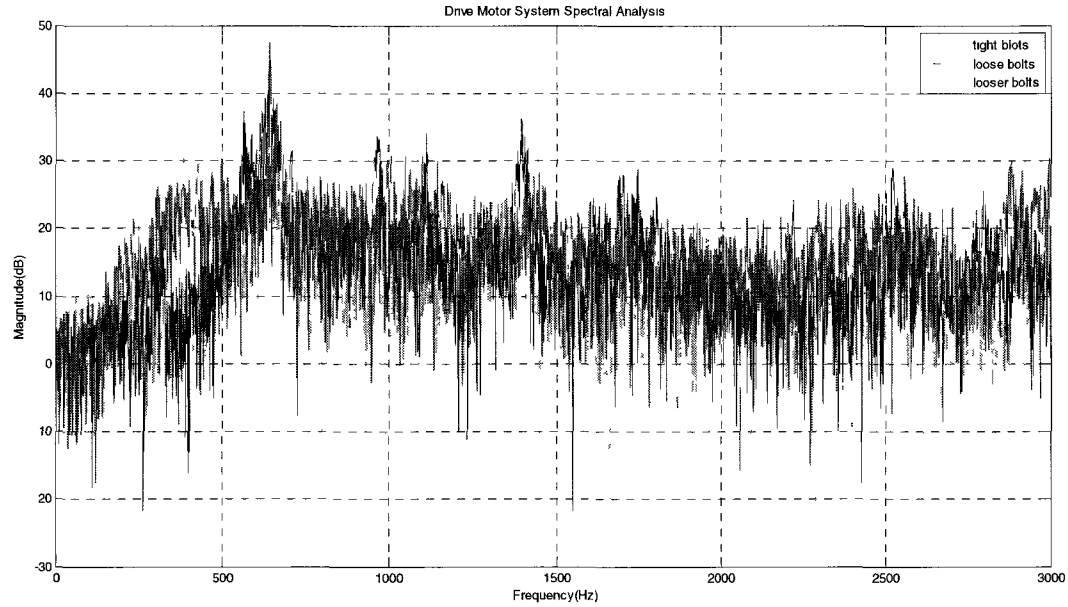


Fig. 11 750 rpm at point 5

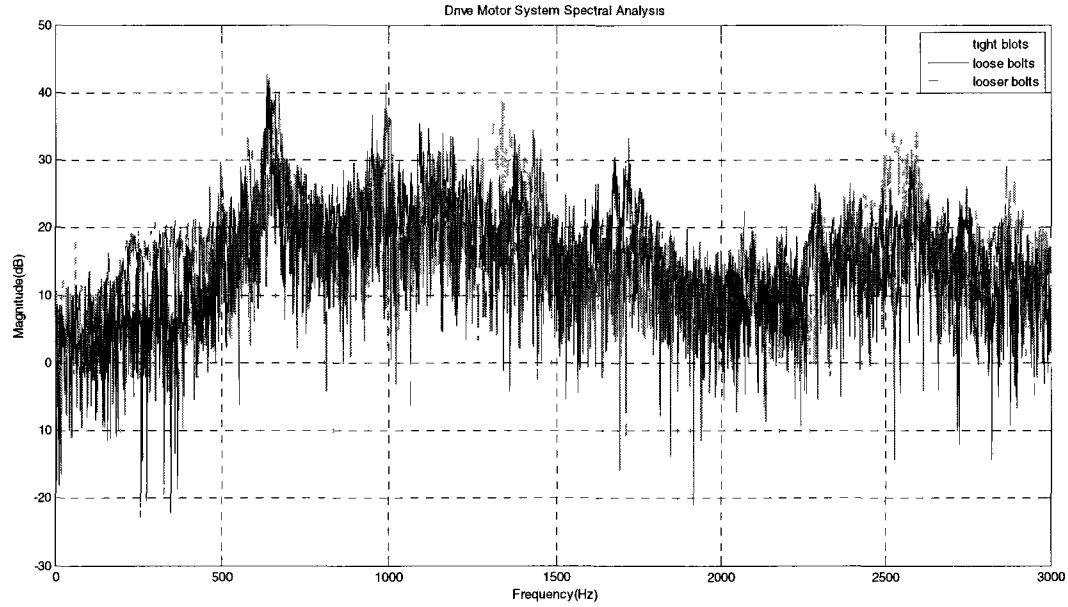


Fig. 12 750 rpm at point 6

3) 6-point acoustic measurement experiment results from 1050 rpm :

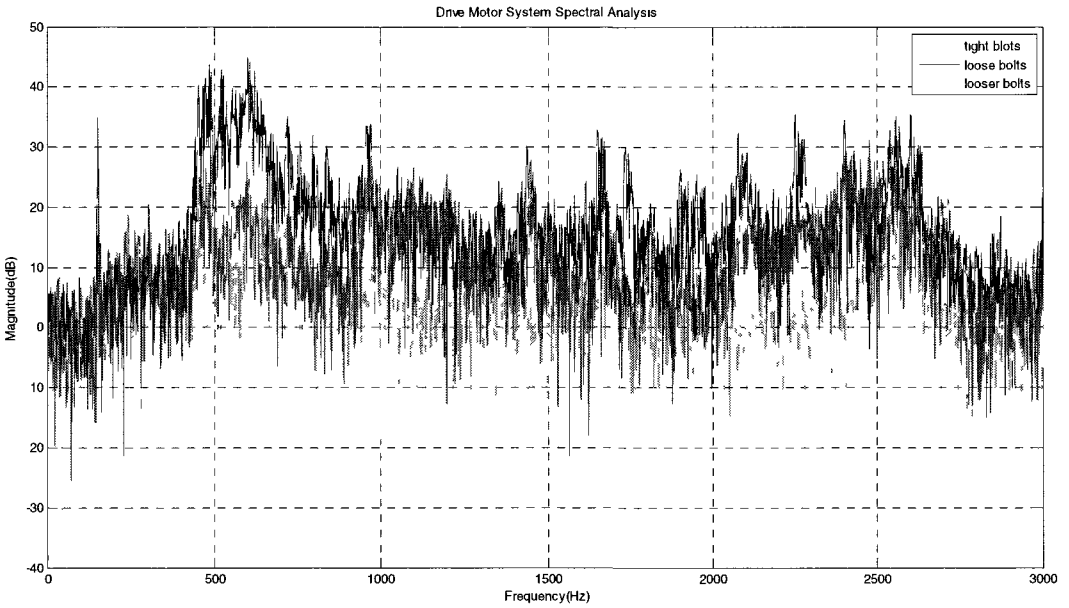


Fig. 13 1050 rpm at point 1

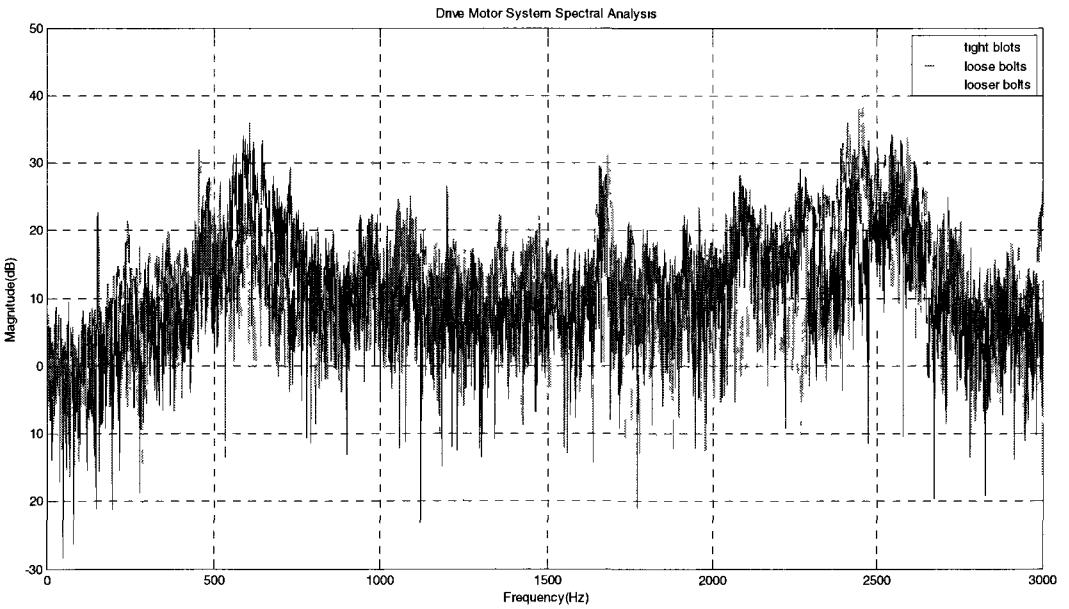


Fig. 14 1050 rpm at point 2

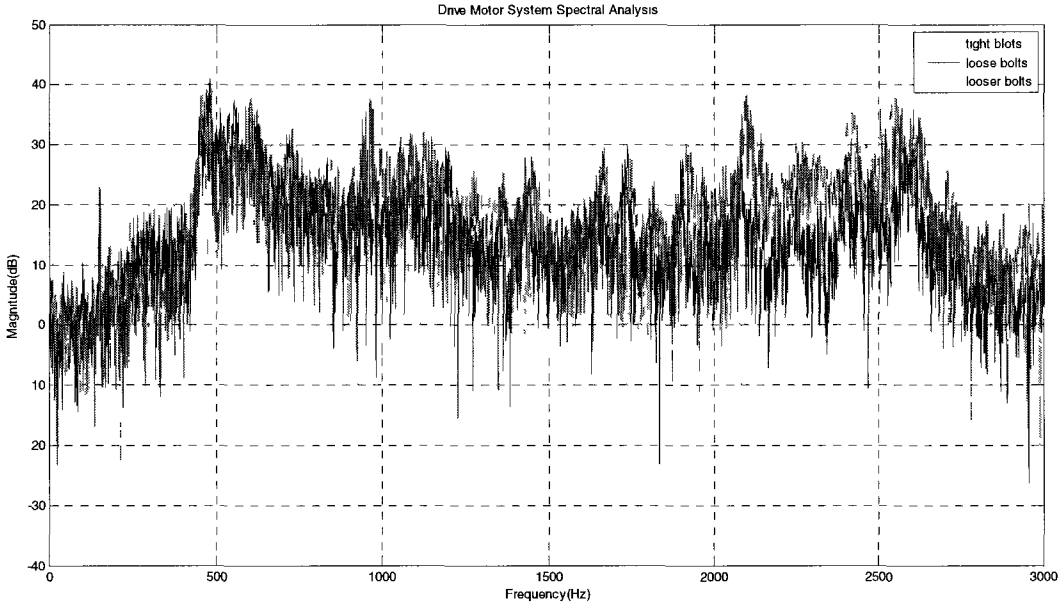


Fig. 15 1050 rpm at point 3

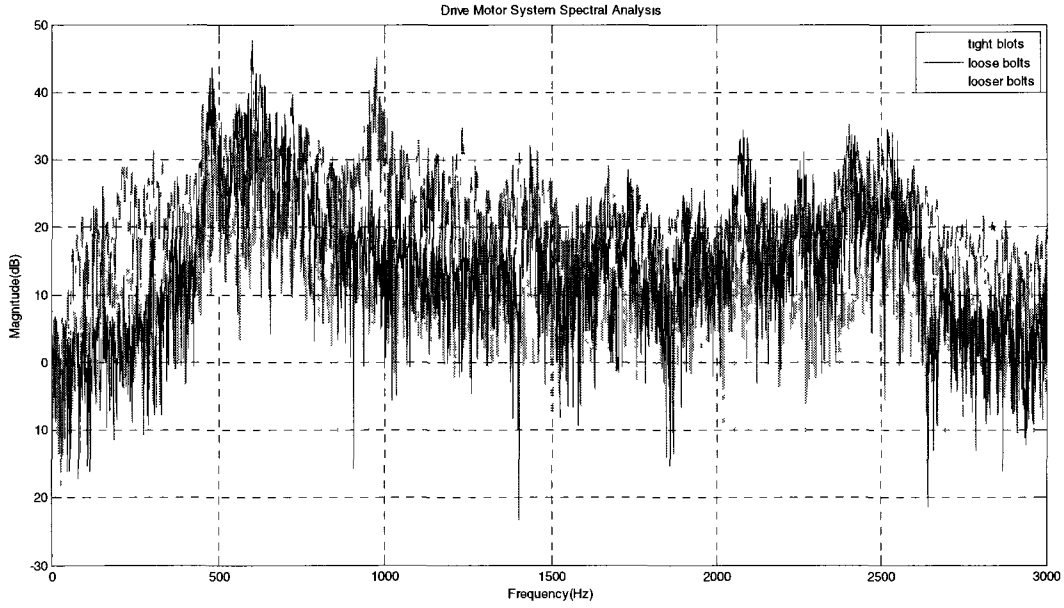


Fig. 16 1050 rpm at point 4

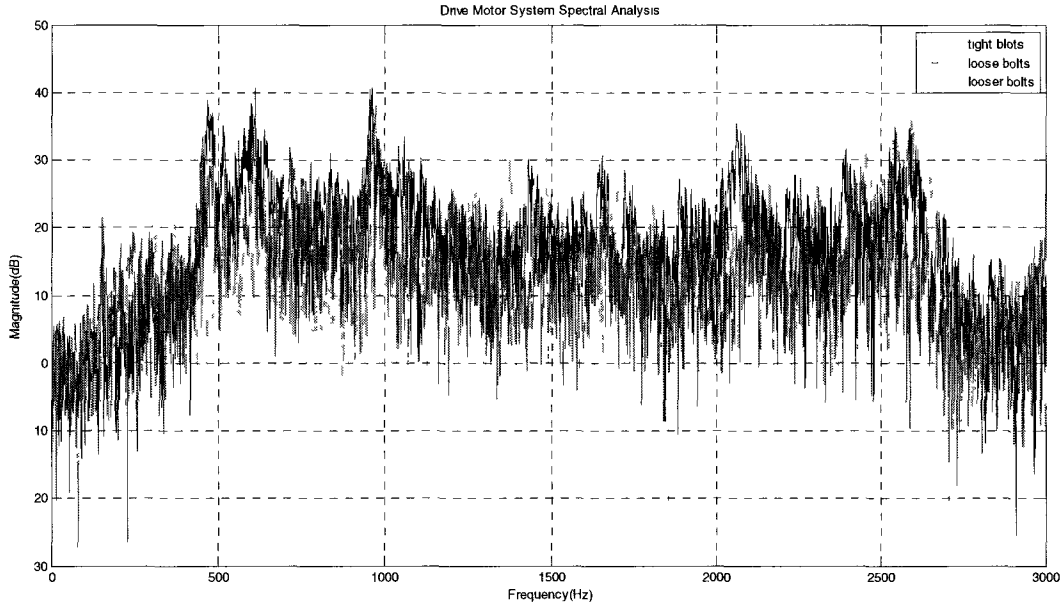


Fig. 17 1050 rpm at point 5

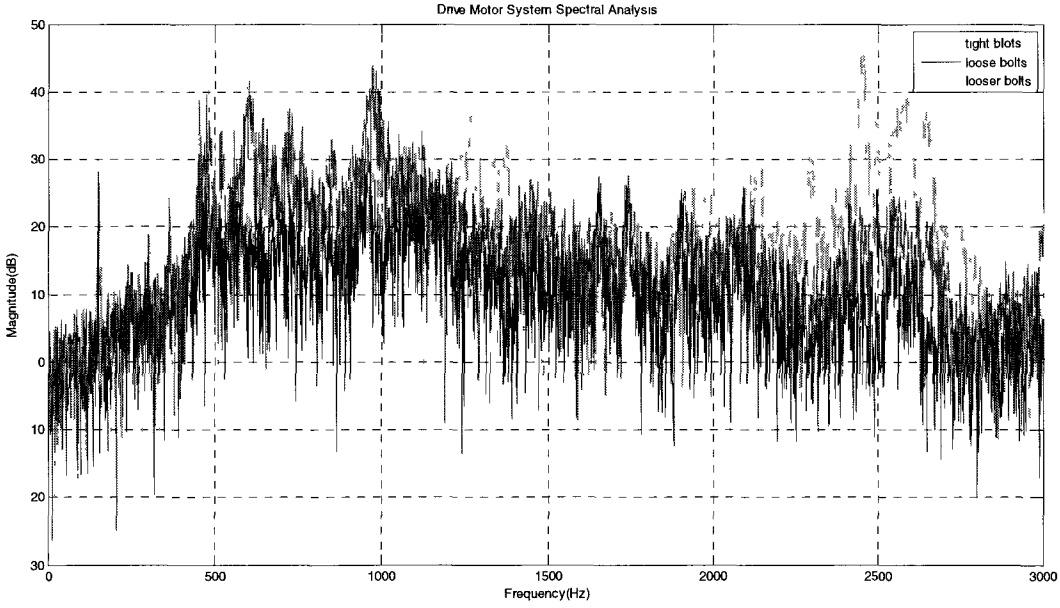


Fig. 18 1050 rpm at point 6

4) 6-point acoustic measurement experiment results from1350 rpm :

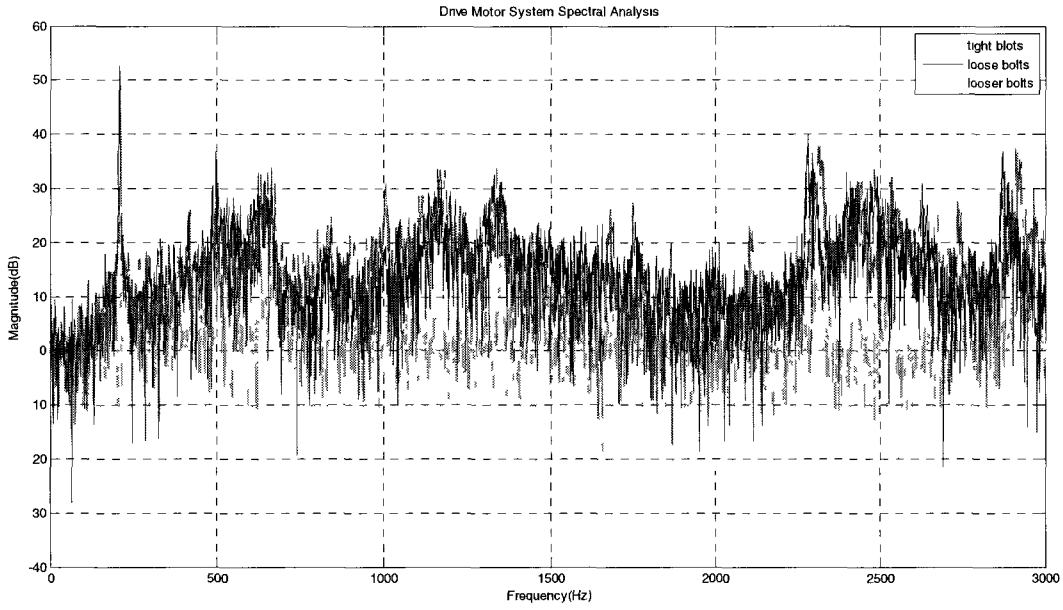


Fig. 19 1350 rpm at point 1

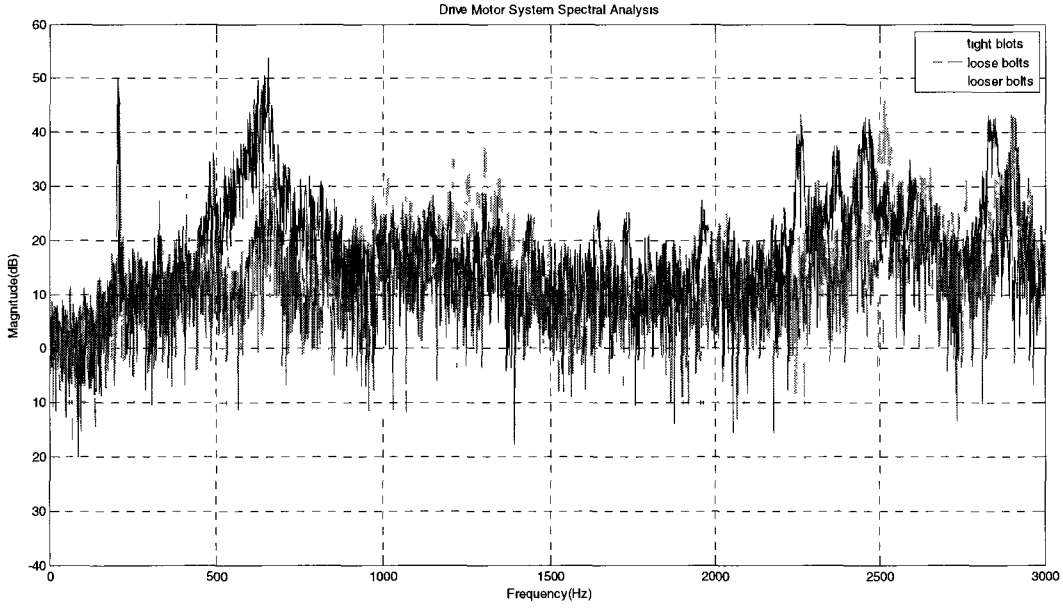


Fig. 20 1350 rpm at point 2

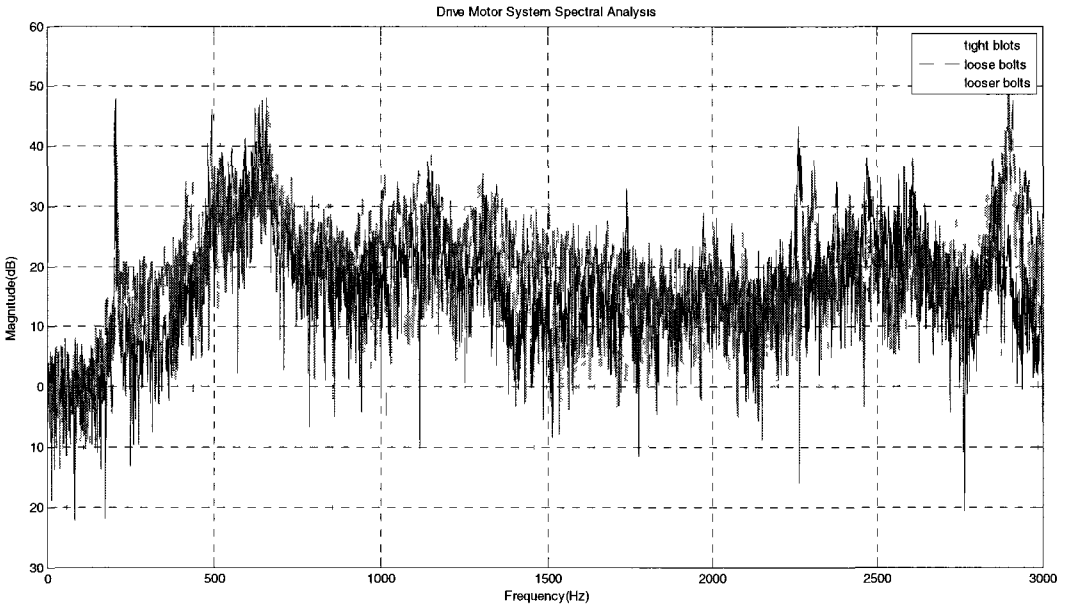


Fig. 21 1350 rpm at point 3

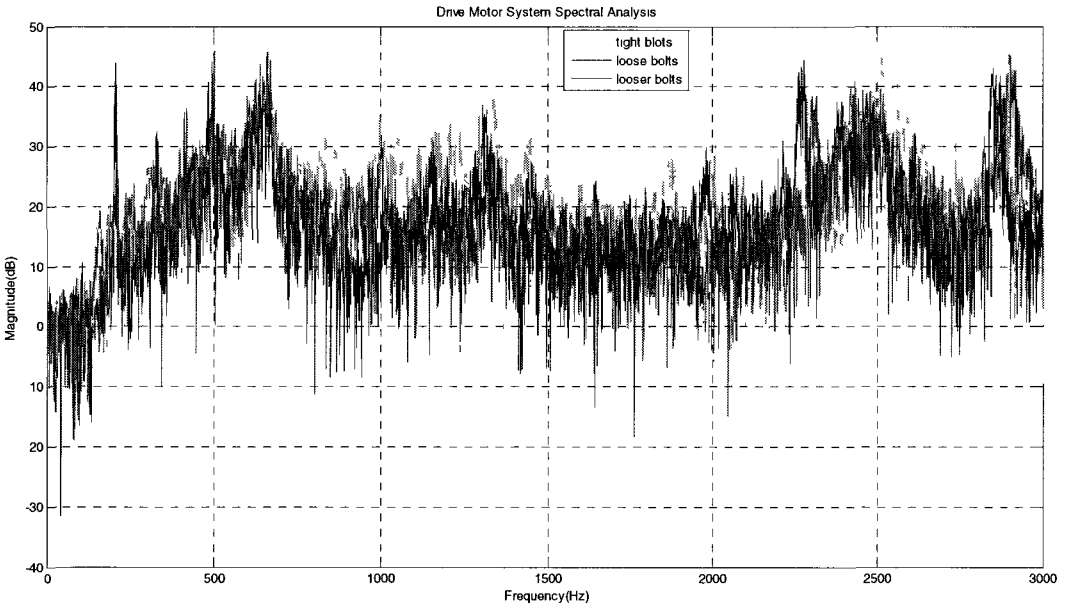


Fig. 22 1350 rpm at point 4

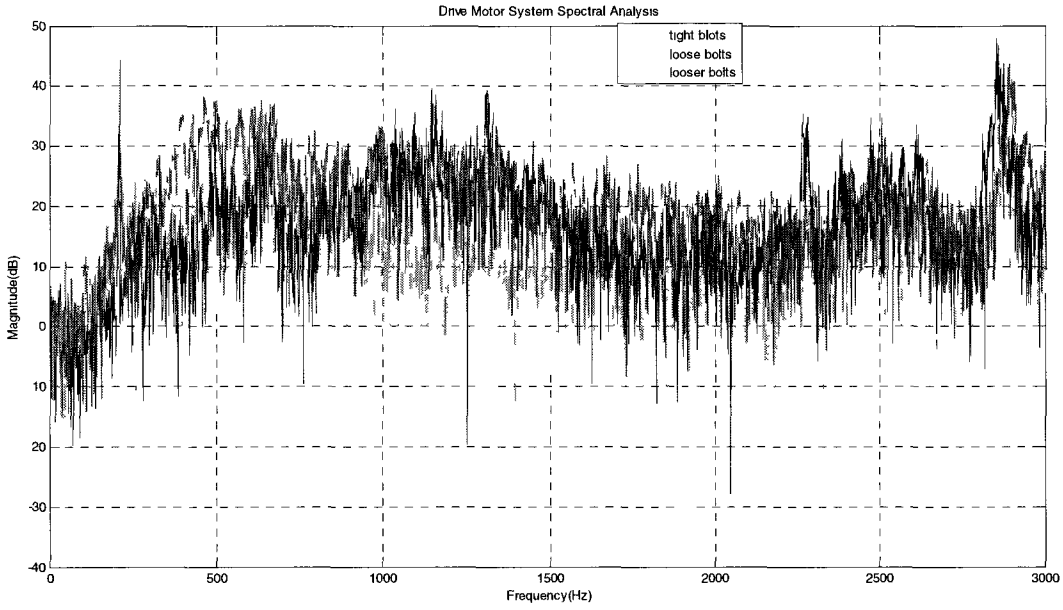


Fig. 23 1350 rpm at point 5

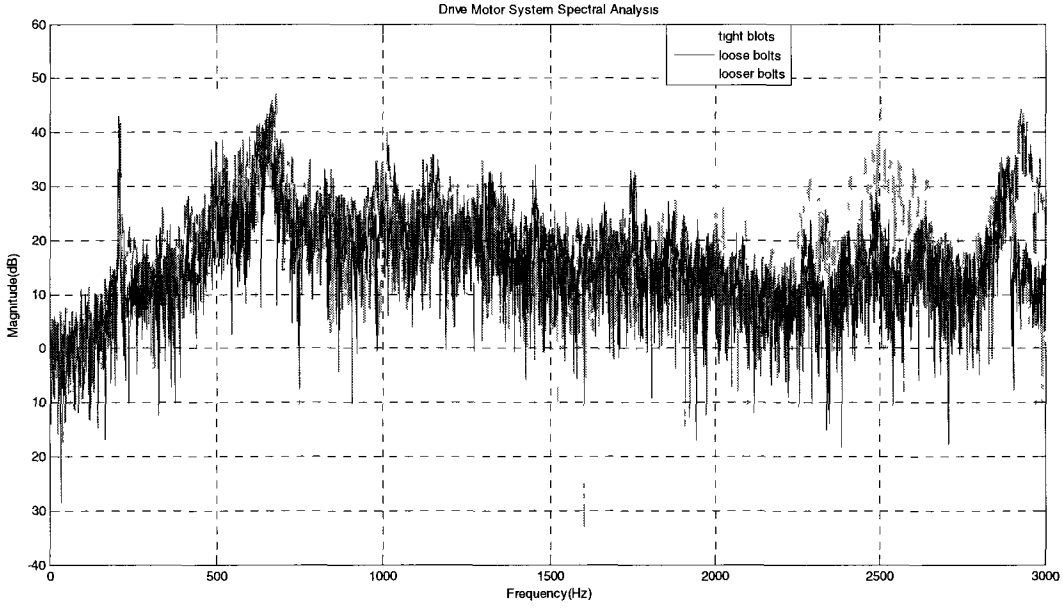


Fig. 24 1350 rpm at point 6

5) 6-point acoustic measurement experiment results from1800 rpm :

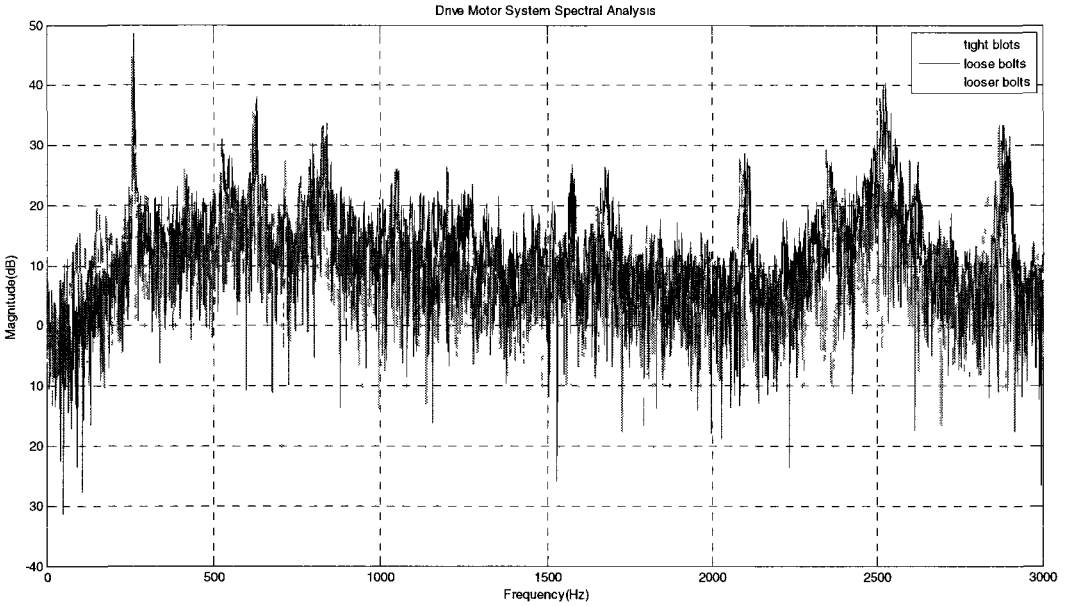


Fig. 25 1800 rpm at point 1

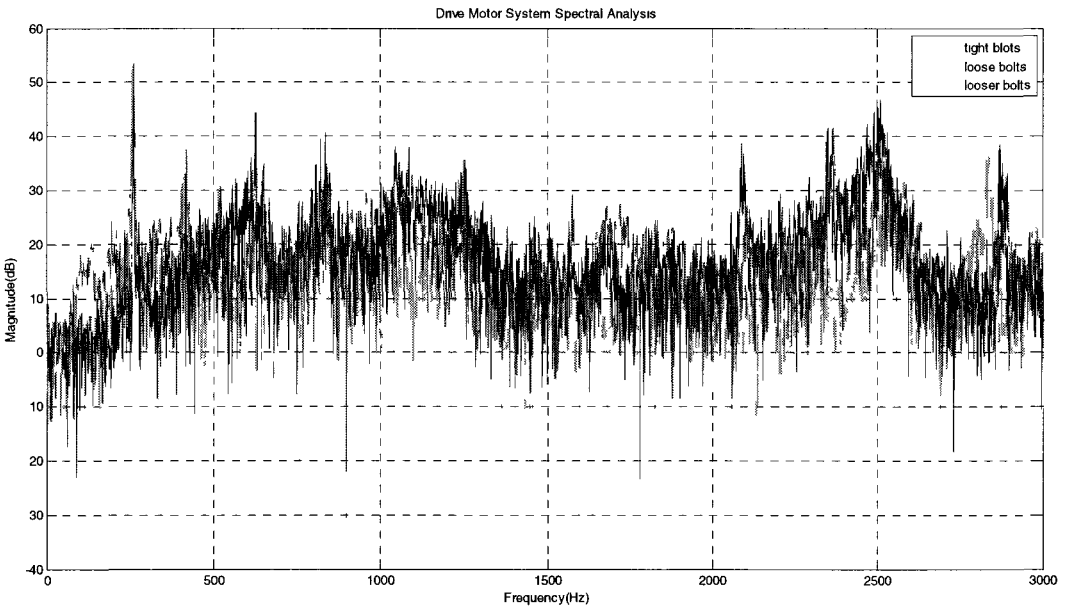


Fig. 26 1800 rpm at point 2

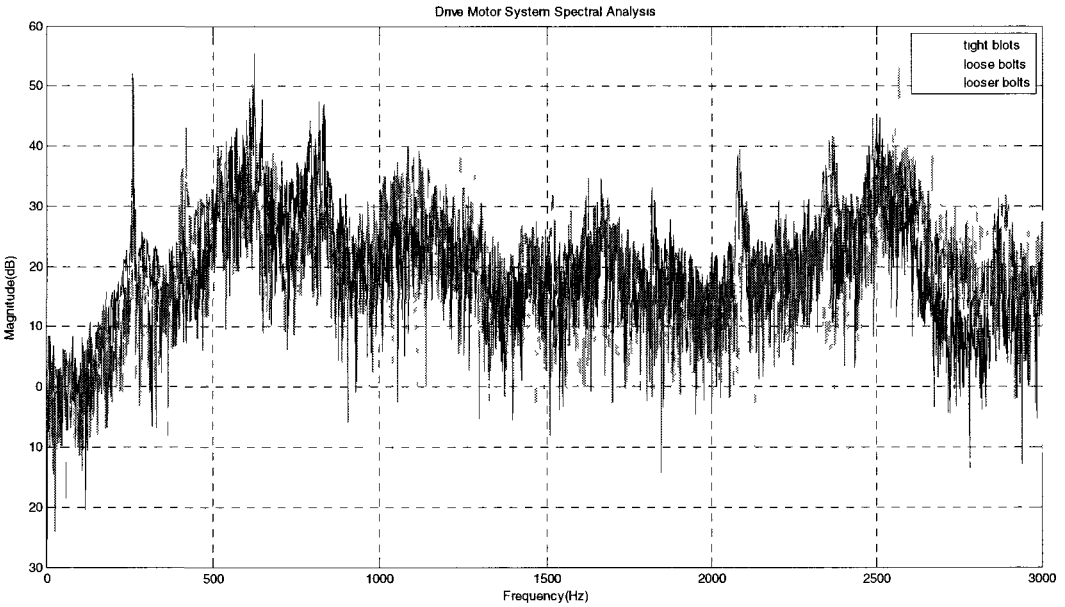


Fig. 27 1800 rpmat point 3

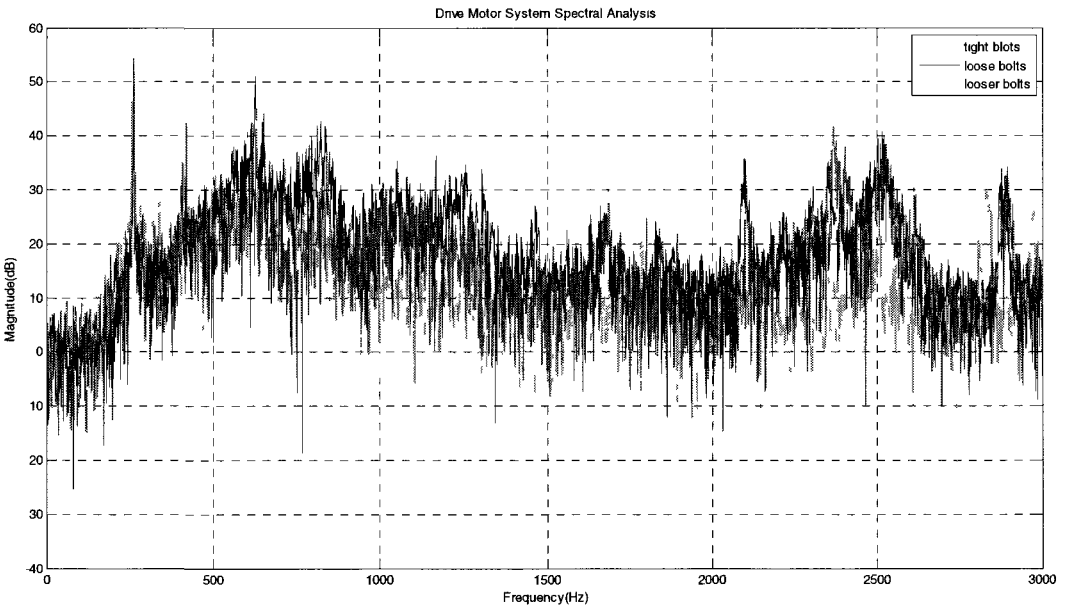


Fig. 28 1800 rpm at point 4

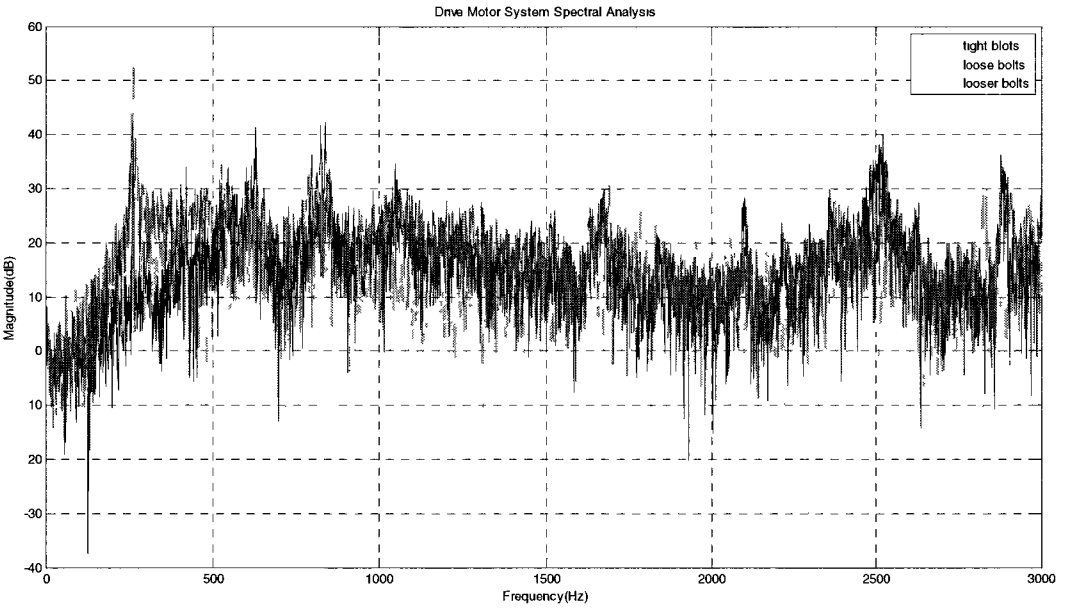


Fig. 29 1800 rpm at point 5

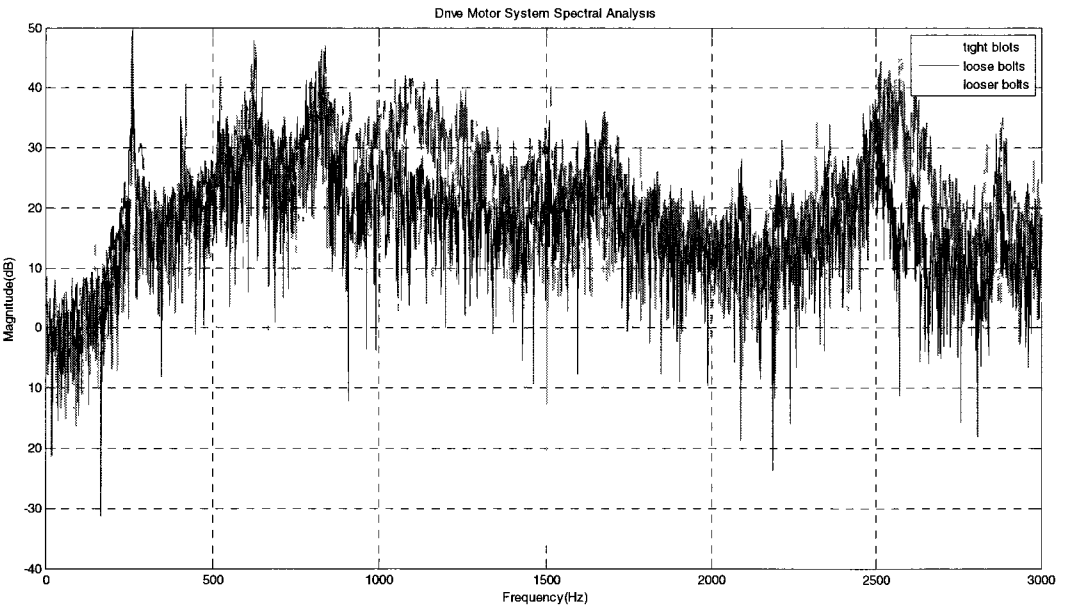


Fig. 30 1800 rpm at point 6

6) 6-point acoustic measurement experiment results from 2100 rpm :

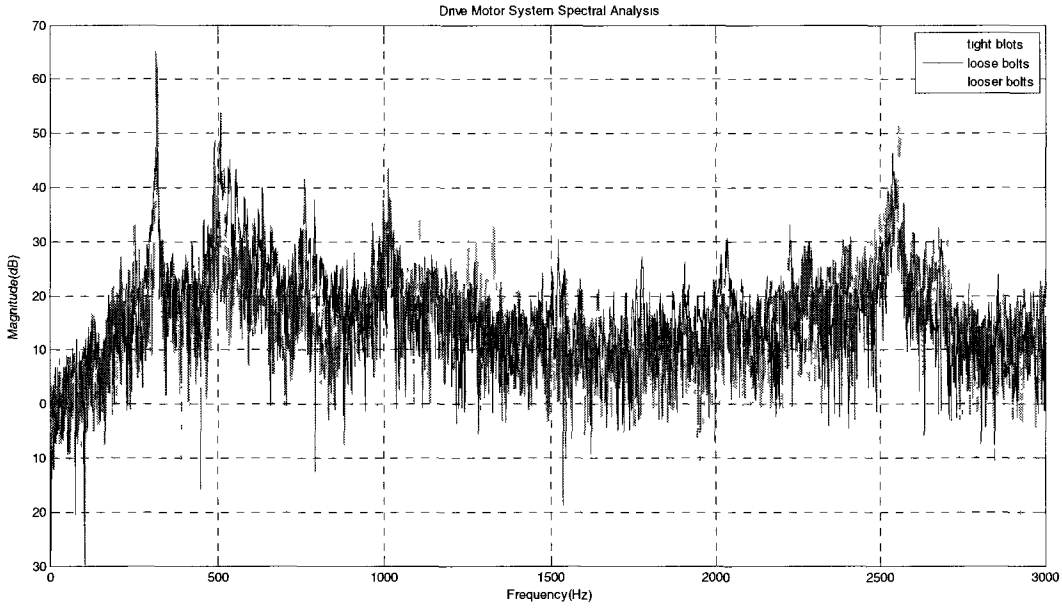


Fig. 31 2100 rpm at point 1

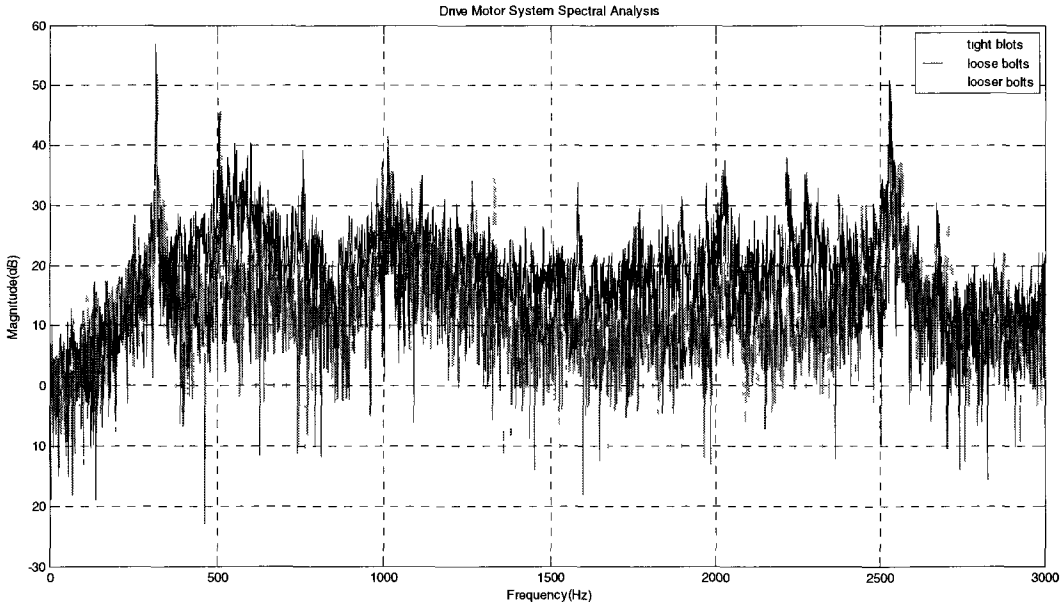


Fig. 32 2100 rpm at point 2

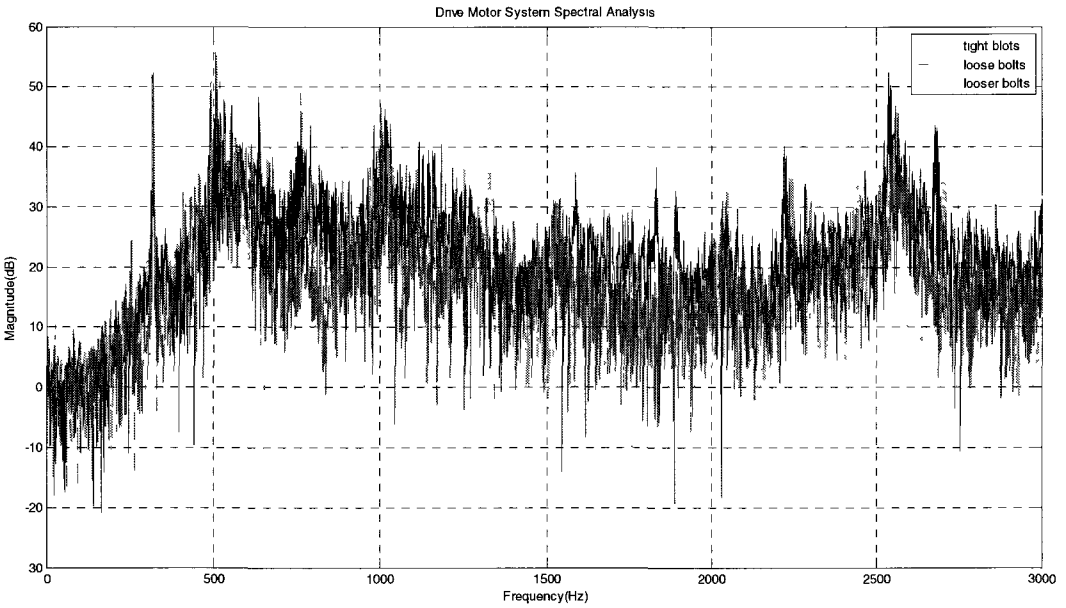


Fig. 33 2100 rpm at point 3

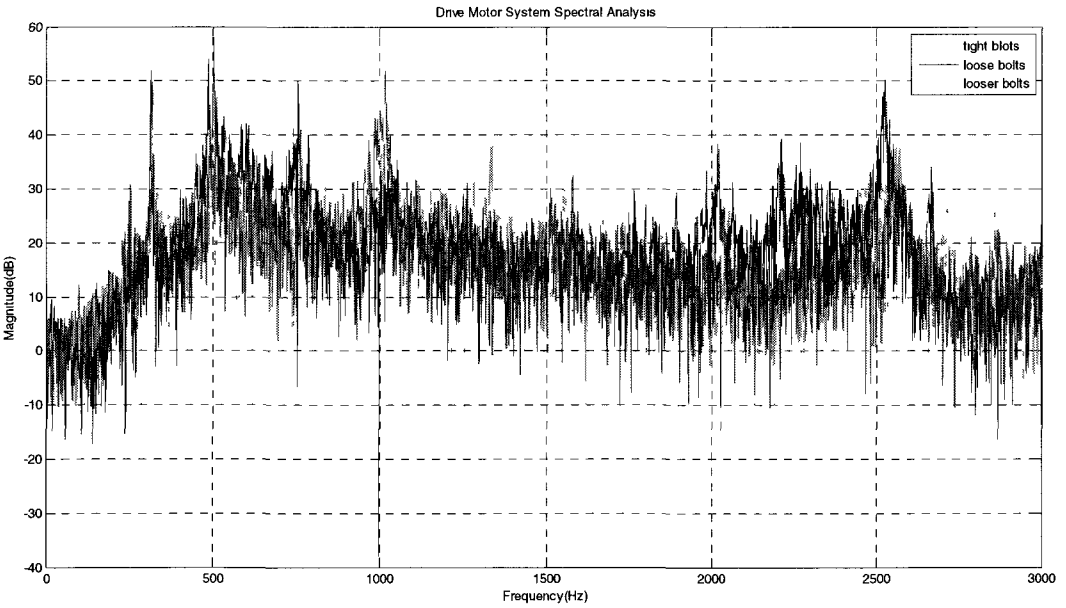


Fig. 34 2100 rpm at point 4

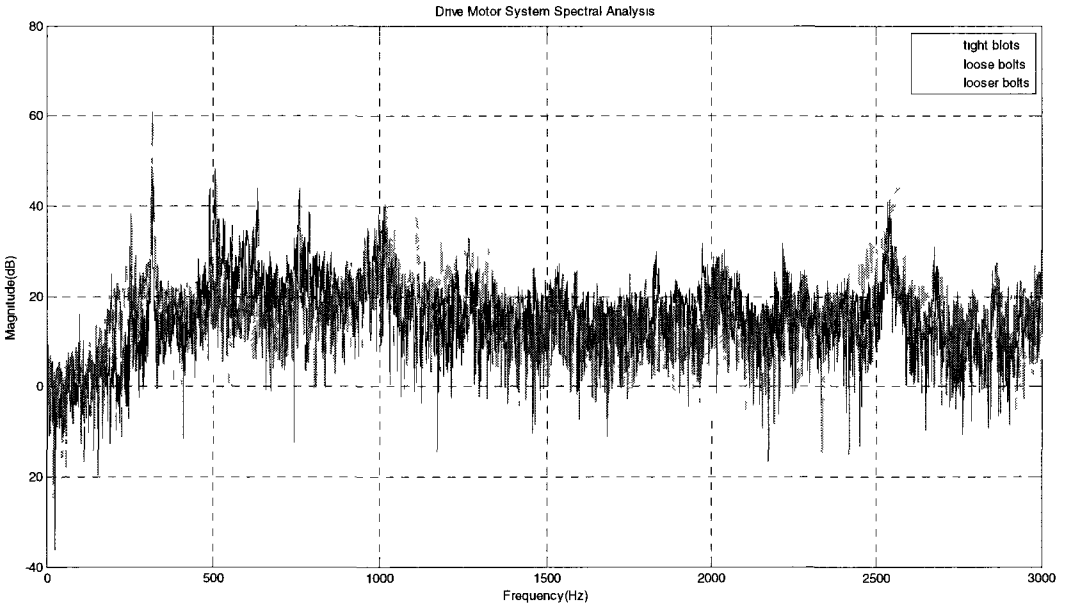


Fig. 35 2100 rpm at point 5

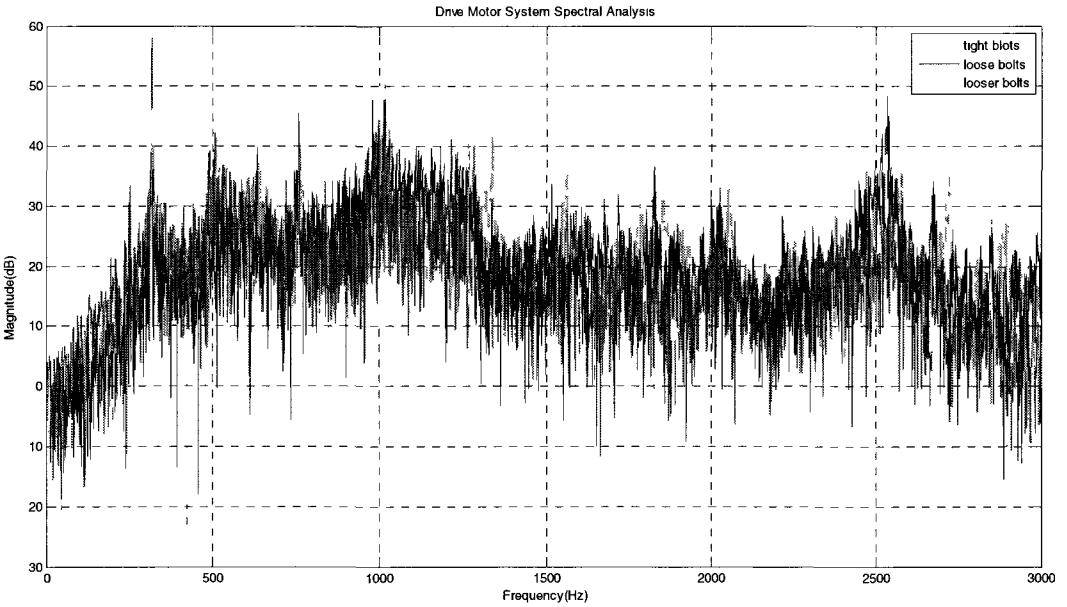


Fig. 36 2100 rpm at point 6

7) 6-point acoustic measurement experiment results from 2400 rpm :

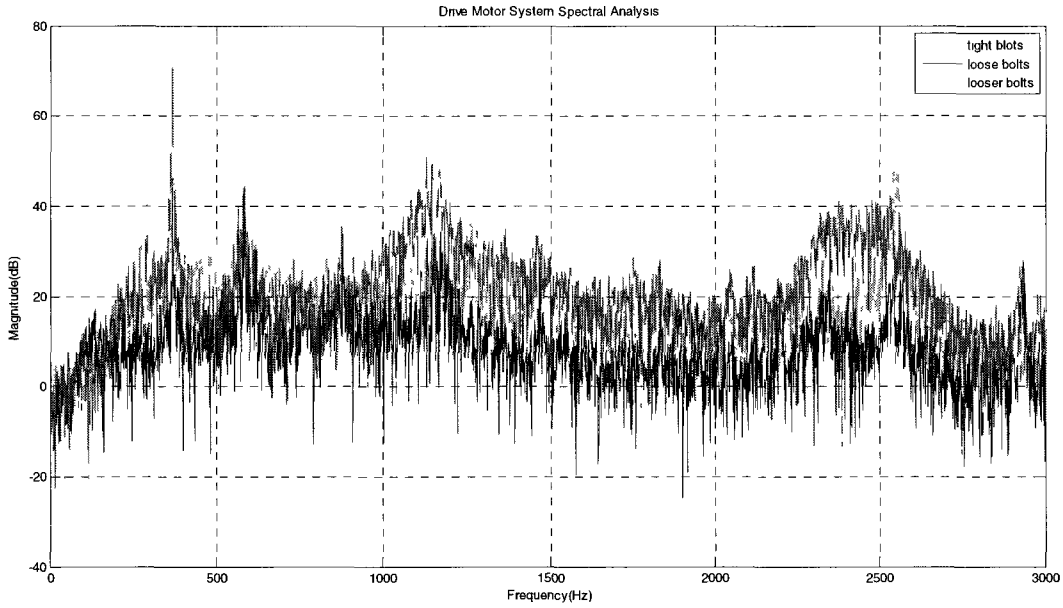


Fig. 37 2400 rpm at point 1

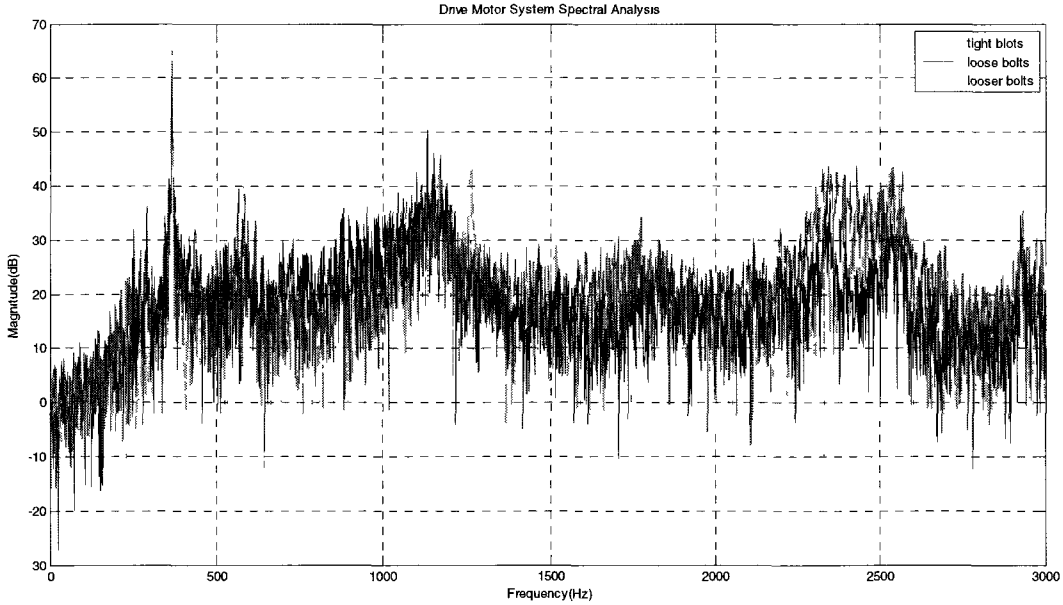


Fig. 38 2400 rpm at point 2

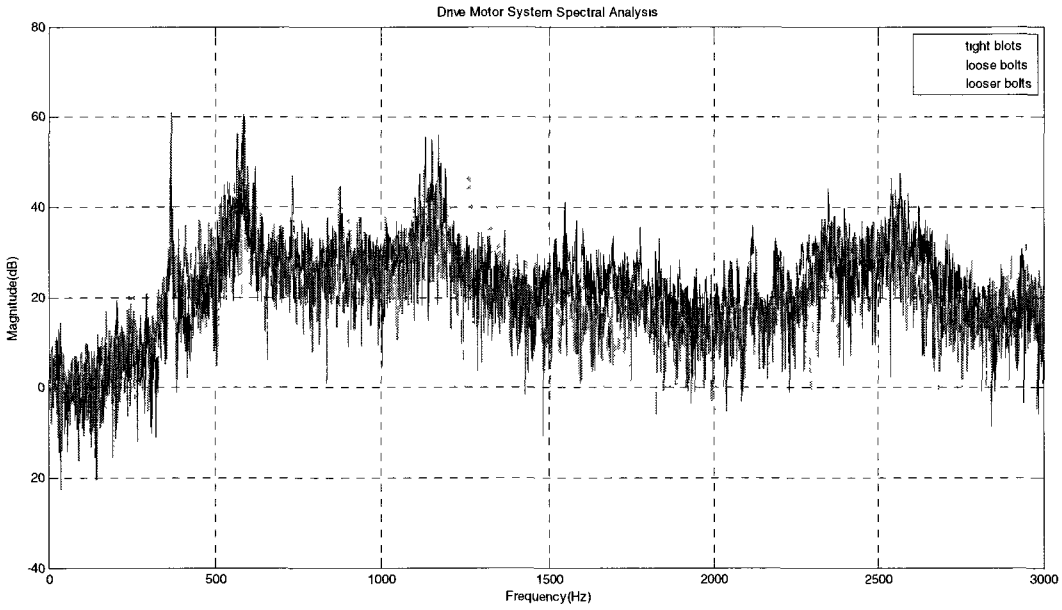


Fig. 39 2400 rpm at point 3

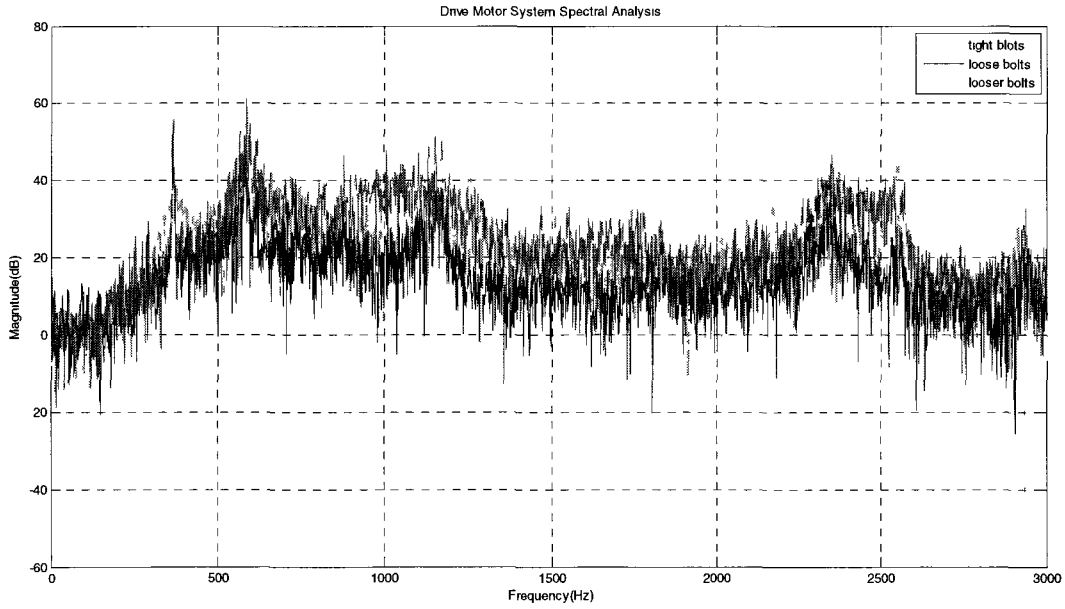


Fig. 40 2400 rpm at point 4

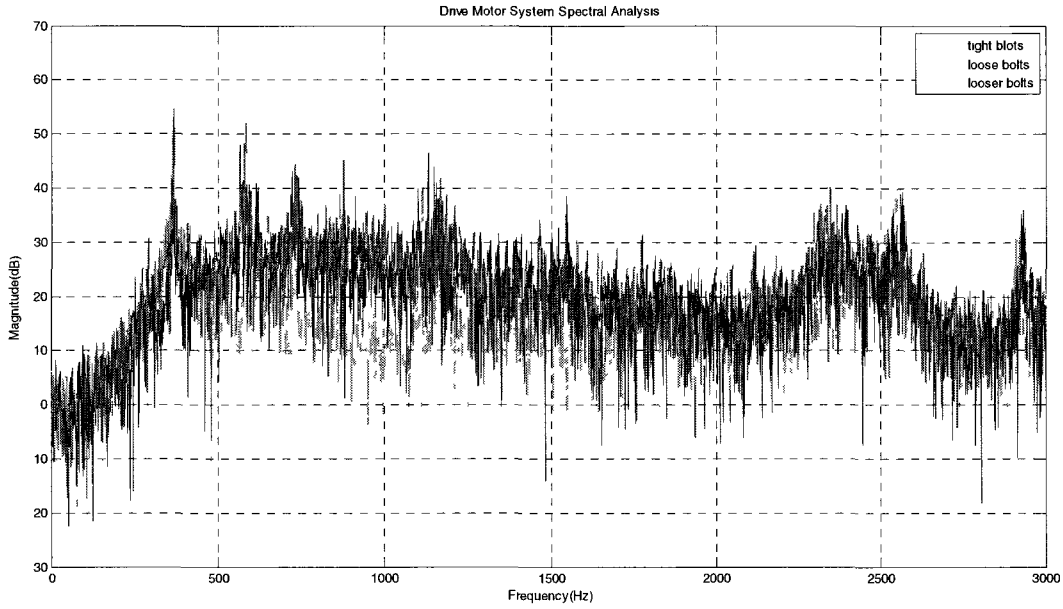


Fig. 41 2400 rpm at point 5

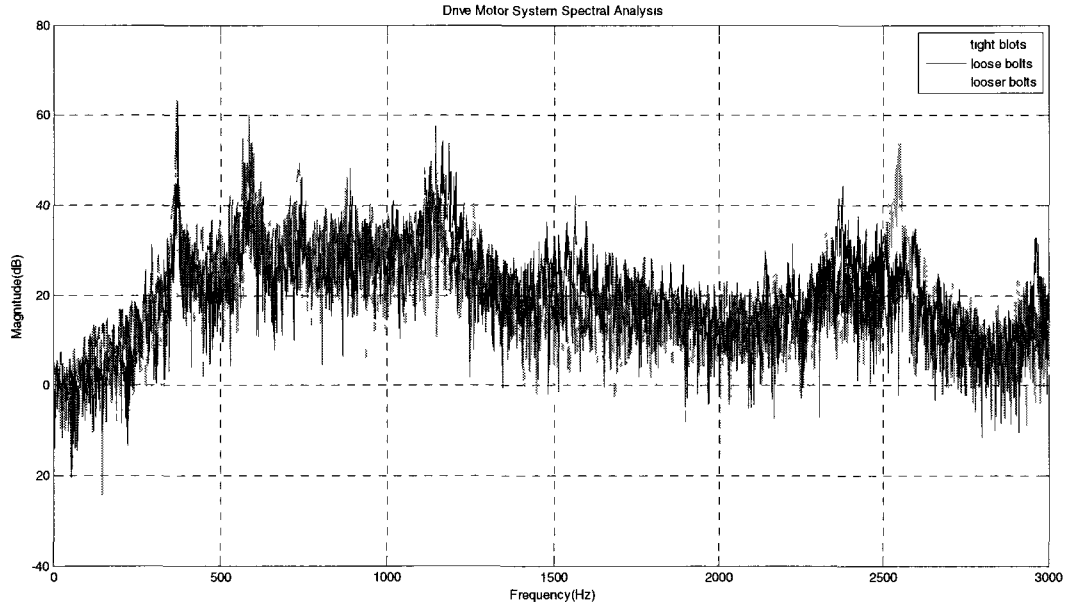


Fig. 42 2400 rpm at point 6

8) 6-point acoustic measurement experiment results from 2700 rpm :

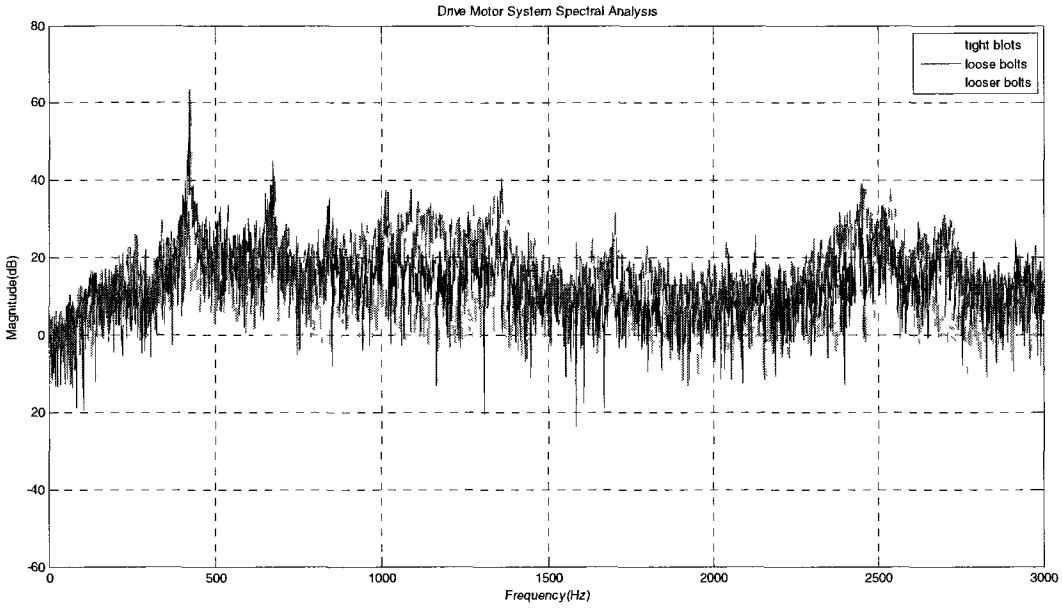


Fig. 43 2700 rpm at point 1

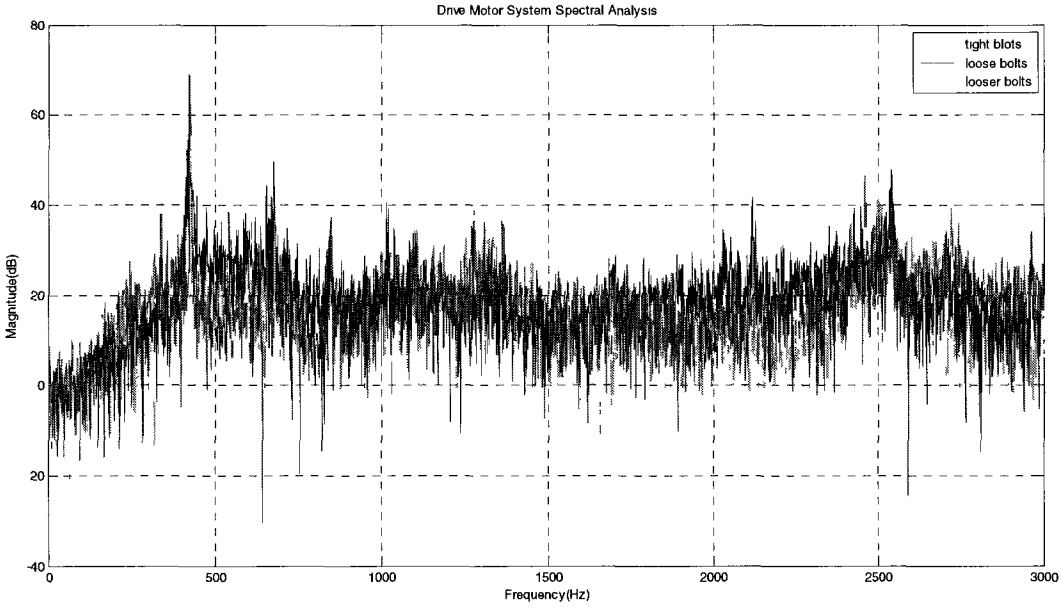


Fig. 44 2700 rpm at point 2

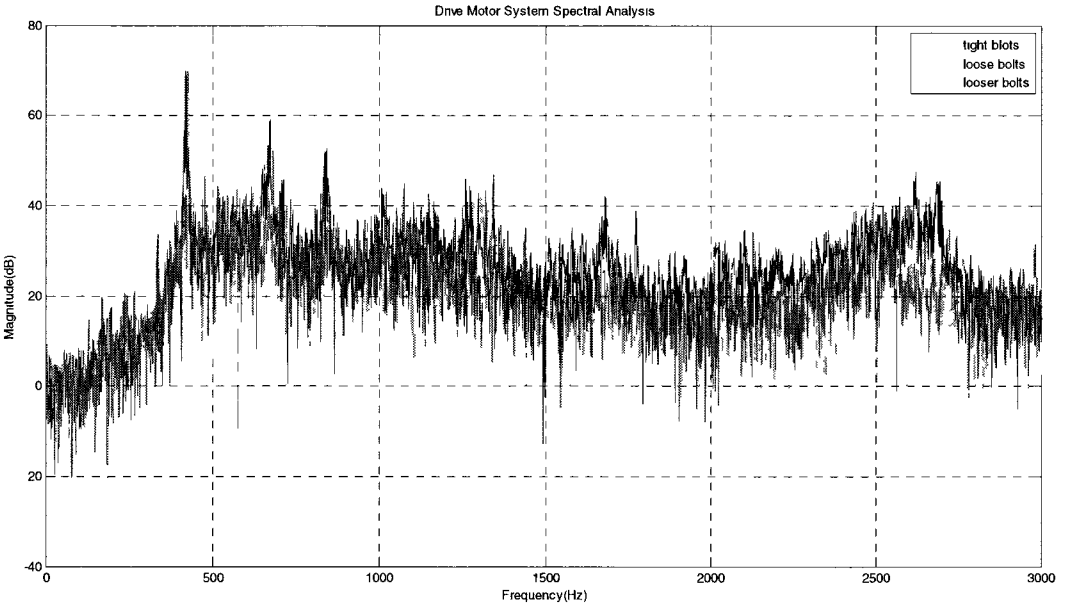


Fig. 45 2700 rpm at point 3

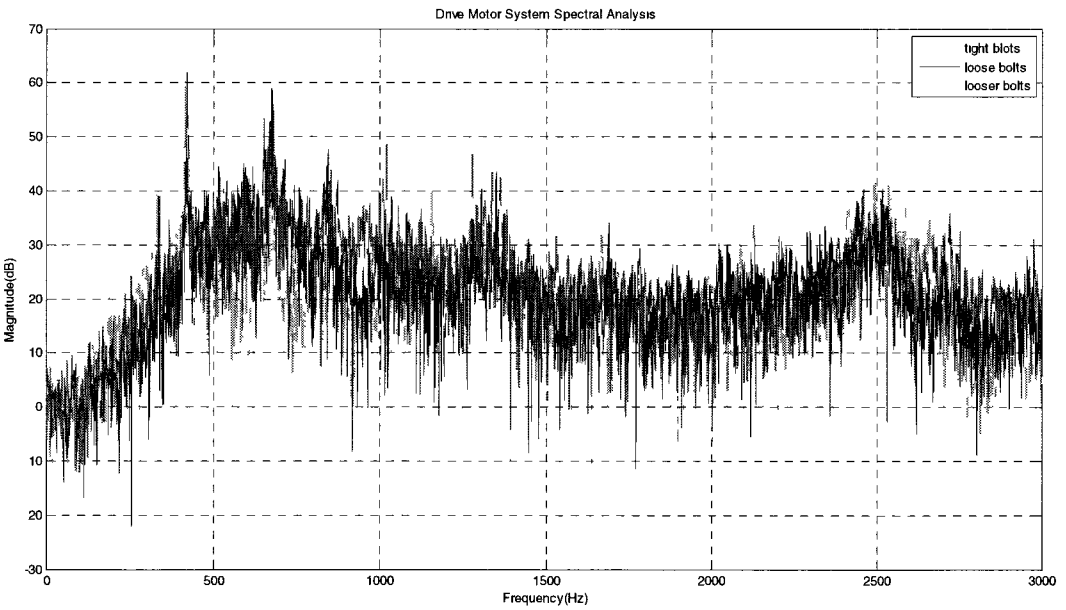


Fig. 46 2700 rpm at point 4

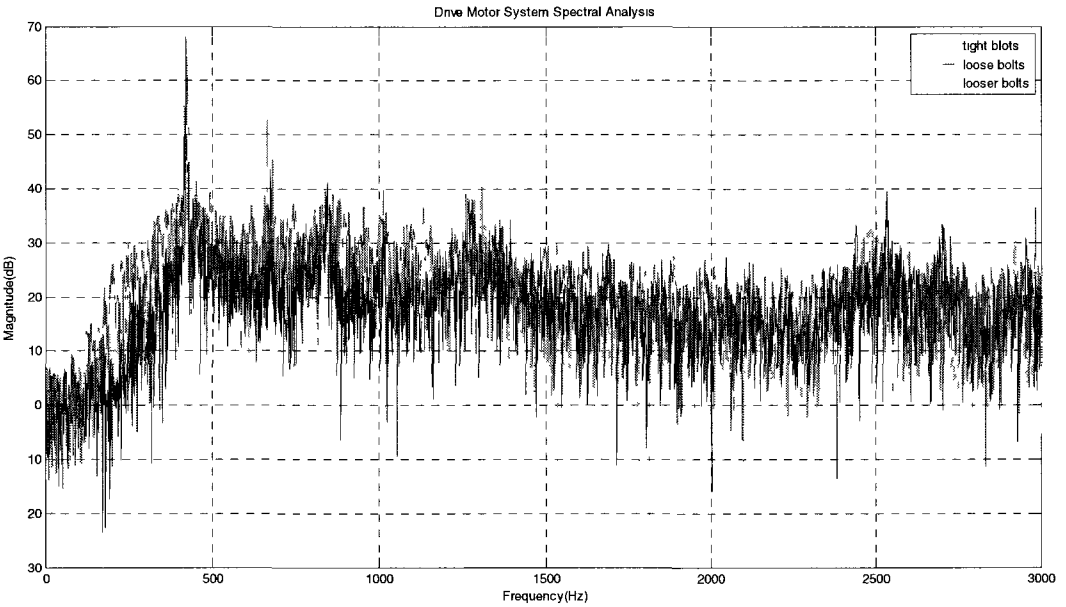


Fig. 47 2700 rpm at point 5

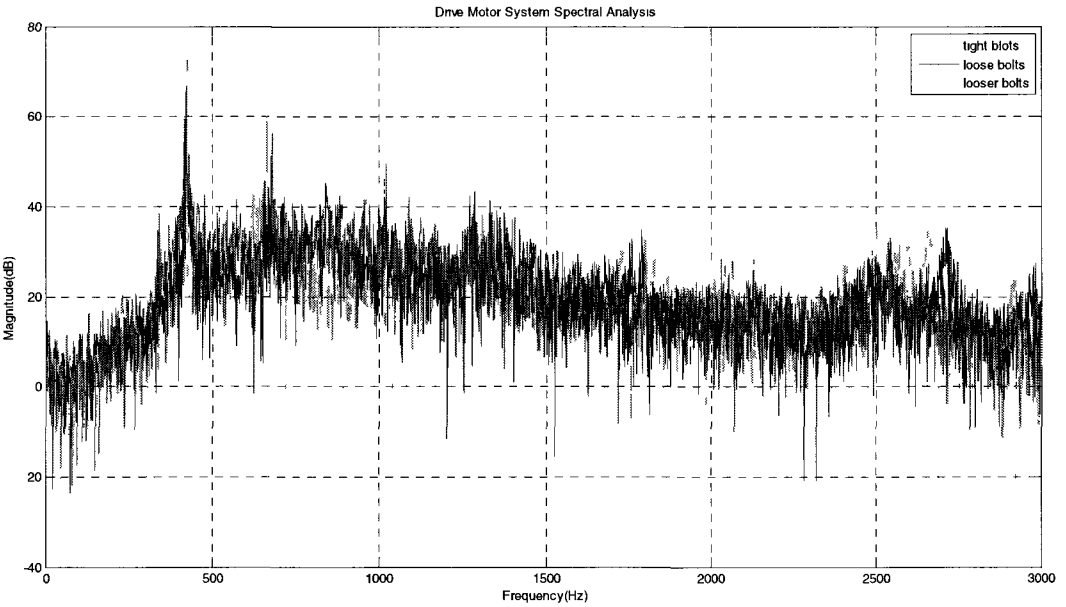


Fig. 48 2700 rpm at point 6

9) 6-point acoustic measurement experiment results from 3000 rpm :

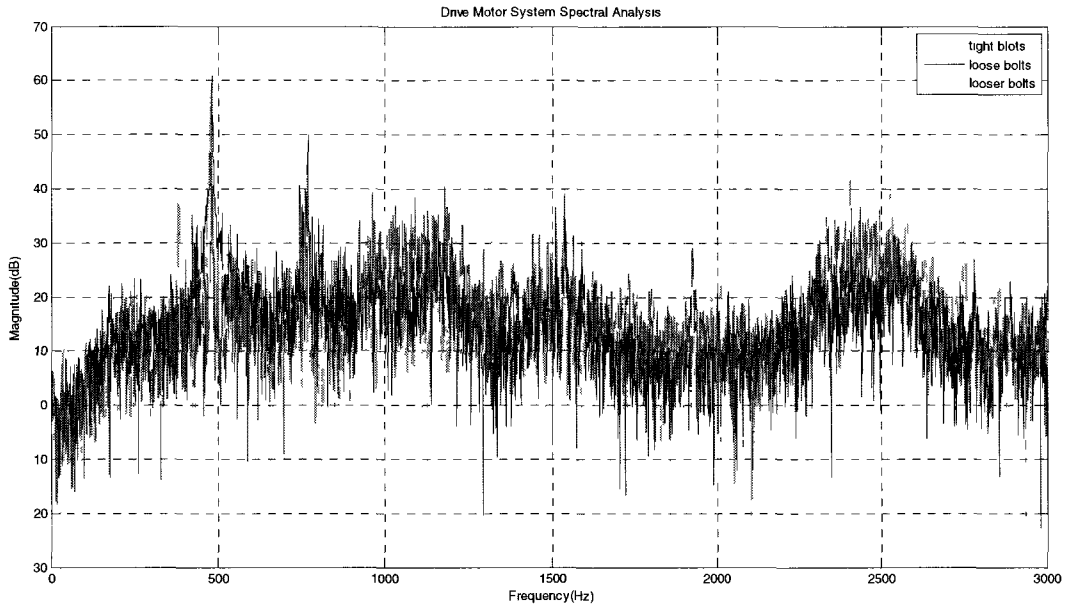


Fig. 49 3000 rpm at point 1

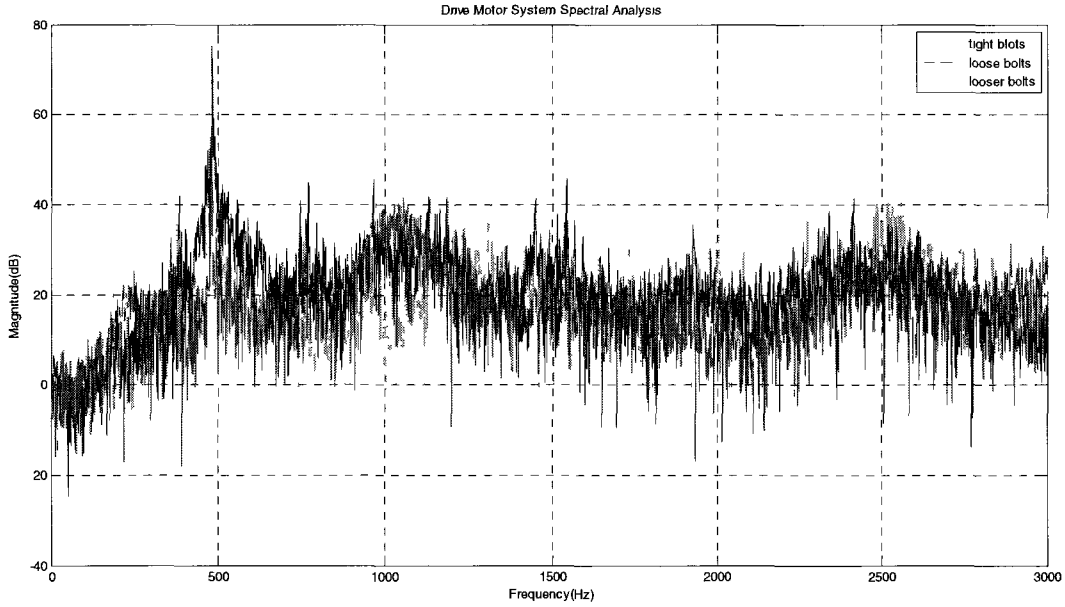


Fig. 50 3000 rpm at point 2

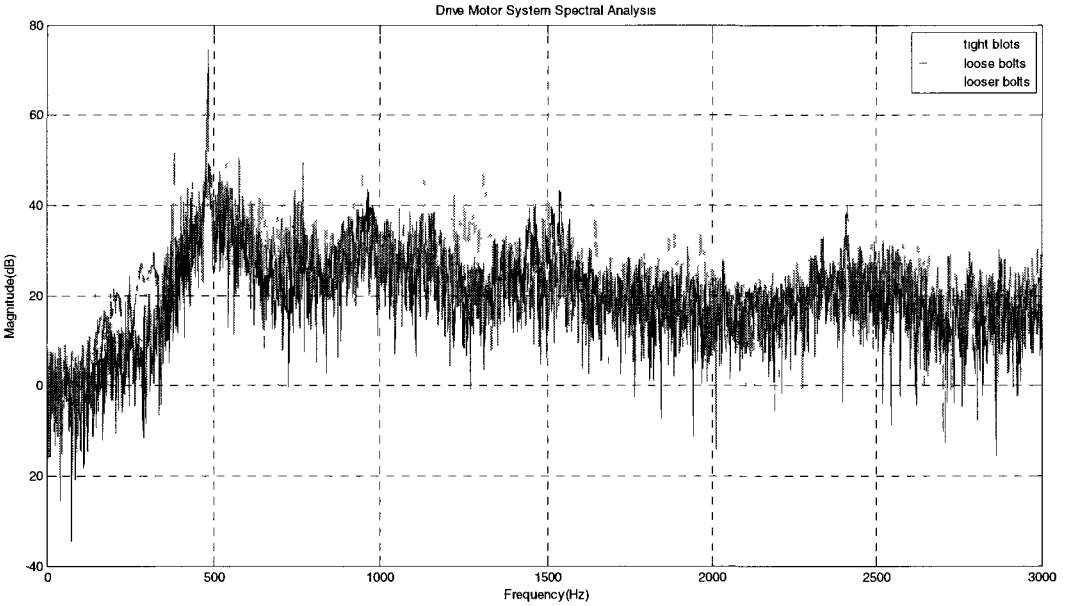


Fig. 51 3000 rpm at point 3

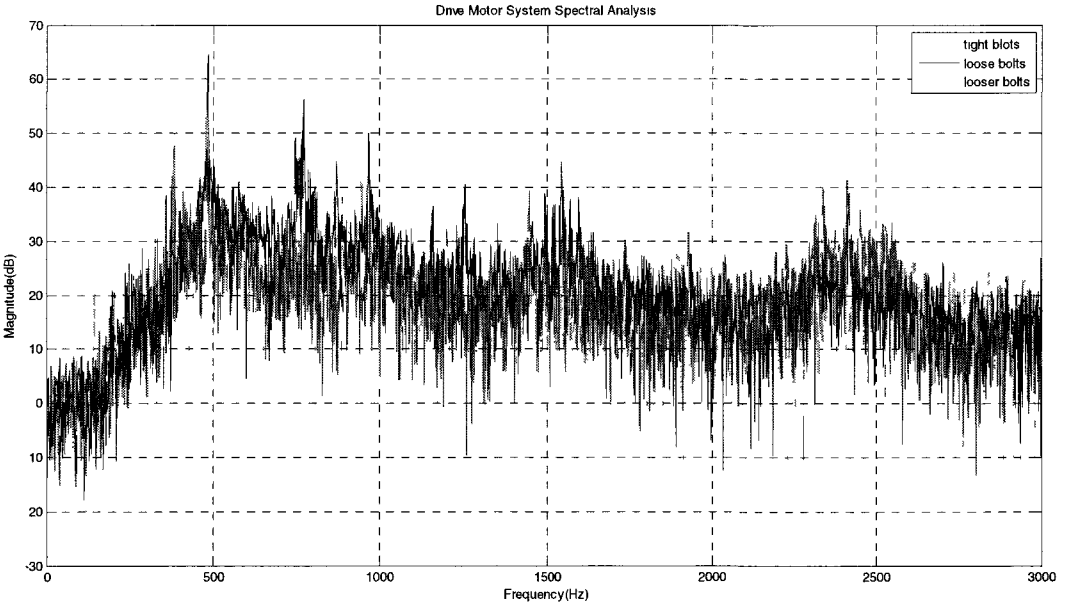


Fig. 52 3000 rpm at point 4

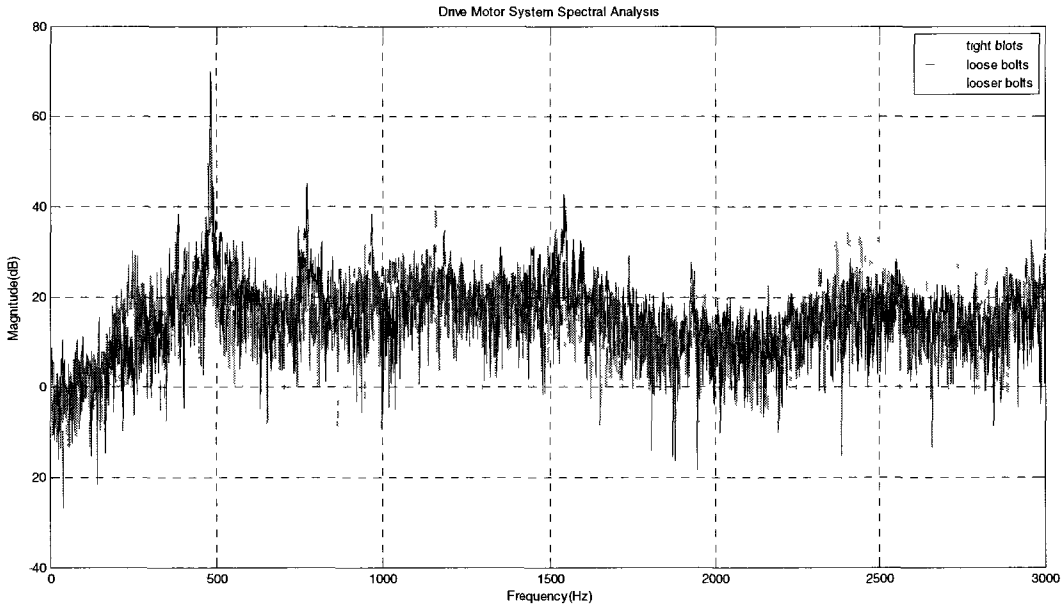


Fig.53 3000 rpm at point 5

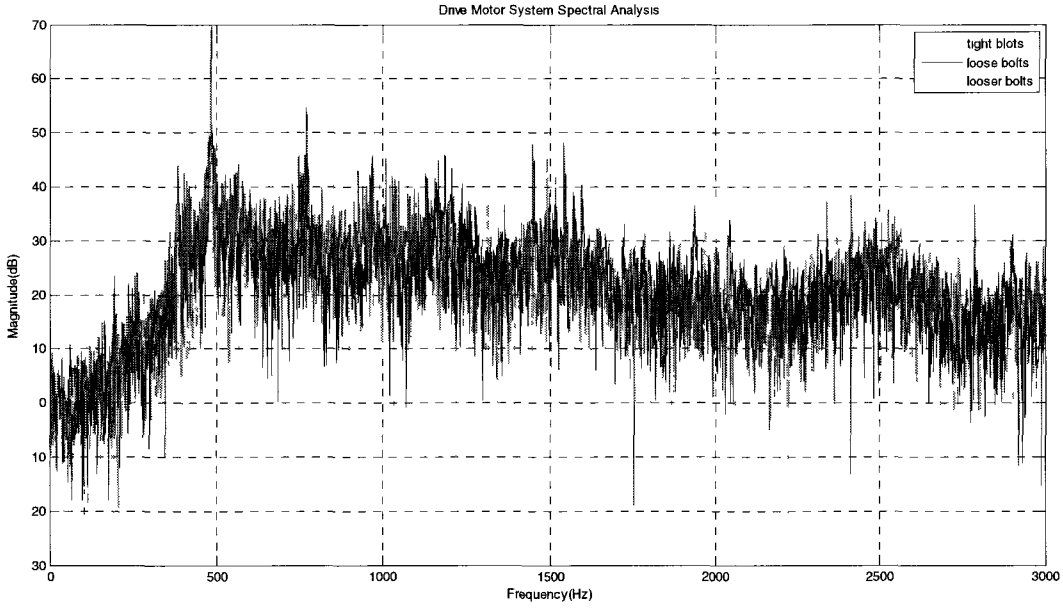


Fig. 54 3000 rpm at point 6

10) 6-point acoustic measurement experiment results from 3300 rpm :

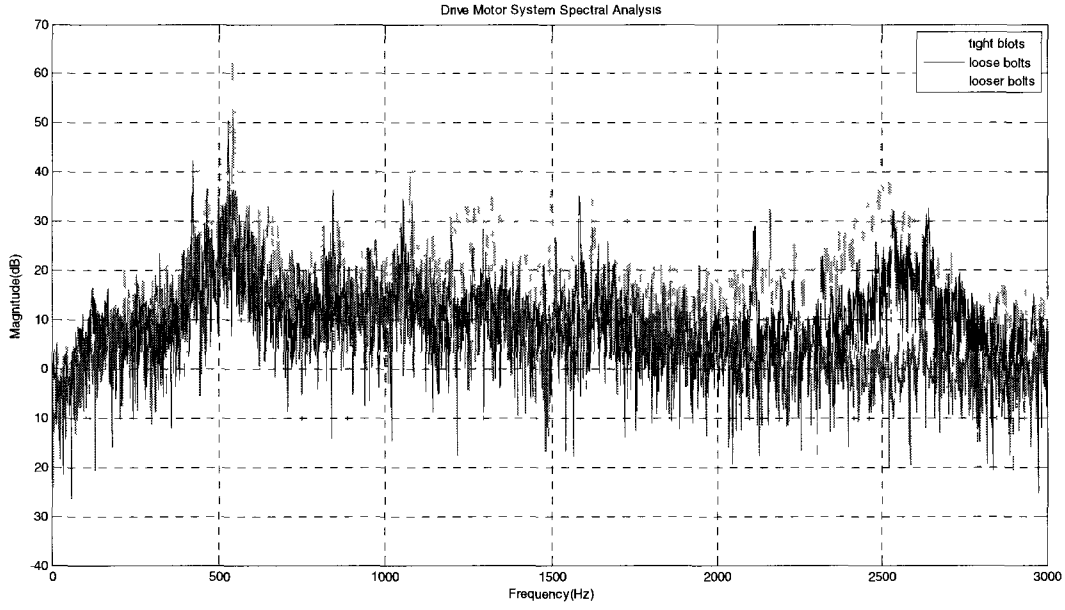


Fig. 55 3300 rpm at point 1

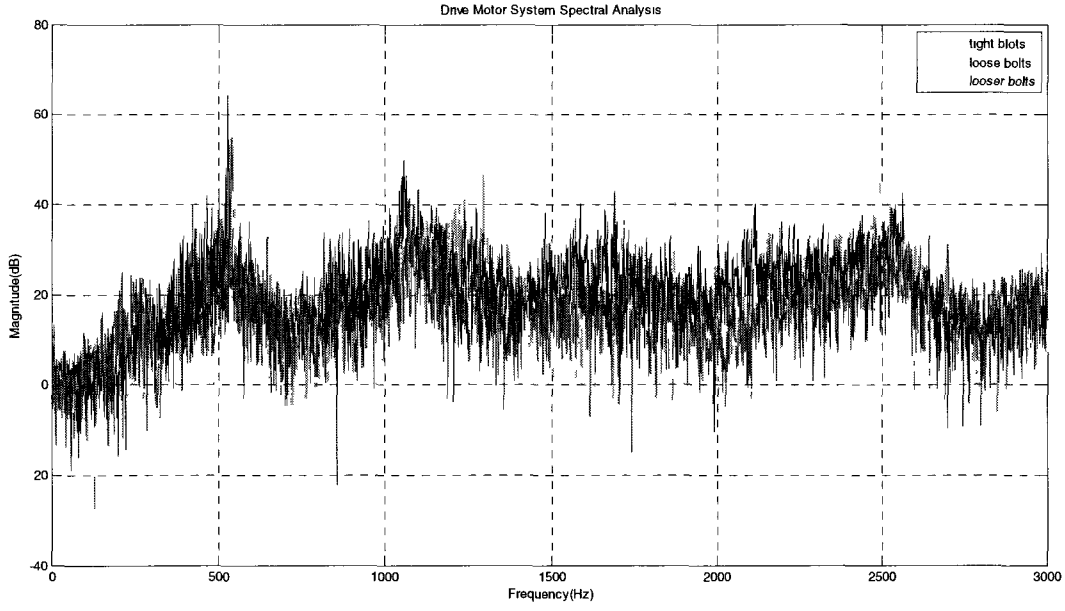


Fig. 56 3300 rpm at point 2

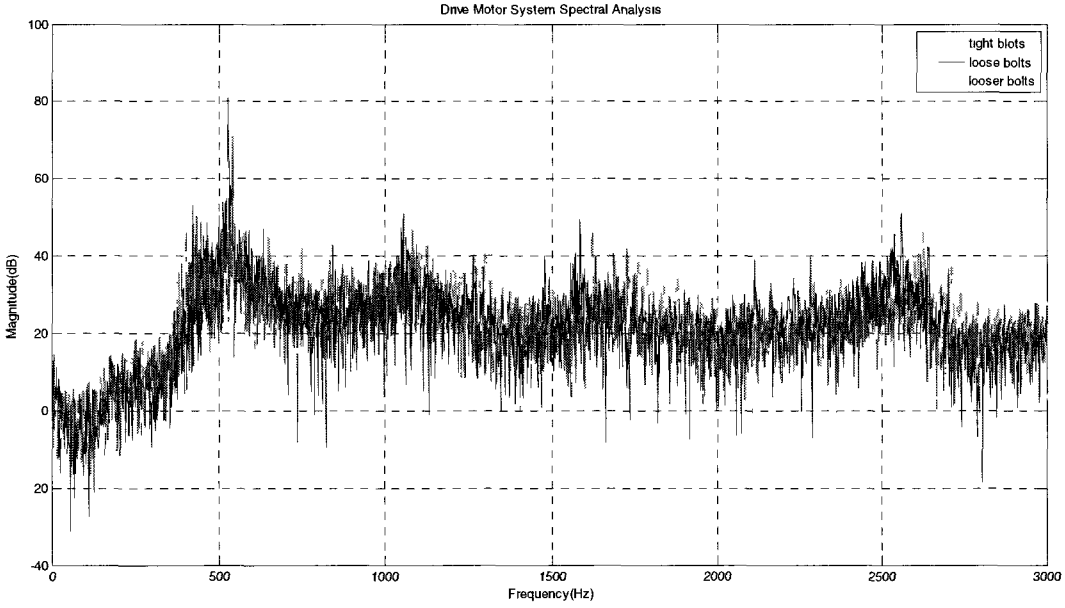


Fig. 57 3300 rpm at point 3

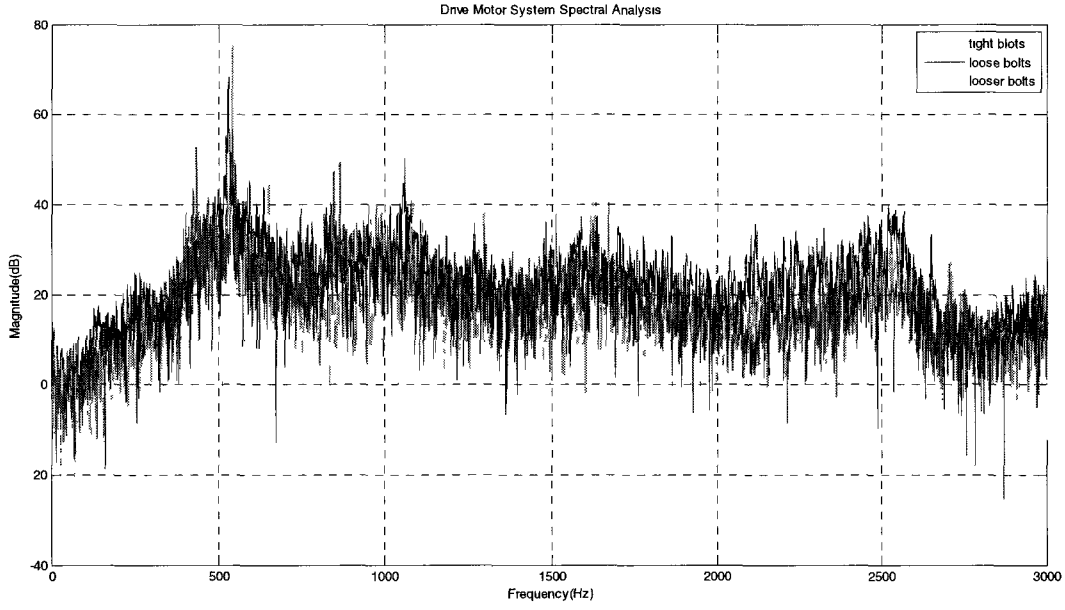


Fig. 58 3300 rpm at point 4

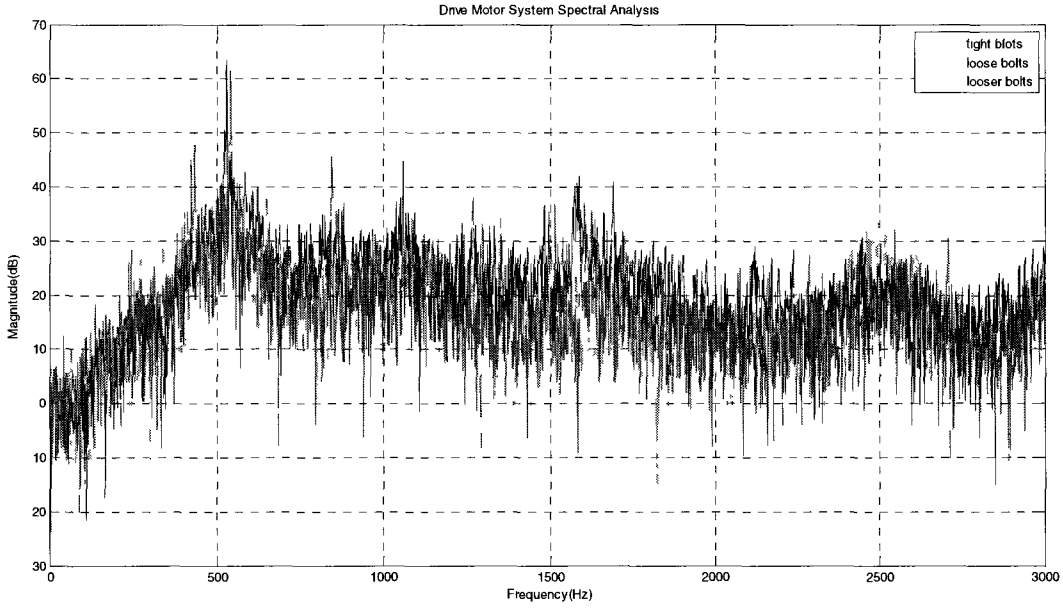


Fig. 59 3300 rpm at point 5

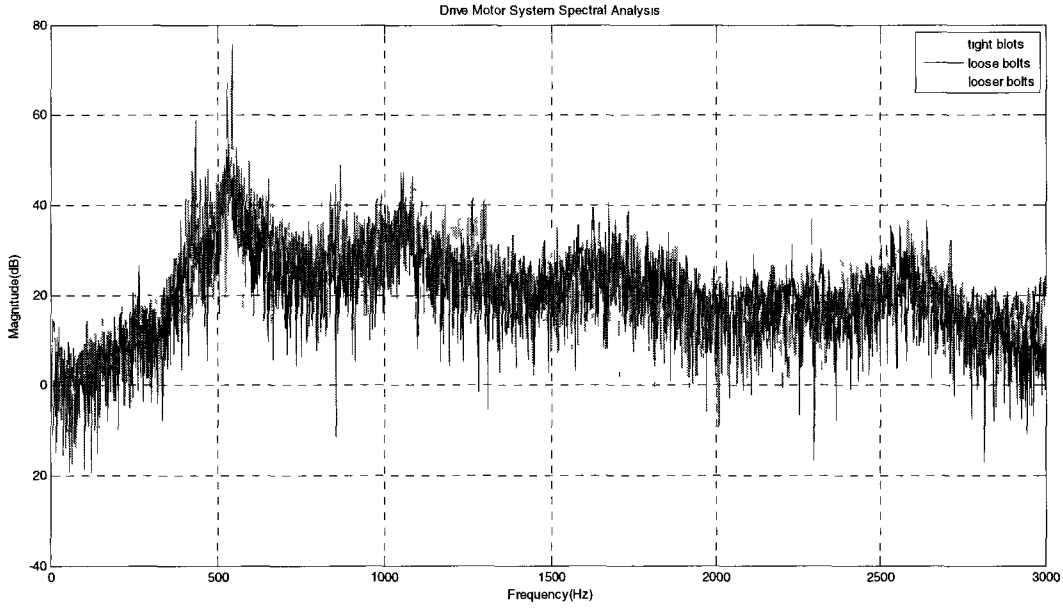


Fig. 60 3300 rpm at point 6

# Appendix E: Resonance Tube Measurement Experimental Results

1) Resonance tube measurement experiment results from 2100 rpm :

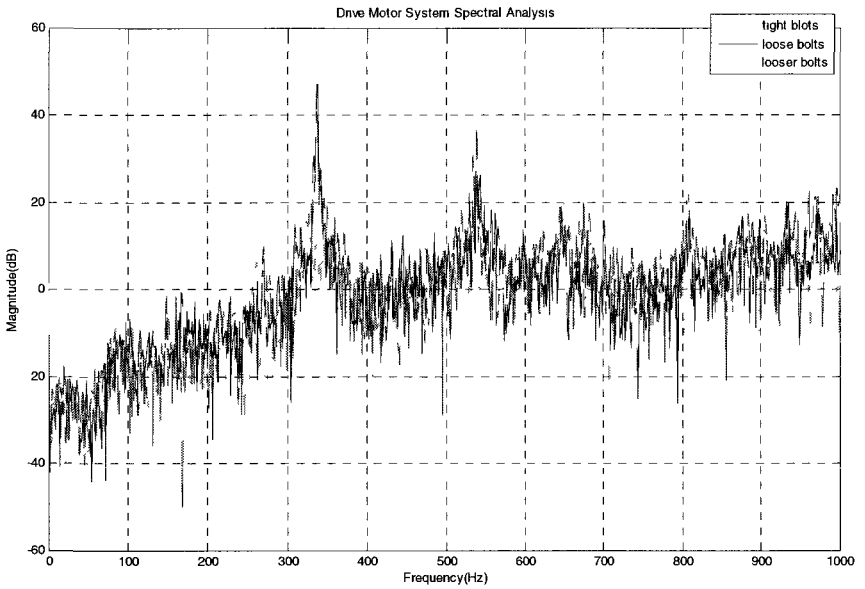


Fig 1. 2100 rpm at point 1

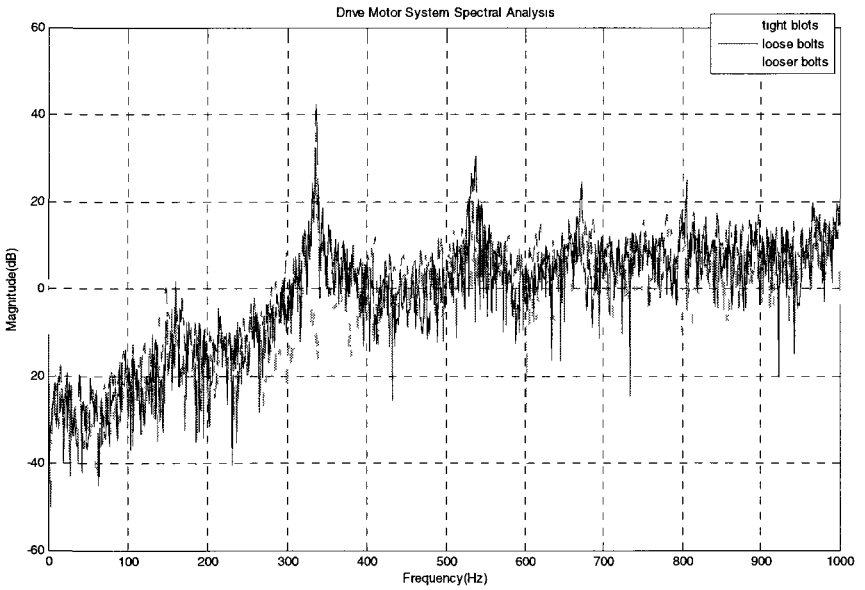


Fig. 2 2100 rpm at point 2

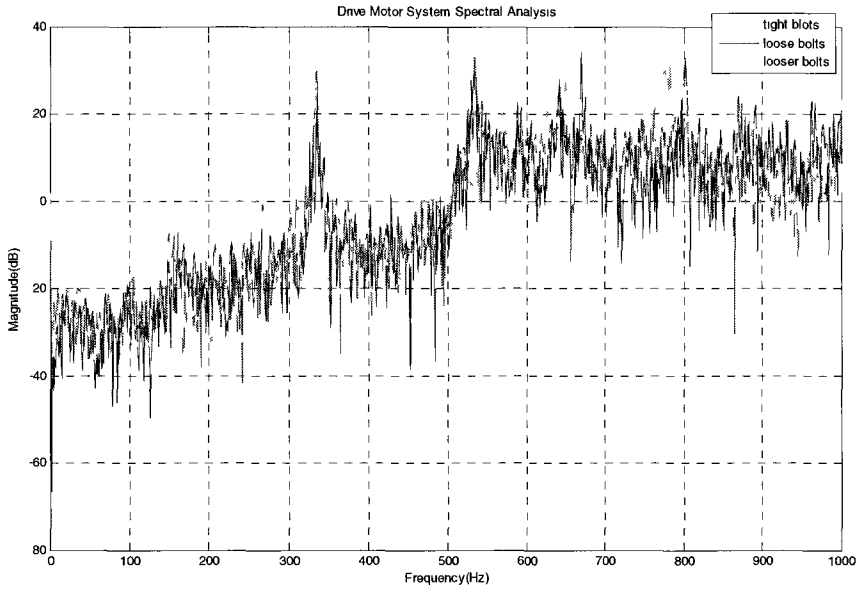


Fig. 3 2100 rpm at point 3

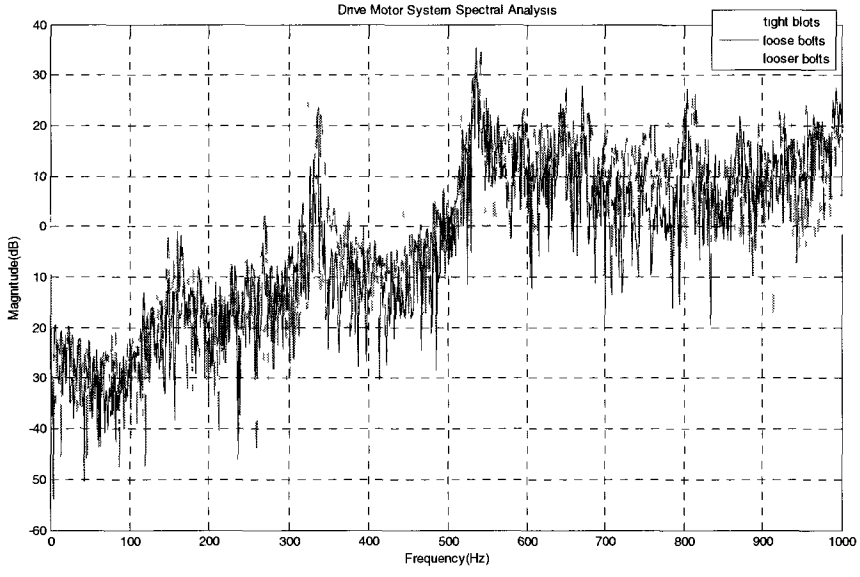


Fig. 4 2100 rpm at point 4

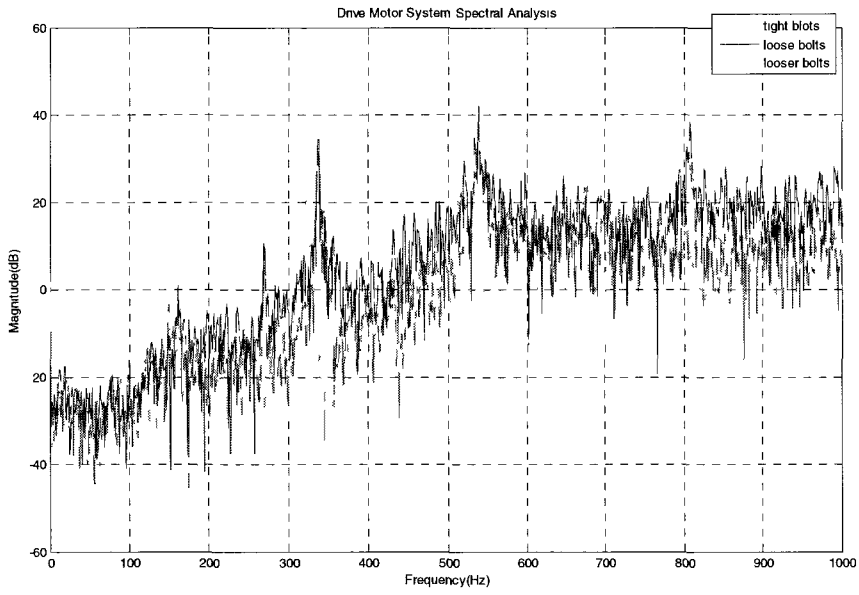


Fig. 5 2100 rpm at point 5

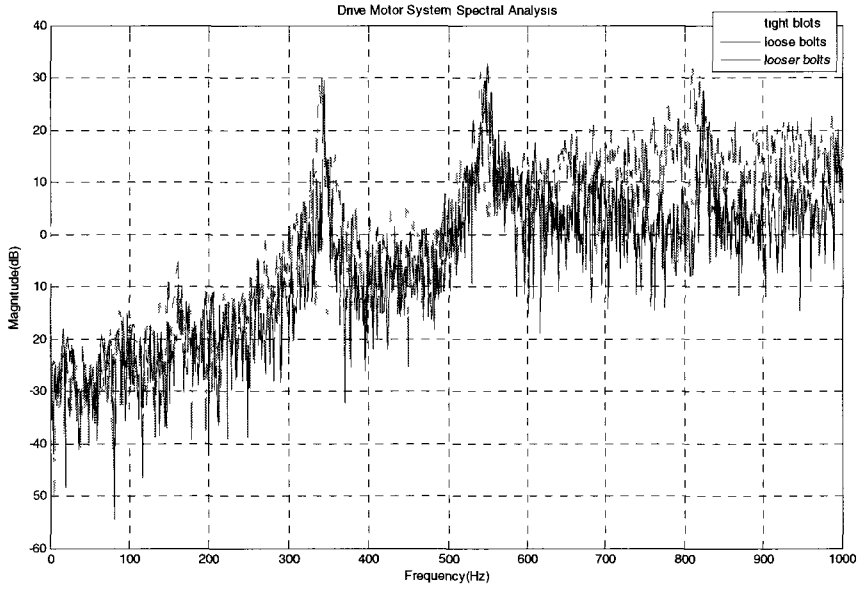


Fig. 6 2100 rpm at point 6

2) Resonance tube measurement experiment results from 2400 rpm :

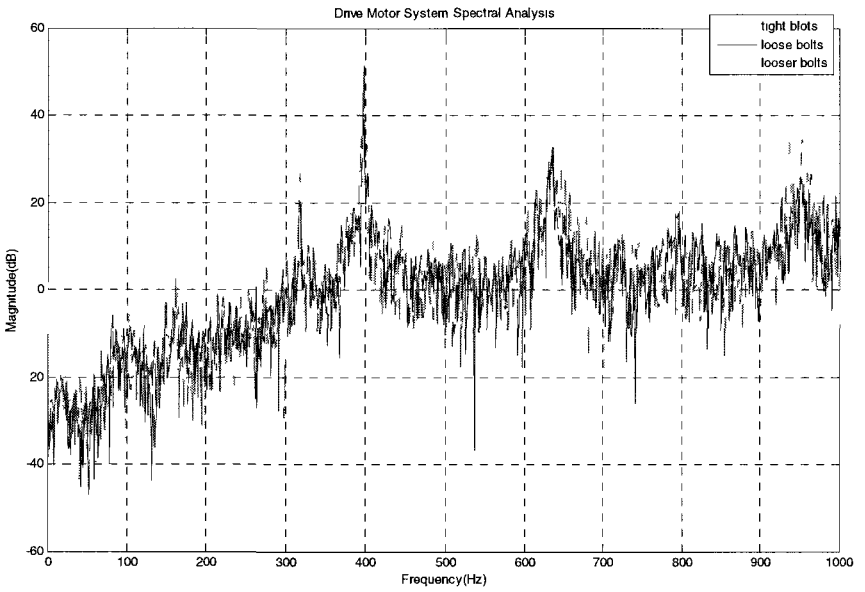


Fig. 7 2400 rpm at point 1

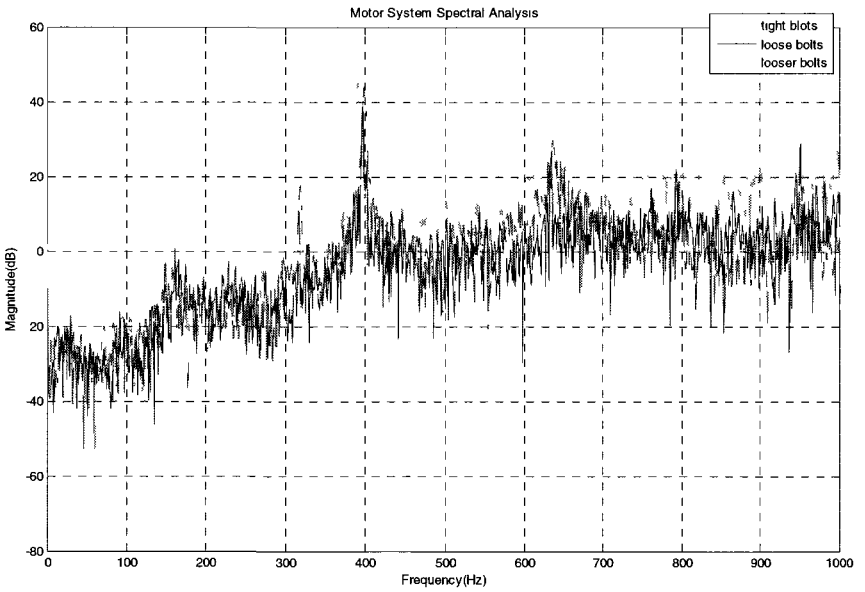


Fig. 8 2400 rpm at point 2

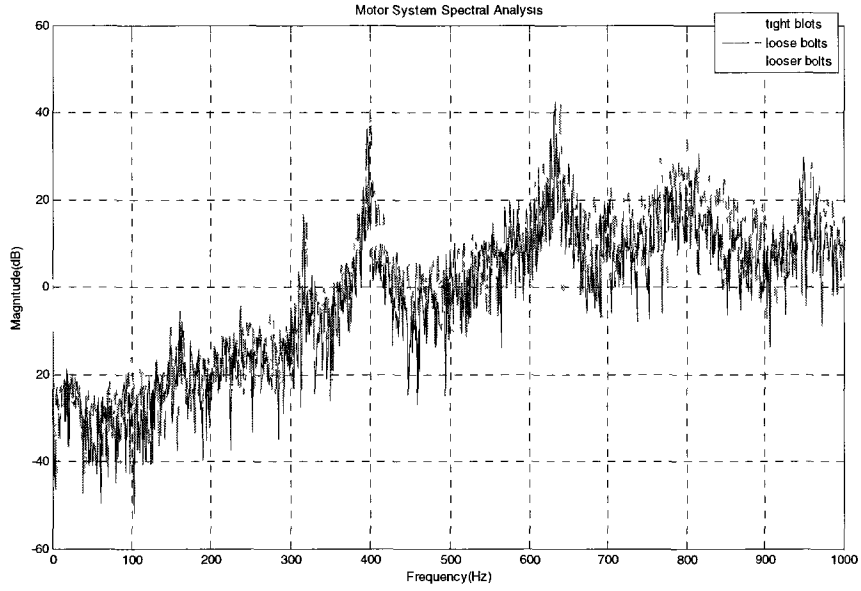


Fig. 9 2400 rpm at point 3

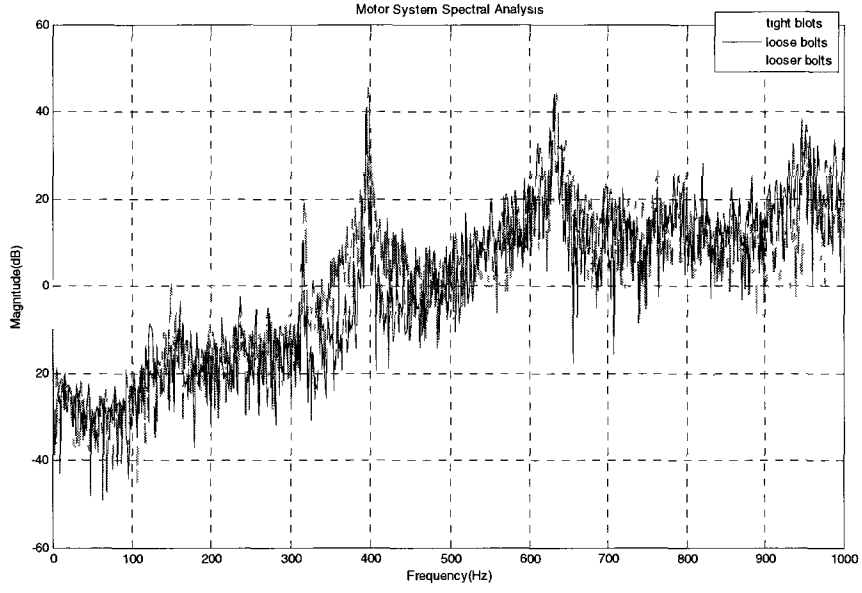


Fig. 10 2400 rpm at point 4

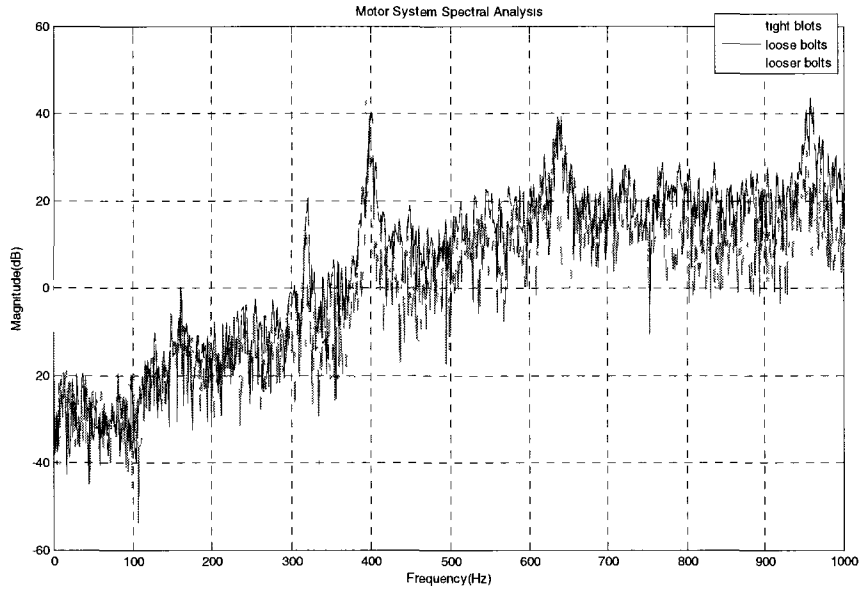


Fig. 11 2400 rpm at point 5

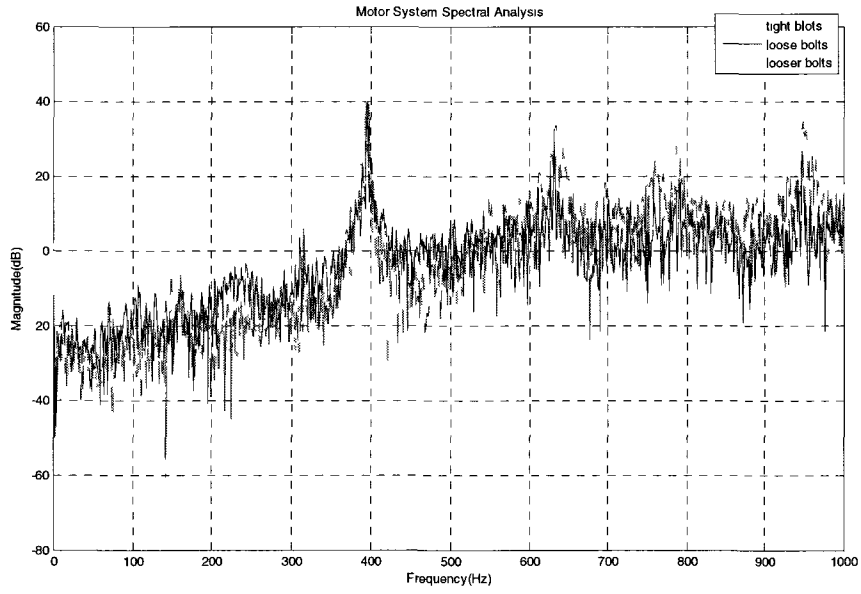


Fig. 12 2400 rpm at point 6

# Appendix F: Results for the Speed at 2100rpm with Frequency up to 1000 Hz

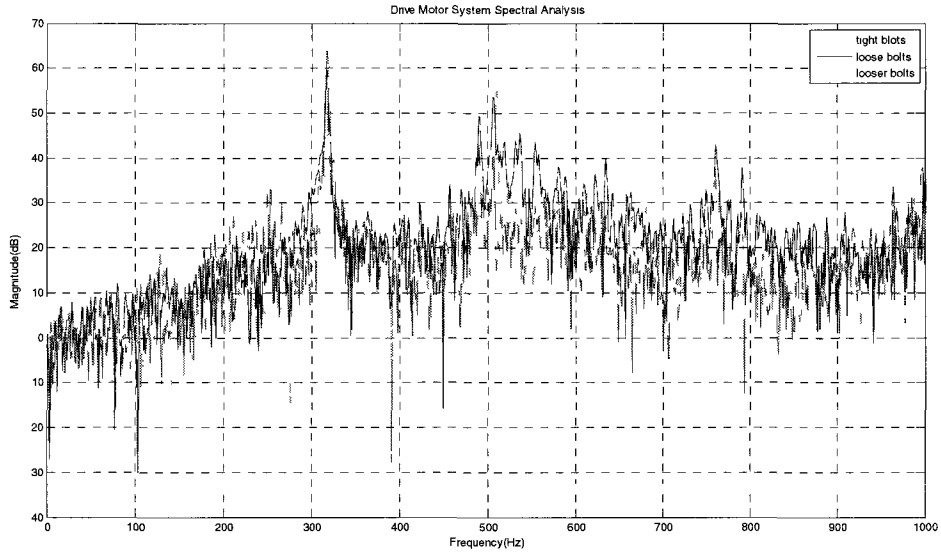


Fig. 1 2100 rpm at point 1

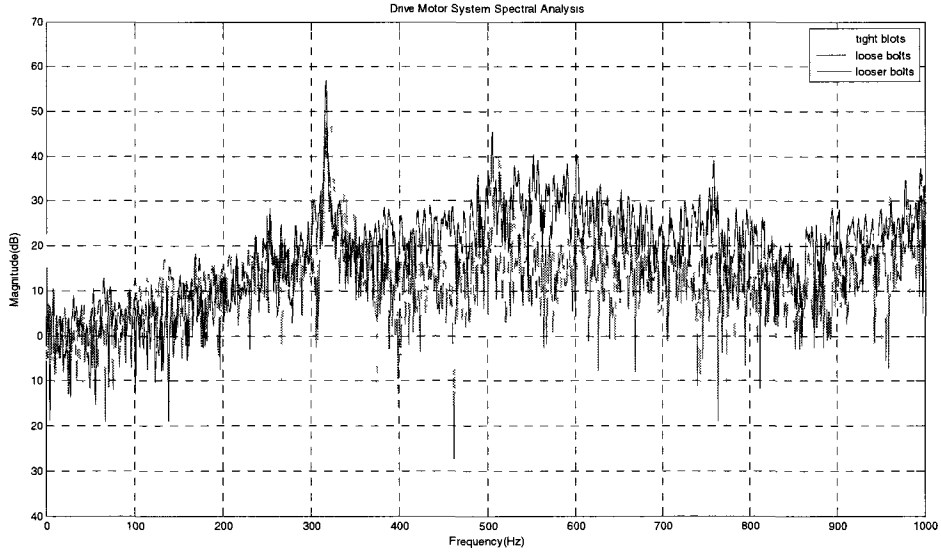


Fig. 2 2100 rpm at point 2

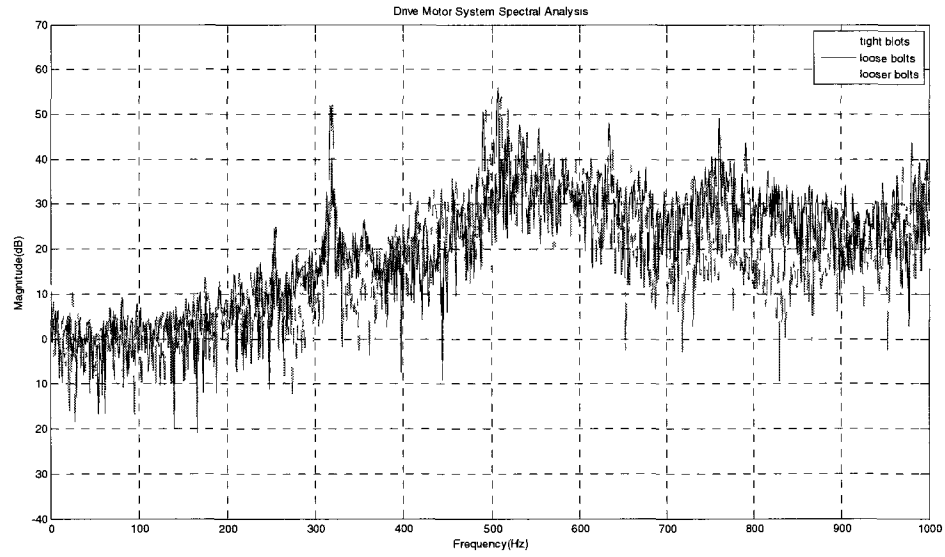


Fig. 3 2100 rpm at point 3

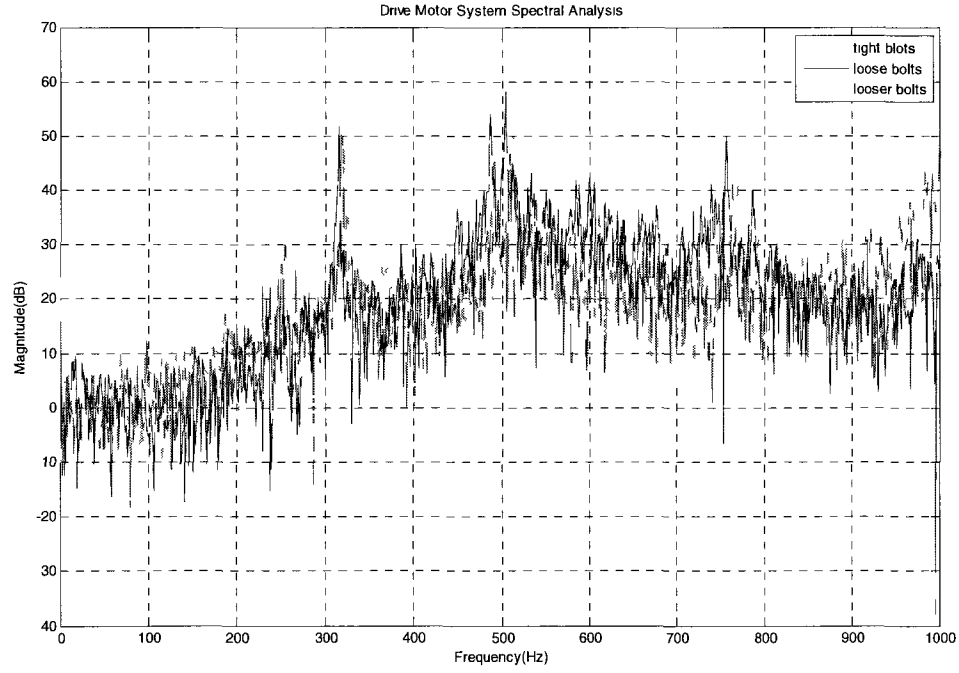


Fig. 4 2100 rpm at point 4

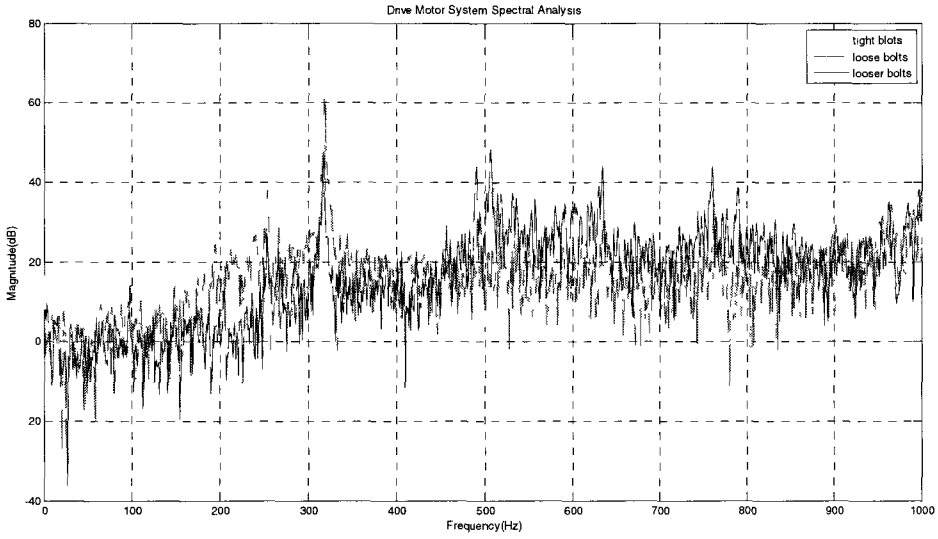


Fig. 5 2100 rpm at point 5

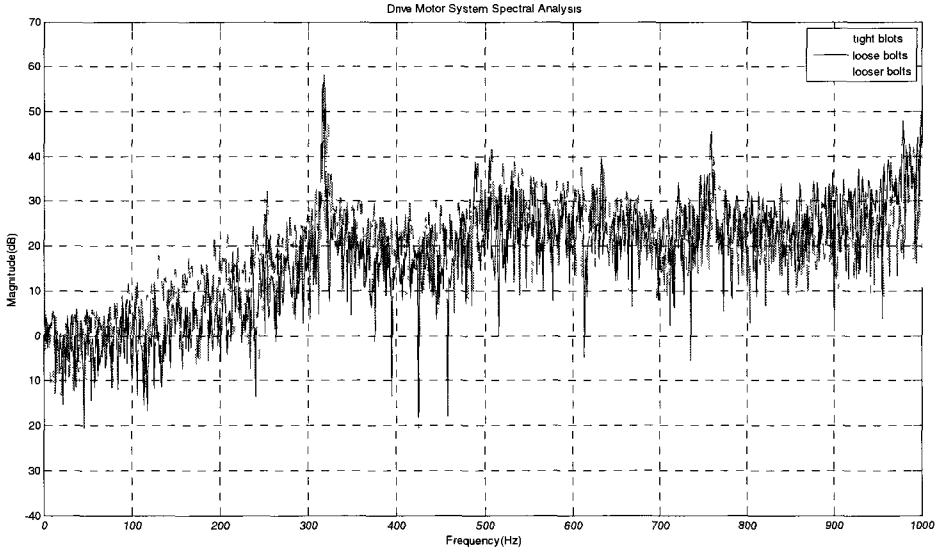


Fig. 6 2100 rpm at point 6